이학박사 학위논문

방선균 *Streptomyces coelicolor*에서 전사인자 WblC를 통한 항생제 저항성의 유도

Induction of antibiotic resistance mediated by transcriptional regulator WblC in *Streptomyces coelicolor*

2020년 8월

서울대학교 대학원

생명과학부

이 주 형

Abstract

Induction of antibiotic resistance mediated by transcriptional regulator WblC in *Streptomyces coelicolor*

Ju-Hyung Lee

Biological Sciences

The Graduate School

Seoul National University

Many antibiotics target bacterial translation, a fundamental metabolic process of protein synthesis. Translation-inhibitory antibiotics interfere with ribosome and other translational apparatus by diverse mode of action. Bacteria exhibit intrinsic resistance to antibiotics by utilizing indigenous genetic factors. Many types of intrinsic resistance mechanisms are known, but it has been observed that there are many undiscovered mechanisms as well.

Actinomycetes of the gram-positive phylum Actinobacteria include environmental microbes, animal and plant symbionts, and pathogens. Actinomycetes include *Streptomyces*, which not only produce most of the commercial antibiotics but retains many antibiotic resistance mechanisms, and *Mycobacterium*, which includes major pathogens causing antibiotic resistance problems such as *M. tuberculosis*. WblC or WhiB7 of actinomycetes is a factor conferring intrinsic resistance to translation-inhibitory antibiotics. WblC (WhiB7), along with HrdB (SigA) is known to bind to target gene promoters and activate transcription. WblC (WhiB7) target gene products execute multiple antibiotic resistance mechanisms. However, the composition of WblC (WhiB7) regulon varies greatly among species as well as encompasses many genes of unknown functions. Moreover, there were several problems in the mode of defining WhiB7

regulon. On the other hand, while *wblC* (*whiB7*) is thought to be regulated by ribosome-mediated transcriptional attenuation, experimental evidences were insufficient and, most of all, no explanations were suggested regarding how the transcriptional attenuation is suppressed during antibiotic stress.

The regulatory targets of WblC in *Streptomyces coelicolor* were examined in this study. 7.8% of all *S. coelicolor* genes exhibited WblC-dependent changes in transcript level during antibiotic stress, and 312 of these genes were confirmed as WblC regulon with observed direct binding of WblC to the promoters. As in mycobacteria, promoters of 288 WblC-upregulated regulon genes had 2 promoter sequence elements and a WblC-binding site in common, and showed WblC binding and transcriptional activation correlated to the degree of conservation of these common sequences. On the contrary, promoters of 24 WblC-downregulated regulon genes had no consensus sequence and exhibited no recruitment of HrdB by WblC. Meanwhile, WblC also regulated expression of many noncoding RNAs other than the regulon genes.

Many of the WblC regulon products were identified to associate with ribosome and function as novel antibiotic resistance factors. *S. coelicolor* WblC regulon consists of multiple known antibiotic resistance genes and several overrepresented functional groups of genes, especially those involved in translation. WblC caused increase in global intracellular translation rate and a corresponding increase in growth rate at low-concentration antibiotic stress conditions, which may be due to diminished effective antibiotic concentration or stimulation of translation by WblC regulon products. Proteins showing both antibiotic stress- and WblC-dependent increase in ribosome association were identified, most of which were products of WblC regulon and many of which were reported to relieve translation stress. Respective mutation of 3 ribosome associate protein-coding WblC regulon genes resulted in increased susceptibility to erythromycin and/or tetracycline, which were recovered by complementation of the mutated genes.

This study also deals with the mechanism how transcriptional attenuation is

suppressed during antibiotic induction of *wblC*. First, the sequence elements of transcriptional attenuation were confirmed to be conserved among most of the *wblC* leader sequences of actinomycetes. Then, transcriptional termination caused by the Rho-independent terminator (RIT) of the leader sequence was verified to attenuate *wblC* expression. Putative antiterminator RNA structures were conserved in *wblC* leader sequences of sub-clades of actinomycetes, and the putative antiterminator of *S. coelicolor* actually functioned as an mechanism facilitating transcription readthrough during antibiotic stress. Lastly, it was found that amino acid starvation can also induce *wblC* expression by suppressing premature transcription termination, implying that ribosome-mediated attenuation of *wblC* responds to diverse translation deficiencies.

Keywords : WblC (WhiB7), antibiotic resistance, regulon, ribosome-mediated transcriptional attenuation, antiterminator, *Streptomyces*

Student Number : 2014-21296

Table of Contents

List of Figures

List of Tables

Chapter 1. Introduction

1-1. Translation-inhibitory antibiotics

Translation, or protein biosynthesis, is one of the fundamental cellular processes, and thus a common target of many antibiotics (Figure 1-1). Translation mainly occurs on ribosome that engages with translation factors and tRNAs in a multi-step procedure of polypeptide synthesis, which can be divided into three phases; initiation, elongation, and termination (Rodnina, 2018). Large and small ribosomal subunits join and form a ribosome (that is 70S in bacteria) at mRNA start codon bound by an initiator tRNA during initiation. Arriving of the aminoacyl-tRNA with an anticodon matching the next codon, peptidyl transfer reaction between peptidyl-tRNA and aminoacyl-tRNA, translocation of tRNAs and exit of free tRNA occurs in the order during each cycle of elongation, which requires the action of elongation factor Tu and elongation factor G. During termination, release factors recognize stop codon at the A-site and hydrolyzes the peptidyl-tRNA to release nascent peptide from the P-site tRNA. Subsequent dissociation of ribosomal subunits from mRNA occurs, which is necessary for recycling of the translation machinery.

Each of the structurally and functionally various translation-inhibitory antibiotic classes targets a specific site and step during translation (Wilson, 2014). The mechanisms of action for many of the translation-inhibitory antibiotic classes – tetracycline antibiotics, macrolides, lincosamides, amphenicols, oxazolidinones, and aminoglycosides, and many others – have been established. Tetracycline and its derivatives bind to the 30S subunit at A-site and prevents aminoacyl-tRNA entry (Brodersen et al., 2000). Macrolides, including erythromycin, bind within and occlude the nascent peptide exit tunnel in the 50S subunit (Kannan and Mankin, 2011; Tu et al., 2005). Lincosamide antibiotics lincomycin and clindamycin, as

well as chloramphenicol (an amphenicol) and linezolid (an oxazolidinone), bind to the 50S subunit within A-site near the peptidyl transfer center and inhibit peptide bond formation (Dunkle et al., 2010; Tu et al., 2005; Wilson et al., 2008). Aminoglycosides such as spectinomcyin, streptomycin, and hygromycin B targets 30S subunit decoding center to prevent either tRNA entry to A-site or translocation during elongation (Brodersen et al., 2000; Carter et al., 2000). The majority of known antibiotics, including all of the antibiotics described above, target and block a step of the elongation cycle (Wilson, 2014).

1-2. Intrinsic antibiotic resistance of bacteria

Antibiotic resistance of bacteria can be either acquired or intrinsic. Acquired resistance arises from a divergence from the normal genetic composition of the bacterium, such as mutations or acquisition of exogenous genetic factors, whereas intrinsic resistance means that the resistance is a phenotype of the indigenous genetic factors. In contrast to acquired resistance that arises mostly due to the selective pressure imposed by human use of antibiotics, intrinsic resistance is a natural phenomenon that predates the human activity (D'Costa et al., 2011).

Because intrinsic antibiotic resistance are the outcomes of a long biological history, there is a great diversity in the mechanisms of resistance (Aminov and Mackie, 2007). Nevertheless, there are several major principles commonly found in antibiotic resistance strategies. A cell envelope impermeable to an antibiotic, enzymatic inactivation of antibiotic, efflux pumping of antibiotic, and antibiotic target site modification or protection are the most frequently observed mechanistic principle of antibiotic resistance (Blair et al., 2015; Cox and Wright, 2013; Peterson and Kaur, 2018). Still, screening of bacterial mutant libraries for increased antibiotic susceptibility often shows that a myriad of uncharacterized genetic factors contribute to intrinsic antibiotic resistance (Fajardo et al., 2008; Xu et al.,

2017). Therefore, the current understanding of intrinsic resistance mechanisms is far from complete, and it is highly possible that there are yet undiscovered mechanisms of antibiotic resistance.

1-3. Intrinsic antibiotic resistance of actinomycetes

Actinomycetes consist an order of actinobacteria, a phylum of gram-positive bacteria with a high genomic guanine-cytosine content. Most of the actinomycetes grow as multicellular filaments that resembles the mycelial morphology of fungi, and form spores as a way of reproduction, while others grow as unicellular organisms. Actinomycetes include both environmental species as well as symbionts and pathogens of animals and plants. The most distinguished genera of actinomycetes are *Streptomyces* and *Mycobacterium*, among many others like *Corynebacterium*, *Propionibacterium*, *Nocardia*, *Micromonospora*, and *Frankia*.

Streptomyces is a large genus of actinomycetes consisting of a great number of species. The genus have been studied in depth, especially using model species like the soil-dwelling *S. coelicolor*. Streptomycetes are abundant in soil as well as in fresh and seawater, and some are symbionts of insects and plants (Chater, 2016). Streptomycetes are widely known for its ability to produce diverse secondary metabolites that can act as bioactive compounds like antibiotics, antifungals, and anti-tumor agents. About three-fourths of all available antibiotics derived from *Streptomyces* (Genilloud, 2017; Kieser et al., 2000). At the same time, Streptomycetes are intrinsically resistant to many antibiotics, thus protecting themselves from their own antibiotics as well as from diverse xenobiotics produced by other bacteria (Cundliffe and Demain, 2010). Most *Streptomyces* retain a rich arsenal of resistance to multiple classes of antibiotics (D'Costa et al., 2006). Some argue that these antibiotic producers are the source origin of antibiotic resistance of pathogens of different phylogenetic clades, although this remains controversial

(Forsberg et al., 2012; Gibson et al., 2015; Jiang et al., 2017).

The genus *Mycobacterium* includes *M. tuberculosis*, one of the deadliest pathogens that causes tuberculosis. The genus also includes several other important human pathogens such as *M. leprae* that causes leprosy and non-tuberculous *M. abscessus* that causes lung, skin, and mucosal infections. Some other mycobacteria are non-pathogenic, like the saprophytic *M. smegmatis*. Antibiotic resistance is one of the major concerns during medical treatment of pathogenic mycobacteria. Development of acquired resistance due to chromosomal mutations as well as intrinsic resistance to many available drugs make tuberculosis one of the most difficult infections to treat (Smith et al., 2013). Mycobacteria are intrinsically resistant to many antibiotics, due to factors such as complex cell envelope that limits antibiotic permeability and retention of numerous antibiotic resistance genes (Nessar et al., 2012; Nguyen and Thompson, 2006). Regarding the regulatory mechanisms of mycobacterial intrinsic resistance, only a few transcriptional regulators are studied in depth that play roles in the antibiotic-dependent activation or derepression of resistance genes. Some of the few examples are LfrR, a TetR-like repressor of efflux pump LfrA (Buroni et al., 2006), and WhiB-like multidrug resistance regulator WhiB7 (Morris et al., 2005).

1-4. WblC/WhiB7, a transcriptional regulator of intrinsic antibiotic resistance

WhiB7, or WblC (WhiB-like protein C) in *Streptomyces*, was discovered in *M. tuberculosis* as a factor conferring multiple drug resistance (Morris et al., 2005). The role of WblC/WhiB7 as an antibiotic resistance factor is widely conserved among actinomycetes like *Mycobacterium*, *Streptomyces*, and others, where mutation of *wblC*/*whiB7* results in increased susceptibility to many classes of antibiotics (Fowler-Goldsworthy et al., 2011; Hurst-Hess et al., 2017; Morris et al.,

2005; Pryjma et al., 2017; Ramon-Garcia et al., 2013). While a wide spectrum of chemicals can induce expression of mycobacterial *whiB7*, most of the strongest inducers are antibiotics targeting translation; tetracyclines, macrolides, amphenicols, etc. (Burian et al., 2012b). Current and previously applied anti-tuberculosis drugs, such as linezolid, amikacin, streptomycin, kanamycin, and capreomycin (World Health Organization, 2019), can activate WhiB7-mediated resistance (Burian et al., 2012b; Hurst-Hess et al., 2017). Several drug-resistant clinical isolates exhibited mutations in the mycobacterial *whiB7* operon, emphasizing the role of WhiB7 in clinical antibiotic resistance of mycobacteria (Chakravorty et al., 2015; Kaur et al., 2016; Koser et al., 2013).

WblC/WhiB7 is a member of WhiB-like protein family of monomeric transcriptional factors conserved within Actinobacteria (Bush, 2018; Chandra and Chater, 2014). WblC/WhiB7 shares the conserved sequence elements of WhiB-like family – four cysteine residues that anchors an iron-sulfur cluster and a conserved glycine-tryptophan-rich motif – and possesses an AT hook motif for A/T-rich DNA sequence binding (Figure 1-2) (Morris et al., 2005; Ramon-Garcia et al., 2013). All of these conserved elements are required for the role of WhiB7 in antibiotic resistance (Ramon-Garcia et al., 2013). The transcription factor is known to bind with domain 4.2 of primary sigma factor SigA (or HrdB in *Streptomyces*) to form a stable WhiB7-SigA complex via WhiB family-specific middle domain that includes glycine/tryptophan-rich motif (Burian et al., 2013). This complex is speculated to recognize the sequence motif of WhiB7 target promoters; -10 and -35 promoter elements and an A/T-rich region 3 bp upstream of the -35 element (Burian et al., 2012b; Burian et al., 2013). In this way, WblC/WhiB7 would recruit the sigma factor to the target promoters and activate transcription. WhiB7 also autoregulates *whiB7* promoter that possesses the WhiB7 promoter sequence motifs (Burian et al., 2012b; Burian et al., 2013). This generates a positive feedback amplifying WhiB7 expression that can explain the drastic surge of *whiB7* mRNA level upon antibiotic stress (Burian and Thompson, 2018).

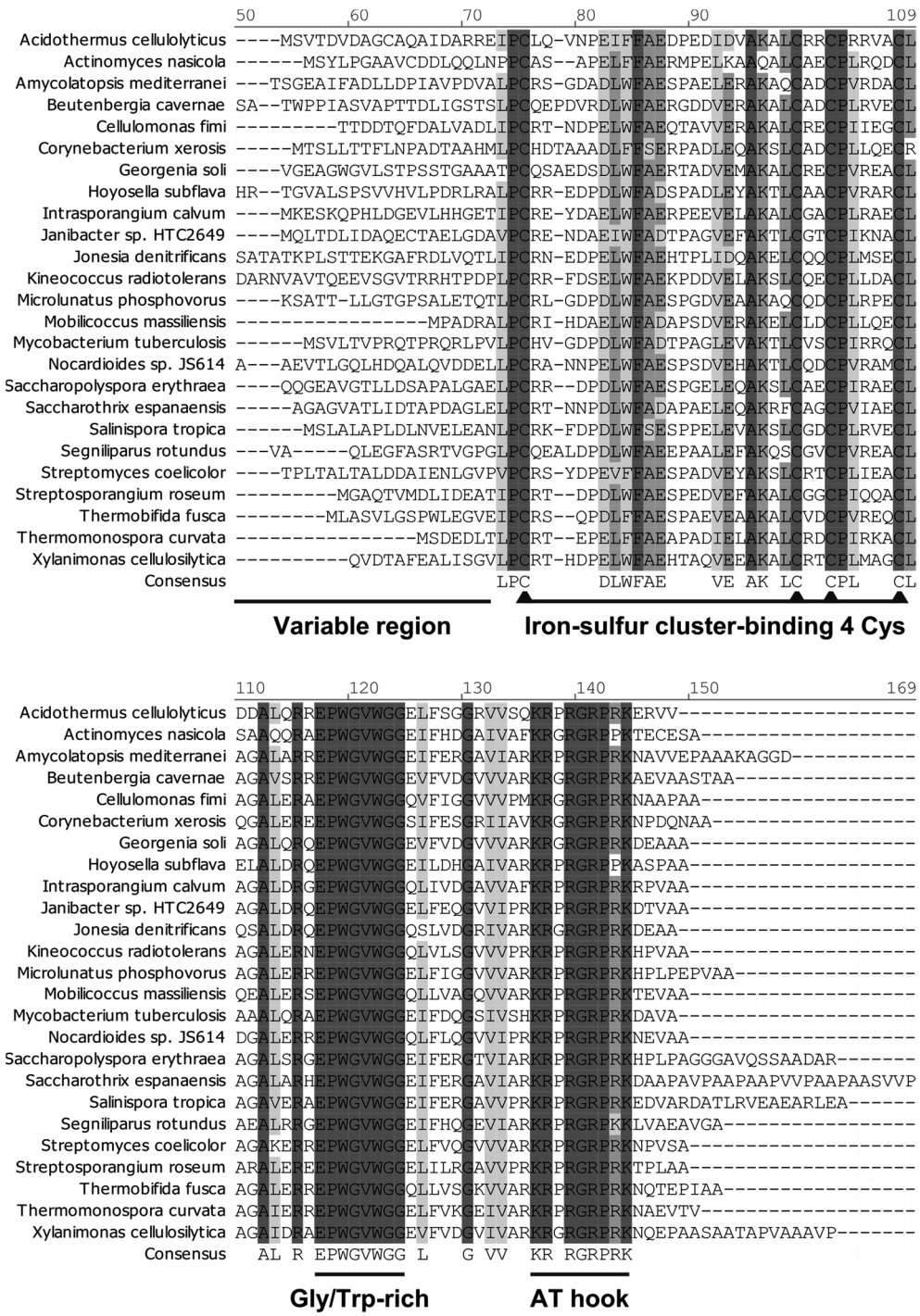

Figure 1-1. Conserved sequence motifs of WblC/WhiB7 orthologs.
Cys, cysteine; Gly, glycine; Trp, tryptophan.

1-5. Antibiotic resistance genes of WblC/WhiB7 regulon

WblC/WhiB7 directs transcription of its regulon – the regulated target genes of WblC/WhiB7 – to confer resistance to a wide spectrum of translation-inhibitory antibiotics. The resistance profile resulting of WblC/WhiB7-mediated gene regulation differs from species to species, indicating that the antibiotic resistance factors of WblC/WhiB7 regulon can vary among species (Ramon-Garcia et al., 2013). This is supported by studies that identified WhiB7 regulons in three different mycobacterial species. WhiB7 regulon of *M. tuberculosis* consists of 12 genes (Morris et al., 2005), while the regulon in *M. abscessus* and *M. smegmatis* consist of 127 and 96 genes, respectively (Hurst-Hess et al., 2017).

The mycobacterial WhiB7 regulons encompass many antibiotic resistance genes of known action mechanisms. *eis* genes are found in WhiB7 regulons of all three species, and the product Eis can acetylate and inactivate aminoglycoside antibiotics to confer kanamycin resistance (Zaunbrecher et al., 2009). MAB_4395 encoding aminoglycoside 2'-N-acetyltransferase and MAB_2989 encoding chloramphenicol acetyltransferase are two other WhiB7 regulon genes encoding antibiotic-inactivating enzymes. *erm* genes are also common to the three species, which encodes a methyltransferase that modifies a residue in 23S rRNA to prevent binding of macrolide-lincosamide-streptogramin B antibiotics to the ribosome (Park et al., 2010). *hflX* is another WhiB7 regulon gene that is common in all three species, which encodes a ribosome-associated GTPase. The heat-induced *Escherichia coli* HflX is capable of GTPase activity-dependent splitting of ribosomes stalled amidst translation due to heat stress (Coatham et al., 2016; Zhang et al., 2015). Additional functions of HflX are ATPase activity-dependent unwinding of rRNA within a heat-stressed ribosome (Dey et al., 2018) and dissociation of hibernating 100S ribosome into 70S ribosomes (Basu and Yap, 2017). HflXr, A firmicute-specific paralog of HflX, contributes to erythromycin and lincomycin resistance presumably by splitting and recycling stalled ribosomes

during antibiotic stress (Duval et al., 2018). It was only recently discovered that mycobacterial HflX can also endow macrolide and lincosamide resistance by a similar activity (Rudra et al., 2020). Some other antibiotic resistance factors of WhiB7 regulons include antibiotic efflux pumps. A major facilitator superfamily (MFS) efflux pump named Tap confers resistance to aminoglycosides and tetracycline (Ainsa et al., 1998), and another MFS protein TetV confers tetracycline resistance (De Rossi et al., 1998). Rv1473 encoding an ABC transporter confers macrolide resistance (Duan et al., 2019). Many other WhiB7 regulon transporters of unknown substrate and function are annotated as probable antibiotic efflux proteins, but needs validation.

The relationship between the remainder of the WhiB7 regulon genes and antibiotic resistance is largely unknown. Moreover, as the antibiotic resistance profile and the composition of WhiB7 regulon differ among species, novel antibiotic resistance mechanisms may be discovered within WblC/WhiB7 regulons of other species. This was exemplified by the discovery of *sigR* as a directly regulated target of WblC in *S. coelicolor* (Yoo et al., 2016). Although SigR and its own regulon had been only known to govern thiol oxidative stress response, the study discovered that SigR and its regulon is responsible for greater resistance to multiple translation-inhibitory antibiotics (Yoo et al., 2016).

1-6. Criteria of defining WblC/WhiB7 regulon

The way of defining WhiB7 regulon in the two previous studies on mycobacterial WhiB7 regulon has some shortcomings that can mislead or limit the understanding of its antibiotic resistance mechanisms. Both studies defined WhiB7 regulon based on transcript level analysis; the genes exhibiting *whiB7*-dependent shifts in transcript level were defined as WhiB7 regulon. Hurst-Hess et al. defined WhiB7 regulon based on the difference between the transcriptomes of *whiB7*

mutant and *whiB7* constitutive expression strain, which does not reflect the context of antibiotic stress-mediated induction. This is exemplified by the fact that the fold induction of *whiB7* was about 2~20-fold between the two strains while *whiB7* is ordinarily induced up to several thousand-fold upon antibiotic treatment (Hurst-Hess et al., 2017). On the other hand, Morris et al. carefully defined WhiB7 regulon after cross-validation of RNA level upregulation through a short time course after various antibiotic treatments as well as constitutive expression of *whiB7*. Yet another problem remains that the transcriptome analysis of *whiB7*-dependent expression cannot discriminate direct WhiB7-mediated regulation, which accompanies WhiB7 binding to promoters, from indirect secondary effects of WhiB7-mediated regulation. Therefore, a precise definition of WblC/WhiB7 regulon should reflect the following criteria; 1) the regulon gene transcripts should be expressed in a *wblC*/*whiB7*-dependent manner and 2) WblC/WhiB7 binding to the promoters of the genes should be identified, 3) within an antibiotic stress condition where a substantial level of *wblC*/*whiB7* induction is observed.

1-7. Regulation of antibiotic resistance by ribosome-mediated attenuation

Attenuation refers to a type of post-transcriptional regulation mechanism that is played by *cis*-acting RNA elements at 5' leader of a transcript. The RNA element acts as a riboregulator that can alternate between different structures/states and thereby conditionally attenuates expression of downstream gene(s) in the transcription unit. Attenuation can be divided into ribosome-mediated, riboswitch-mediated, and RNA-binding protein-mediated attenuation, according to the molecular mechanism by which the alternative structure/state is determined (Merino and Yanofsky, 2005; Turnbough, 2019). Attenuation can also be divided into transcriptional attenuation and translational attenuation, based on the stage at

which downstream gene expression is attenuated (Bedard et al., 2020; Dar and Sorek, 2017; Dersch et al., 2017).

E. coli tryptophan operon (*trp* operon) is a classical model of ribosome-mediated transcriptional attenuation. In the *trp* operon leader sequence, a short upstream ORF (uORF) precedes the attenuator that includes an RIT (or intrinsic terminator) (Yanofsky, 1981). Ribosomes translating the uORF immediately follows RNA polymerase transcribing the RNA, which prevents folding of antiterminator – an alternative RNA structure of RIT – that overlaps with the end of uORF (Turnbough, 2019). This favors formation of leader RIT and transcriptional attenuation of downstream gene(s). However, if the translation of the uORF is uncoupled from transcription, antiterminator can form preemptively before transcription of the distal half stem of the RIT hairpin is complete (Yanofsky, 1981). Therefore, antiterminator formation outcompetes RIT formation and allows transcription of downstream gene(s).

Each attenuator has a specific environmental or physiological cue that allows expression of downstream genes. In case of ribosome-mediated attenuation, shortage of a specific amino acid or nucleotide can couple or uncouple transcription and translation to determine alternative RNA structures/states (Turnbough, 2019). Translation-inhibitory antibiotics can also regulate ribosome-mediated attenuation. Translation-inhibitory antibiotic causes ribosome to stall during uORF translation, which favors expression of the downstream gene either by antiterminator formation or exposure of ribosome-binding site (Figure 1-3). Some antibiotic-responsive attenuators such as those of *ermC* of *Staphylococcus aureus* and *lmo0919* of *Listeria monocytogenes* exhibit high antibiotic specificity, while some others respond to various antibiotics (Dar and Sorek, 2017). Induction of many resistance genes are known to be regulated by ribosome-mediated attenuation upon translation-inhibitory antibiotic stress (Dersch et al., 2017). A recent development and application of term-seq, a high-throughput RNA 3' end-mapping technique, identified novel antibiotic-responsive transcription

antitermination events in leader RNA sequences of various known and putative antibiotic resistance genes (Dar et al., 2016). This implied that antibiotic-responsive regulation by ribosome-mediated transcriptional termination is a widespread regulatory mechanism that controls diverse antibiotic resistance genes.

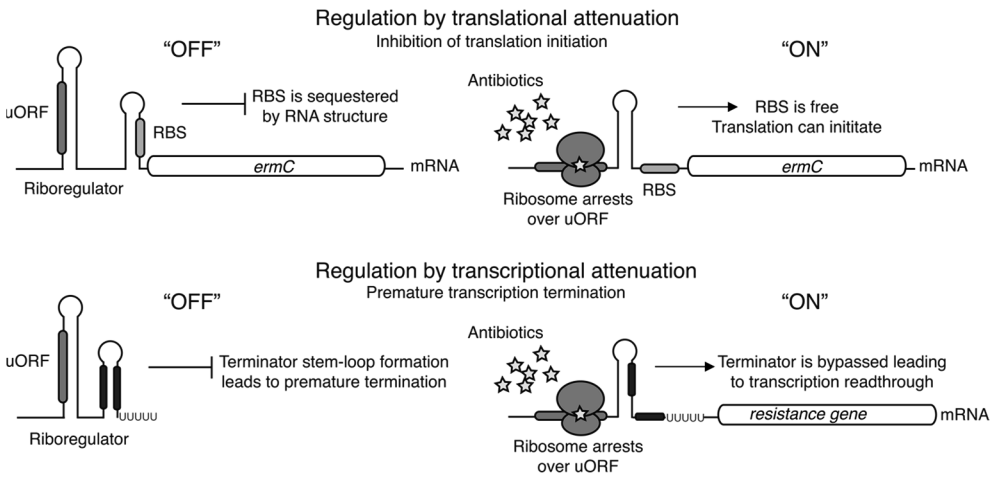

Figure 1-2. Model of antibiotic-responsive ribosome-mediated attenuators (Dar and Sorek, 2017).
RBS, ribosome-binding site; U, uridine.

1-8. Ribosome-mediated transcriptional attenuation of *wblC*/*whiB7*

Ribosome-mediated transcriptional attenuation is thought to be the regulatory mechanism underlying antibiotic-responsive expression of WblC/WhiB7. *wblC* orthologs have a long leader sequences (Burian et al., 2012b). *whiB7* promoters of two mycobacterial species were found to be constitutively active without antibiotic stress, but the transcript level dwindles sharply at the leader sequences, in which uORF and a conserved RIT were predicted (Dinan et al., 2014). The presence of the uORF is conserved among actinomycetes and ribosomal protection of uORF RNA suggests that it is actually translated, but the coding domain sequence is highly variable among species and had no effect on *whiB7* expression *in trans*, implying the importance of uORF translation *in cis* but not of its product (Burian and Thompson, 2018). Treatment of inducer antibiotics increased readthrough of the putative RIT of *M. smegmatis whiB7* leader (Burian and Thompson, 2018). Several studies have identified the increase of *whiB7* expression and/or antibiotic resistance by either insertion/deletions in uORF or base substitutions in the putative RIT of the leader sequence, supporting the hypothesized transcriptional attenuation at *whiB7* leader sequence (Burian and Thompson, 2018; Chakravorty et al., 2015; Kaur et al., 2016; Reeves et al., 2013).

However, the ribosome-mediated transcriptional attenuation hypothesis of *wblC*/*whiB7* requires further substantiation for a complete illustration. Transcriptional termination by the conserved putative leader RIT and translation of uORF have not been directly demonstrated. Most importantly, no explanation is currently available of how the leader RIT can be conditionally antiterminated, and how translation-inhibitory antibiotic stress would facilitate this antitermination. How this hypothesized ribosome-mediated transcriptional attenuation system would sense such a broad spectrum of WblC/WhiB7-inducing antibiotics is also an interesting question that awaits investigation.

Chapter 2. Materials and Methods

2-1. Strains, plasmids, and reagents

All strains used in this study are listed in Table 1. All plasmids and primers used in this study are listed in Table 2 and Table 3, respectively. *S. coelicolor* strains were kept in freezer as spores that were harvested according to standard procedures (Kieser et al., 2000). *E. coli* strain stocks were made from full-grown liquid cultures by adding glycerol to a final concentration of 20% and stored in deep freezer. Antibiotics used in this study are listed in Table 4, along with solvents used for making respective stock solutions. In the case of tetracycline hydrochloride, the solution was either made in ethanol as a stock solution or freshly made in ultrapure water before use.

Table 1. Strains used in this study.

Name	Description	Reference
S. coelicolor		
M145 (wild type)	SCP1- SCP2-	(Kieser et al., 2000)
M145+pSET162 (wild type +vector)	M145::pSET162	(Shin et al., 2011)
Δ*wblC*	M145 *wblC*::*aac(3)IV*	(Fowler-Goldsworthy et al., 2011)
Δ2532	M145 ΔSCO2532	This study
Δ*hrpA*	M145 *hrpA*::*aac(3)IV*	This study
Δ*hflX*	M145 *hflX*::*aac(3)IV*	This study
Δ*arfB*	M145 *arfB*::*aac(3)IV*	This study
Δ*helY*	M145 *helY*::*aac(3)IV*	This study
Δ2532+2532	Δ2532::pSET162-2532	This study
Δ*hrpA*+*hrpA*	Δ*hrpA*::pSET162-*hrpA*	This study
Δ*hflX*+*hflX*	Δ*hflX*::pSET162-*hflX*	This study
ΔuORF*wblC*	M145 (uORF-*wblC*)::*aac(3)IV*	This study
ΔuORF*wblC*+pSET162	ΔuORF*wblC*::pSET162	This study
ΔuORF*wblC*+uC5191	ΔuORF*wblC*::pSET162-uC5191	This study
ΔuORF*wblC*+uC5191(A)	ΔuORF*wblC*::pSET162-uC5191(A)	This study
ΔuORF*wblC*+uC5191(UD)	ΔuORF*wblC*::pSET162-uC5191(UD)	This study
ΔuORF*wblC*+CL-*gusA*	ΔuORF*wblC*::pGUS-CL	This study
ΔuORF*wblC*+CL(U)-*gusA*	ΔuORF*wblC*::pGUS-CL(U)	This study
ΔuORF*wblC*+CL(D)-*gusA*	ΔuORF*wblC*::pGUS-CL(D)	This study
ΔuORF*wblC*+CL(A)-*gusA*	ΔuORF*wblC*::pGUS-CL(A)	This study
ΔuORF*wblC*+CL(UD)-*gusA*	ΔuORF*wblC*::pGUS-CL(UD)	This study
M600	SCP1- SCP2-	(Kieser et al., 2000)
M570	M600 *relA*::*hyg*	(Sun et al., 2001)
E. coli		
DH5α	Strain used for cloning	(Hanahan, 1983)
BW25113/pIJ790	Strain containing λ RED recombination plasmid	(Gust et al., 2003)
ET12567/pUZ8002	Methylation-defective strain containing conjugal donor plasmid	(Paget et al., 1999)

Table 2. Plasmids used in this study.

Name	Description	Reference
pIJ773	Plasmid carrying *aac(3)IV-oriT*(RK2) disruption cassette	(Gust et al., 2003)
PKC1139	*E. coli* shuttle vector with temperature-sensitive pSG5-derived replicon *lacZα ori*(pMB1) *aac(3)IV oriT*(RK2) *rep(pSG5)*	(Bierman et al., 1992)
pSET162	pSET152-derived integrative vector with thiostrepton resistance marker *lacZα ori(pMB1) aac(3)IV oriT*(RK2) *attP-int*(phiC31) *tsr*	(Kim et al., 2006)
pSET162-2532	pSET162 carrying SCO2532	This study
pSET162-*hrpA*	pSET162 carrying *hrpA*	This study
pSET162-*hflX*	pSET162 carrying *hflX*	This study
pSET162-uC5191	pSET162 carrying *wblC* operon (uORF-*wblC*-SCO5191)	This study
pSET162-uC5191(A)	pSET162 carrying 'Anti-switched' *wblC* operon (uORF-*wblC*-SCO5191) variant	This study
pSET162-uC5191(UD)	pSET162 carrying 'Swap-paired' *wblC* operon (uORF-*wblC*-SCO5191) variant	This study
pGUS	Integrative vector pSET152-derived vector carrying promoterless *gusA ori*(pMB1) *aac(3)IV oriT*(RK2) *attP-int*(phiC31) *gusA aadA*	(Myronovskyi et al., 2011)
pGUS-CL	pGUS carrying *wblC* leader transcriptionally fused to *gusA*	This study
pGUS-CL(U)	pGUS carrying 'Up-switched' *wblC* leader variant transcriptionally fused to *gusA*	This study
pGUS-CL(D)	pGUS carrying 'Down-switched' *wblC* leader variant transcriptionally fused to *gusA*	This study
pGUS-CL(A)	pGUS carrying 'Anti-switched' *wblC* leader variant transcriptionally fused to *gusA*	This study
pGUS-CL(UD)	pGUS carrying 'Swap-paired' *wblC* leader variant transcriptionally fused to *gusA*	This study

Table 3. Primers used in this study.

Name	Sequence (5' to 3')*
qPCR	
tuf3-ChIP-F	cattcgacgtgcgacgaagcg
tuf3-ChIP-R	ggtgaagtgggcgacggca
tetM-ChIP-F	catgatggcgccgtccgaac
tetM-ChIP-R	ggaaggggcgctgggggaa
sigR-ChIP-F	acctggactggaccgtgctg
sigR-ChIP-R	tcactcgaatcggaggatagacgacg
cvnA1-ChIP-F	cttctacgtccggtgatccg
cvnA1-ChIP-R	gcacagtgcaggatctccaac
SCO4914-ChIP-F	ggtggtcatgctgccgattg
SCO4914-ChIP-R	gggcatggtcaccagacgag
guaB2-ChIP-F	gggattatcggccacccgtcat
guaB2-ChIP-R	gctgcacatcccagtcgatcag
SCO3064-ChIP-F	tccgcgtctcaagtccttcc
SCO3064-ChIP-R	cgtcgaactgtcgccaaagg
wblE-ChIP-F	gagtctcttcttggcgatcggg
wblE-ChIP-R	gcgtggtcctgtggtttgaaga
citA-ChIP-F	caaacgagtcggaaaggtcacacag
citA-ChIP-R	ctcggggtcgaccatcggg
5UTR-RT-F	aacagcggccttcccgga
5UTR-RT-R	tctcggcgtctcgggggga
Post-RIT-RT-F	tccccgaacgggggcgac
gusA-RT-R	ccgttgctcgactagtgccaat
16S-RT-F	caatgggcgaaagcctgatg
16S-RT-R	caggtaccgtcactttcgct
Mutant strain construction	
SCO2532-up-HindIII-F	gcacAAgcTttgacttcgctcacc
SCO2532-up-BamHI-R	tcatggATcCgcgctctaggcctgc
SCO2532-down-BamHI-F	cagcGGATccatgtcgatcgacgtc
SCO2532-down-EcoRI-R	cgacgaaTTcccggcgatcggga
hrpA-disrupt-F	ccaggtttttcccgaggatgagatcctggaacccgtatgATTCCGG GGATCCGTCGACC
hrpA-disrupt-R	ggccgccggtcgaactcaccctccgtacgggcctcgtcaTGTAGG CTGGAGCTGCTTC
hflX-disrupt-F	gccgcgccgacccttcccagctacgtaaggatccaatgATTCCG GGGATCCGTCGACC
hflX-disrupt-R	ctcggtcggtcggcctgctgttcggccgcgcgggtctcaTGTAGG CTGGAGCTGCTTC
arfB-disrupt-F	atattcgagtgacgcgggccgcccgcggacgggaacatgATTCC GGGGATCCGTCGACC
arfB-disrupt-R	cgtactggagctggactgagacgcgggtccttccggtcaTGTAGG CTGGAGCTGCTTC
helY-disrupt-F	cgcccccacggaacccccacacggccgatcccgataatgATTCC

	GGGGATCCGTCGACC
helY-disrupt-R	actcccgccgggccgggtgaggtgtcggggccggggtcaTGTAG GCTGGAGCTGCTTC
uORFwblC-disrupt-F	actcgtcgagaaaatagtttgcgcatgcccggggaatccATTCCG GGGATCCGTCGACC
uORFwblC-disrupt-R	tacgtcaggggcggtcgatcgttcctgcggtgttcatgTAGGCTG GAGCTGCTTC
Gene complementation	
SCO2532-AseI-F	cgaccatTaATgcatcgcctacc
SCO2532-XbaI-R	tcgtTctAgActacttccccttgg
hrpA-NotI-F	tggagCgGCcgccaccctgtcaag
hrpA-XbaI-R	accctcTAGacgggcctcgtcacg
hflX-NotI-F	tgggGcgGccgcaaccaggacgg
hflX-XbaI-R	gggcTctAgAtcggtcggcctgctg
uORFwblC-XbaI-F	ggcgtctaGAagcggttgcgggag
uORFwblC-NotI-R	ctcaacctgcGgccgCcgtatctcctgatc
Confirmation of genotype and vector insert	
SCO2532-seq-F	accggtcggataaacccctcg
SCO2532-seq-R	tggatgtgcagttgctccatgg
hrpA-seq-F	ctgaaaagcgataggtcgccgg
hrpA-seq-R	gctttttctgcgttgcgctgc
hflX-seq-F	gagaaggccgcggggaagcag
hflX-seq-R	ggtcagtgacccgtacaggc
arfB-seq-F	ctaccaccatgaacgtcgagag
arfB-seq-R	ggacccgagaacttctacctgg
helY-seq-F	acgacgtgacctgaggaccg
helY-seq-R	tgcgcacagagcgcggaagg
attB-seq-F	atgcccgccgtgaccgtcgagaacccgctg
attB-seq-R	gttggtgatggtgccgccgccaccgttgga
attP-seq-R	cccagggcgagcaattccgagaca
lacp-seq-F	ggcagtgagcgcaacgcaattaatg
lacZa-seq-R	aagttgggtaacgccagggttttcc
ori-seq-F	gagtgagctgataccgctcg
uORF-seq-R	cttcctcgtctgttcgttccgg
gusA-seq-F	ctcaatcaatcaccggatcc
gusA-seq-R	ttcttgatctcgcgggtcgg
***wblC* leader sequence variation**	
Up-switch-F	cgccttcaCCCGGCcggaaccccacc
Down-switch-F	gggatccgGCCGGGttctgtttgtccc
Anti-switch-F	ccgACCgccagaaGGGtggagtgatc
S1 nuclease mapping probe preparation	
CL-3end-S1-F	taccgcgaccggtgccggattc
CL-3end-S1-R	tacggacggggcgtgcgcttc
pGEMT-T7p-80bp	tgtaatacgactcactatagggcg

wblC-S1-F	cgtcgagaaaatagtttgcgcatgc
wblC-S1-R	ccttggtcggtcgctcattgc
sigR-S1-F	agctgatcaccgacggcgtgg
sigR-S1-R	tgcgtcggtcccagtgaccg
hflX-S1-F	gagaaggccgcggggaagcag
hflX-S1-R	cgcttggtgtcctgggagggg

* Sequences that correspond to variations from genomic DNA or vector sequences are denoted in capital letters.

Table 4. Antibiotics used in this study.

Antibiotic	Vendor	Solvent	Note
Erythromycin	Sigma	EtOH	-
Tetracycline hydrochloride	Sigma	H_2O or EtOH	Light-sensitive, hydrolysis in H_2O
Lincomycin hydrochloride	Fluka	H_2O	-
Thiostrepton from *Streptomyces azureus*	Sigma	DMSO	-
Spectinomycin dihydrochloride pentahydrate	Fluka	H_2O	-
Chloramphenicol	Sigma	EtOH	-
Hygromycin B, concentrated solution	Duchefa	H_2O	-
Streptomycin sulfate salt	Sigma	H_2O	-
Linezolid	Sigma	DMSO	-
Fusidic acid sodium salt	Sigma	H_2O	Light-sensitive
Puromycin dihydrochloride from *Streptomyces alboniger*	Sigma	H2O	-
Apramycin sulfate	Sigma	H2O	-

2-2. Culture conditions

E. coli strains were grown and manipulated according to standard procedures (Green and Sambrook, 2012; Gust et al., 2003). Yeast extract-malt extract liquid medium with 10% sucrose (YEME), minimal liquid medium (NMMP), soya flour mannitol (SFM) agar, and nutrient broth (NB) agar were used as *S. coelicolor* culture media (Kieser et al., 2000). Unless described otherwise, liquid cultures of *S. coelicolor* were performed by inoculation of spores into baffled flasks of YEME and incubation at 30℃ with shaking of 180 rpm for sufficient aeration. In general, antibiotics were treated to liquid cultures of *S. coelicolor* when they reached early-to-mid exponential phase (OD_{600} of 0.1~0.5) at given concentrations and time. For changing culture medium in the middle of growth, cells were pelleted by centrifugation, washed with phosphate-buffered saline, and resuspended in a different media. SFM agar was used for spore collection (Kieser et al., 2000), and NB agar was used for colony-forming unit count measurements and antibiotic selection of genetically manipulated strains.

2-3. RNA sequencing (RNA-seq)

Total RNA was prepared from harvested cells by Dr. Ji-Sun Yoo using sodium dodecyl sulfate and hot phenol RNA extraction method (Kieser et al., 2000). DNA contaminants were removed from prepared RNAs by DNase I treatment, and rRNA was removed using Ribo-Zero rRNA Removal Kit (Epicentre). Sequencing library was constructed using TruSeq Stranded total RNA sample prep kit (Illumina) and sequenced using Illumina HiSeq 4000, with the settings of 101 bp paired-end reading. After quality check using FastQC v0.11.4 (www.bioinformatics.babraham.ac.uk/projects/fastqc) and adapter sequence trimming using Trimmomatic v0.36 (Bolger et al., 2014), the reads were mapped to *S. coelicolor* A3(2) genome

(NC_003888.3) using Bowtie v2.3.2 (Langmead and Salzberg, 2012). Reads mapped to specific genomic features were counted using featureCounts of the Subread package v1.5.3 (Liao et al., 2014), then normalized and analyzed for differential expression between the samples using DESeq2 package of Bioconductor v3.5 (Love et al., 2014). Principal component analysis of the samples was performed using ClustVis (Metsalu and Vilo, 2015).

2-4. Chromatin immunoprecipitation-sequencing (ChIP-seq)

Chromatin immunoprecipitation (ChIP) of WblC-crosslinked DNA was performed by Dr. Ji-Sun Yoo as described previously (Yoo et al., 2016), which includes parallel no-immunoprecipitation (no-IP) control DNA preparation. Biologically independent triplicates of immunoprecipitated DNA and no-IP control DNA were pooled respectively. Sequencing libraries were prepared using KAPA DNA library preparation kit (Roche) and sequenced using Illumina HiSeq 4000, with the settings of 101 bp paired-end reading. Quality check, adapter trimming, and read mapping were performed as same as for the RNA-seq analysis procedure. Duplicated reads were removed using MarkDuplicates of Picard v1.133 (broadinstitute.github.io/picard). Peaks of genomic regions enriched in ChIP samples were identified using MACS v2.1.1 (Zhang et al., 2008), in which no-IP control was used as reference.

2-5. *In silico* sequence analyses

Conserved sequence motifs were discovered from a set of WblC-upregulated regulon promoter sequences using MEME of MEME-suite (Bailey et al., 2009). The location of transcription start sites (TSSs) were approximated as the 5’ ends of

differentially expressed RNAs in the RNA-seq data. Conserved motifs were searched in a strand-specific manner using a 4-order Markov model of *S. coelicolor* A3(2) genome (NC_003888.3). Search for WblC-binding site plus -35 element was performed with sequences from -65 bp to -25 bp relative to the approximate TSSs. Search for -10 element was performed with sequences from -35 bp to -5 bp relative to the approximate TSSs. The discovered motif-matching sites were cross-checked by testing if one of the sites was recursively discovered to match with the motif around a given distance from the other site, which distance restricts the spacing between -35 element and -10 element to be 16~19 bp. Also, only the sites that significantly matched (p-value<0.05) with the motif that was elicited after filtering promoters with all the other criteria were deemed legitimate. Sequence logos of the promoters with legitimate motif matches were made using WebLogo v2.8.2 (Crooks et al., 2004).

Orthologs of *wblC*/*whiB7* genes were identified using TBLASTN from actinomycetes genomes in NCBI Genome database (www.ncbi.nlm.nih.gov/genome). Sequence motifs of ribosome-mediated transcriptional attenuation was elicited from upstream sequences of *wblC*/*whiB7* orthologs in a strand-specific manner using MEME of MEME-suite (Bailey et al., 2009). Sequence logos of the discovered motifs were made using WebLogo v3.7.4 (Crooks et al., 2004).

All sequence alignments were performed using Clustal Omega (Sievers and Higgins, 2018). Prediction of RNA structures were performed using Mfold web server (Zuker, 2003).

2-6. Chromatin immunoprecipitation-quantitative PCR (ChIP-qPCR)

ChIP was performed as described above for ChIP-seq, but with some modifications described below. IP buffer (50 mM Tris-Cl [pH 8.0], 200 mM NaCl,

1 mM EDTA [pH 8.0], 1% Triton X-100, 1 mM phenylmethylsulfonyl fluoride) was used as a substitution for RIPA buffer (50 mM HEPES-K [pH 7.5], 150 mM NaCl, 1 mM EDTA [pH 8.0], 1% Triton X-100, 0.1% sodium deoxycholate, 0.1% sodium dodecyl sulfate, 1 mM phenylmethylsulfonyl fluoride). The Protein A/G PLUS-Agarose beads (Santa Cruz) were blocked with bovine serum albumin fraction V by pre-incubation in IP buffer at 4℃ for 1 hr before being added to lysates, instead of preclearing the lysates with Protein A/G beads. ChIP of WblC- and HrdB-crosslinked DNA was performed using anti-WblC and anti-HrdB polyclonal antibodies (Kim et al., 2020; Yoo et al., 2016), respectively. The degree of enrichment by ChIP compared to no-IP control was analyzed by quantitative PCR (qPCR) using TOPreal qPCR 2x Premix (Enzynomics) and QuantStudio3 Real-Time PCR System (Thermo).

2-7. *In silico* Analyses of gene-protein functions

Functional annotations of *S. coelicolor* chromosomal genes and the encoded proteins were collected from PANTHER Classification System v14.1 (Mi et al., 2019), which used the Gene Ontology release of Feb 2nd, 2019 (The Gene Ontology Consortium, 2019), and InterPro v73.0 (Mitchell et al., 2019). Additionally, the genes were annotated according to EggNOG v4.5.1 (Huerta-Cepas et al., 2016) using EggNOG mapper (Huerta-Cepas et al., 2017). Enrichment, or overrepresentation, of any of the obtained functional annotations within a group of genes compared to the *S. coelicolor* genome was assessed using Fisher's exact test. Genes were hierarchically clustered on the basis of Gene Ontology term and InterPro entry annotations using ClustVis (Metsalu and Vilo, 2015) and were categorized according to the result.

Phylogenetic analyses of SCO2532 and SCO4278 (ArfB) proteins were performed using MEGA7 by Neighbor-joining method (Kumar et al., 2016), from

aligned protein sequences. Synteny of SCO5707 was analyzed using SyntTax (Oberto, 2013).

2-8. *In vivo* ^{35}S-methionine/cysteine incorporation assay

500 μl of cells in culture media with normalized OD_{600} of 0.2 were prepared by adding liquid media to cultures at OD_{600}≈0.4. 1 μCi of EasyTag EXPRESS 35S Protein Labelling Mix (PerkinElmer) was added and the cells were incubated at 30℃ for 10 min with shaking for incorporation of radioisotopic amino acids. 0.5 mg of methionine was added and the incubation was continued for 5 min. Cells were harvested, washed twice with phosphate-buffered saline, and dot-blotted on Whatman filter paper. Phosphor imaging plate was exposed overnight to the filter paper and imaged using BAS-2500 (Fujifilm). Radioactivity of the blots were quantified from radiographs using MultiGauge v3.0 (Fujifilm), and differences in radioactivity between strains were assessed using two-tailed Student's *t*-test.

2-9. Ribosome isolation

Cells were harvested, washed with ice-cold wash buffer (20 mM Tris-Cl [pH 7.4], 100 mM NaCl, 10 mM $MgCl_2$), and resuspended in ice-cold lysis buffer (20 mM Tris-Cl [pH 7.4], 200 mM NH_4Cl, 10 mM $MgCl_2$, 0.5 mM EDTA, 6 mM β-mercaptoethanol) supplemented with 5 U/ml RNase Inhibitor (Applied Biosystems) and 1 mM phenylmethylsulfonyl fluoride. Lysis was performed using Q500 Sonicator (Qsonica) equipped with 3.2 mm micro-tip by 5 times of 1-sec pulses at 20% maximum amplitude. Lysates were treated with 5 U/ml TURBO DNase (Ambion) at 4℃ for 15 min and centrifuged (22,000 x g) twice at 4℃ for 10 min to remove cell debris. Pellets of crude ribosomes were obtained by ultracentrifugation

(100,000 x g) at 4℃ for 1 hr, rinsed with ice-cold lysis buffer by gentle swirling, and resuspended in ice-cold lysis buffer supplemented with 10 U/ml RNase Inhibitor (Applied Biosystems). Crude ribosomes were isolated by ultracentrifugation (150,000 x g) at 4℃ for 2.5 hr after loading onto 5~30% sucrose gradient of lysis buffer. The gradient was fractionated, and ribosomal fractions were identified by measuring absorbance of the fractions at 254 nm and collected.

rRNA was isolated from a small portion of the isolated ribosomes by phenol-chloroform extraction and precipitation with isopropanol and glycogen. The integrity of isolated ribosomes were checked by agarose-formaldehyde gel electrophoresis of the rRNA.

2-10. Liquid chromatography-tandem mass spectrometry

Isolated ribosomes were subjected to mass-spectrometric proteome analysis, which was performed by Dr. Jong-Seo Kim and Mr. Jeesoo Kim of Center for RNA Research, Institute of Basic Sciences (IBS). Samples were denatured with 8 M urea and reduced with 10 mM dithiothreitol. Cysteine thiol groups were alkylated with 40 mM iodoacetamide in darkness. After dilution to a urea concentration of 1 M, samples were trypsinized overnight at 37℃. Tryptic peptides were cleaned up with C18-SPE column (Supelco), dried using a vacuum concentrator, and resuspended in 25 mM ammonium bicarbonate buffer. After peptide quantification by bicinchonic acid assay, 2 μg of peptides were analyzed by liquid chromatography-tandem mass spectrometry. The liquid chromatographic system used was nanoACQUITY UPLC (Waters) equipped with in-house-packed 3 cm-long capillary trapping column of 150 μm inner diameter and 100 cm-long analytical column of 75 μm inner diameter with 3 μm Jupiter C18 particles (Phenomenex). The system was operated at 300 nl/min flow rate, and a 100 min-long linear

gradient was applied for each biological replicate. The liquid chromatographic system was coupled to Q-Exactive Hybrid Quadrupole-Orbitrap Mass Spectrometer (Thermo) operated with a fragmentation mode of higher-energy collisional dissociation (HCD). Acquired data were analyzed using MaxQuant v1.5.3.30 equipped with the peptide search engine Andromeda and the statistical analysis platform Perseus (Tyanova et al., 2016). Precursor ion mass tolerance was set to 10 ppm, and peptide search was performed against Swiss-Prot *S. coelicolor* database at false discovery rate<0.01. Label-free quantification was applied for quantitative analysis, and protein quantity differences between conditions were assessed by two-tailed Student's *t*-test.

2-11. Construction of mutant strains

Genes of interest (*hflX*, *hrpA*, *arfB*, *helY*, and uORF-*wblC*) were respectively knocked out from *S. coelicolor* wild-type strain (M145) by PCR-targeted mutagenesis (Gust et al., 2003), using *aac(3)IV*-containing apramycin resistance cassette of pIJ773, and confirmed by PCR. In the case of constructing ΔuORF*wblC*, genomic DNA region spanning -10 element of *wblC* promoter, uORF, and *wblC* (-629~+364 relative to the start codon of *wblC*) was knocked out by the cassette.

SCO2532 was deleted from *S. coelicolor* wild-type strain by homologous recombination-mediated replacement with a SCO2532-deleted allele. Flanking sequences of target gene was amplified by PCR and inserted side by side, to form a gene-deleted allele, into temperature-sensitive suicide vector pKC1139 (Bierman et al., 1992). After confirming the inserts by sequencing, the recombined vector was conjugated into wild-type strain from non-methylating *E. coli* donor strain ET12567/pUZ8002. Single-crossover exconjugants resistant to 50 μg/ml apramycin were selected at 37℃, confirmed by PCR, and subcultured for double crossover event. Double-crossover deletion mutant sensitive to 50 μg/ml apramycin

were selected and confirmed by PCR.

2-12. Introduction of genes via integrative vectors

Complementation of mutant strains (Δ*hflX*, Δ*hrpA*, Δ2532, and ΔuORF*wblC*) with respective knocked-out or deleted genes was carried out using integrative vector pSET162 (Kim et al., 2006). Each gene with the promoter region was PCR-amplified and cloned into pSET162. In the case of ΔuORF*wblC*, the strain was complemented with full-length *wblC* operon. The vectors were conjugated into respective mutant strains from ET12567/pUZ8002 after confirming the inserted sequences. Vector-integrated exconjugants resistant to 10 μg/ml thiostrepton were selected, and the integrated vector was confirmed by PCR.

For introducing *wblC* operons with leader sequence variations into ΔuORF*wblC*, upstream half of the *wblC* operon that spans an indigenous KpnI site between leader RIT and the start codon of *wblC* was amplified by megaprimer PCR. Megaprimers were prepared by PCR to retain sequence variations, using primer uORF-seq-R and each of the mutagenesis primers, and isolated by gel extraction after agarose gel electrophoresis. Inserts were PCR-amplified from pSET162 carrying *wblC* operon using each of the megaprimers in combination with primer lacZa-seq-R. The inserts were respectively cloned into pSET162 carrying *wblC* operon. In this way, the previously cloned wild-type leader sequence upstream of the indigenous KpnI site was replaced with respective leader sequences with sequence variations. Insert sequence confirmation, vector conjugation, selection, and PCR confirmation were performed as described above for gene complementation using pSET162.

Introduction of *wblC* leader-*gusA* reporter transcriptional fusion into ΔuORF*wblC* was carried out using pGUS, an integrative vector carrying *gusA* (Myronovskyi et al., 2011). The upstream half of the *wblC* operon was excised

from pSET162 carrying *wblC* operon with XbaI and KpnI and cloned into pGUS. *wblC* leader sequence variations were generated by megaprimer PCR as described above and respectively inserted into pGUS. Insert sequence confirmation, vector conjugation, and PCR confirmation were performed as described above, whereas selection of the vector-integrated exconjugants was done with 200 μg/ml spectinomycin.

2-13. Minimum inhibitory concentration (MIC) test

MICs of antibiotics were determined by resazurin assay of cell viability. 150 μl aliquots of YEME inoculated with 10^6 colony-forming unit/ml spores was made on 96-well plates and serially treated with 2-fold different concentrations of antibiotics. After 21 hr culture, 15 μl of 0.03% resazurin (Fluka) was added into each well. After additional 1 hr incubation at culture condition, cell viability in each well was determined by colorimetric assay of resazurin reduction into resofurin. The ratio of absorbance by resofurin at 570 nm to absorbance by resazurin at 600 nm, was measured as an indicator of viability. >1.2-fold increase in the ratio compared to no-growth control was regarded as a signal of growth, and the lowest concentration that inhibited increase in the ratio was determined as MIC.

2-14. S1 nuclease protection assay

Harvested cells added with modified Kirby's mixture (Kieser et al., 2000) were lysed using Q500 Sonicator (Qsonica) equipped with 3.2 mm micro-tip by 5 times of 1-sec pulses at 20% maximum amplitude. Total RNA was extracted with phenol-chloroform, precipitated with isopropanol, resuspended in ultrapure water and dissolved by heating at 65℃, and quantified by measuring absorbance at 260

nm.

50 μg of the total RNA was dried using a vacuum concentrator and resuspended in 20 μl of S1 hybridization solution (40 mM PIPES-Na [pH 6.4], 400 mM NaCl, 1 mM EDTA [pH 8.0], 80% formamide) supplemented with probe DNA. The mixture was incubated at 95℃ for 10 min for denaturation and slowly cooled overnight to 50℃ for probe-RNA annealing. 300 μl of S1 nuclease buffer (40 mM NaOAc [pH 4.5], 300 mM NaCl, 2 mM $ZnSO_4$) supplemented with 60 U of S1 nuclease (Thermo) was added and incubated at 37℃ for 40 min. The reaction was quenched by adding 80 μl of S1 termination solution (2.5 M NH_4OAc, 50 mM EDTA [pH 8.0]). S1 nuclease-digested probe-RNA hybrids were precipitated with isopropanol and resolved by urea-acrylamide gel electrophoresis. The gel was dried onto Whatman filter paper using a vacuum-heated slab gel dryer, and a phosphor imaging plate was exposed to the filter paper. Phosphor imaging was performed as described above for *in vivo* ^{35}S-methionine/cysteine incorporation assay. Total RNA was analyzed by agarose-formaldehyde gel electrophoresis in parallel to check RNA integrity and to visualize rRNAs as internal control of RNA quantity.

2-15. Probe preparation for S1 nuclease protection assay

For preparing the probe DNA for 3' end mapping of *wblC* leader RNA, genomic DNA region spanning the putative RIT of *wblC* leader (-270~+30 relative to the start codon of *wblC*) was PCR-amplified and cloned into pGEM-T Easy Vector (Promega). S1 nuclease probe with a 80-bp vector body sequence was PCR-amplified from the recombined vector. The probe DNA was radiolabeled with T4 DNA polymerase and [α-^{32}P]-dATP (PerkinElmer) following standard procedure of labeling 3' termini of double-stranded DNA (Green and Sambrook, 2012).

For preparing probe DNAs for 5' end protection assay, genomic DNA regions spanning the target TSSs were PCR-amplified. Probe DNA was radiolabeled with

T4 polynucleotide kinase and [γ-^{32}P]- ATP (PerkinElmer) following standard procedure of labeling the 5' termini of DNA in forward reaction (Green and Sambrook, 2012).

2-16. Quantitative reverse transcription-PCR (qRT-PCR)

Total RNA was prepared from harvested cells as described above for S1 nuclease mapping. 5 μg of the total RNA was treated with TURBO DNase (Ambion) to remove DNA contamination, extracted with phenol-chloroform, and precipitated with isopropanol and glycogen. The RNA dissolved in ultrapure water was quantified from absorbance at 260 nm, annealed with random hexamer by incubation at 65℃ for 5 min and chilling on ice. cDNA was synthesized using RevertAid Reverse Transcriptase (Thermo) in a thermocycler that was programmed as follows; 10 min at 25℃, 1 hr at 45℃, and 10 min at 70℃. 1/20-diluted cDNA was analyzed by qPCR as described above for ChIP-qPCR. Quantity of each RNA species was calculated by ΔΔCt method, where the quantity of 16S rRNA was adopted as control in the process of normalization.

Chapter 3. WblC-regulated targets in *S. coelicolor*

3-1. Direct target genes controlled by WblC

In order to define WblC regulon in *S. coelicolor*, I utilized RNA-seq-derived transcriptome data and ChIP-seq-derived genome-wide WblC binding data, all of which were performed and analyzed by Dr. Ji-Sun Yoo. The comparative transcriptome analysis of duplicates of wild type (strain M145) and Δ*wblC*, all of which were treated with 2 μg/ml tetracycline for 30 min, had elicited 614 genes of which RNA level were significantly different (BH-adjusted *p*-value<0.01) by >2-fold between the strains (Figure 3-1). Analysis of ChIP-seq data obtained from wild type treated with 2 μg/ml tetracycline for 1 hr had identified 830 WblC-binding peaks with >2-fold enrichment (Figure 3-1). I checked promoter regions (-500 ~ +200 bp from start codon) of the 614 differentially expressed genes identified from the tetracycline-treated transcriptomes to see if they contain WblC-binding peaks. I manually curated each WblC-binding peak within these regions to filter out peaks that are not linked to the differentially expressed transcript but to another transcript. As a result, 206 promoters were identified as direct target promoters regulated by WblC, and 312 differentially expressed genes that are transcribed from these promoters were defined as WblC regulon (Figure 3-1). This number of genes consists 4% of all chromosomal genes of *S. coelicolor*. WblC-binding peak summits of 153 (74%) out of the 206 WblC target promoters were located within -100 ~ +50 bp from the start codon of the first gene in the transcription unit (Figure 3-2).

The WblC regulon, comprising of 312 genes, makes up 4.0% of the 7,853 chromosomal genes of *S. coelicolor*, which demonstrates that WblC is a global regulator of transcription under antibiotic stress. 288 genes (92%) of the 312 WblC regulon genes showed greater expression in wild type, indicating that WblC

activated transcription of most of its target genes (Figure 3-1 and 3-3A). However, the other 24 target genes showed less expression in wild type than in Δ*wblC*, implying that WblC could also function as a transcriptional repressor on some of its targets (Figure 3-1 and 3-3B). In this document, I term the 288 genes as WblC-upregulated regulon and the 24 genes as WblC-downregulated regulon.

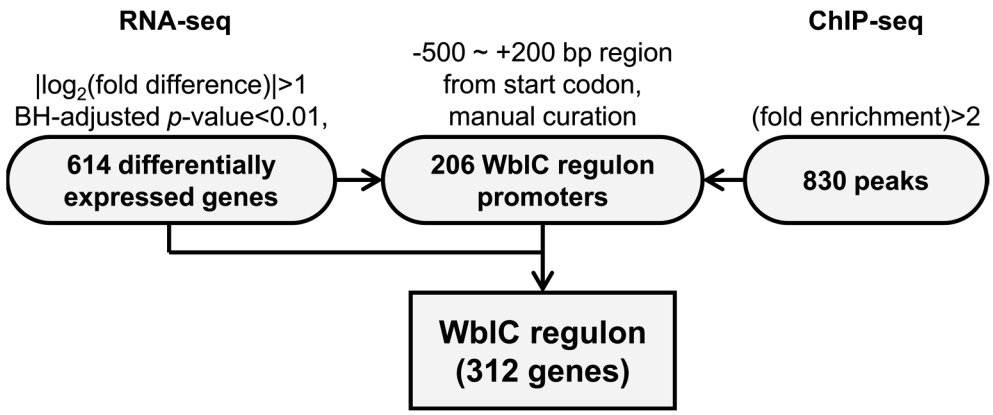

Figure 3-1. Methods and criteria of defining WblC regulon.

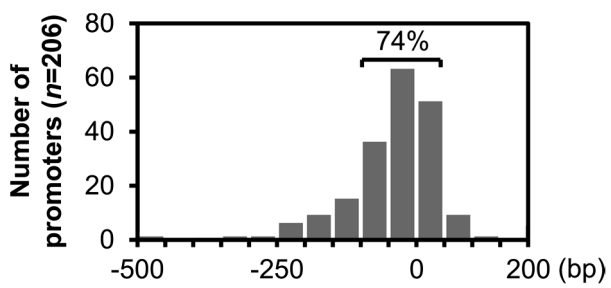

Figure 3-2. Locations of WblC-binding peak summits relative to each start codon of first gene in a transcription unit.

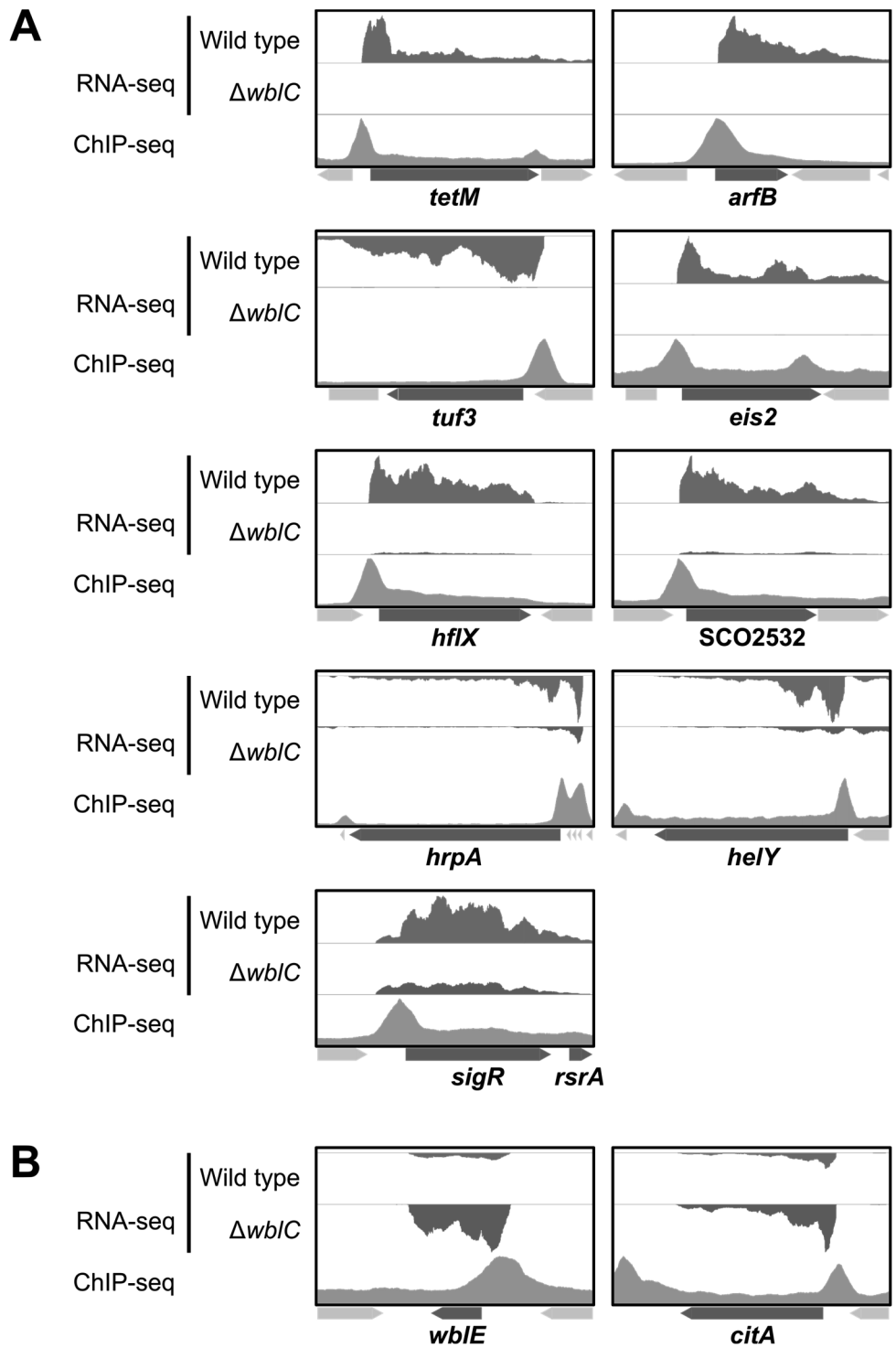

Figure 3-3. Selected examples of WblC-upregulated (A) and WblC-downregulated (B) regulon genes.
WblC regulon genes are labeled and indicated by dark gray arrows. Note that *y*-axis scales are variable among the plots.

3-2. Promoter sequence motif of WblC-upregulated regulon

I examined sequences of the identified WblC regulon promoters in order to discover the conserved sequence motifs similar to that of mycobacterial WhiB7-regulated promoters (Burian et al., 2012b). The search within WblC regulon promoters activated by WblC revealed a conserved sequence motif that is commonly found in 183 (97%) out of 189 promoters. As in mycobacteria, the sequence motif comprises of the two promoter elements (-10 and -35 elements) as well as an A/T-rich WblC-binding motif lying 3 bp upstream of the -35 element (Figure 3-4). I referred to the mapped TSSs in *S. coelicolor*, determined by Jeong et al. (2016), to validate the identified promoter elements. Most TSSs of the WblC-activated promoters were located at legitimate distances of 7~8 bp downstream from the last nucleotides of the identified -10 elements (Figure 3-5). The -10 element consensus is nearly identical to the genome-wide consensus deduced from the TSS data (Jeong et al., 2016). However, the -35 element of the WblC regulon is quite dissimilar from, and less conserved than, the genome-wide consensus (Jeong et al., 2016). Considering that WhiB7 forms and presumably binds to target promoters as a complex with SigA (HrdB) (Burian et al., 2012b; Burian et al., 2013), this low conservation of -35 elements in WblC-activated promoters is consistent with the observation that HrdB-binding promoters have less pronounced -35 element motif (Smidova et al., 2019). For motif elicitation in WblC-activated promoters, I had set the distance between the two promoter elements to be 16~19 bp, which is the optimal and ordinary promoter spacer length in actinomycetes (Agarwal and Tyagi, 2006; Jeong et al., 2016). 84% of the promoters with identified motifs had 17~18 bp spacer (Figure 3-6), implying that the optimal spacer length for WblC-mediated transcription activation is 17~18 bp.

I also discovered that the fold upregulation by WblC correlated with promoter sequence conservation. 20% of the promoters with the greatest WblC-dependent fold upregulation of the first gene in each transcription unit, estimated from RNA-

seq, exhibited stronger conservation of the A/T-rich WblC-binding motif than the 20% of the promoters with the smallest fold upregulation (Figure 3-7A). The more greatly activated promoters also tended to have adenine but not thymine at the 4th positions of WblC-binding motif (Figure 3-7A). WblC-dependent fold increase of RNA level also correlated with biased base usage in several positions of the promoter elements. Specifically, usage of guanine and cytosine at 3rd and 4th positions of -35 element, respectively, and weaker propensity for thymine at 1st position of -10 element correlated with greater fold activation. The WblC-binding motif conservation also affected the degree of WblC binding. 20% of the promoters with the greatest fold enrichment by WblC ChIP exhibited a stronger conservation of the motif and the tendency of having adenine but not thymine at the 4th position (Figure 3-7B), as in the promoters with the greatest WblC-dependent fold increase of RNA level. However, bias of base usage in the promoter elements was less pronounced (Figure 3-7B). This suggests that greater conservation of WblC-binding motif facilitates both WblC binding and subsequent transcription upregulation while the promoter elements affect the degree of transcription activation but is largely irrelevant of the strength of WblC-promoter binding.

I also tried to find any conserved sequence motif in WblC regulon promoters repressed by WblC, but discovered no sequence conservation.

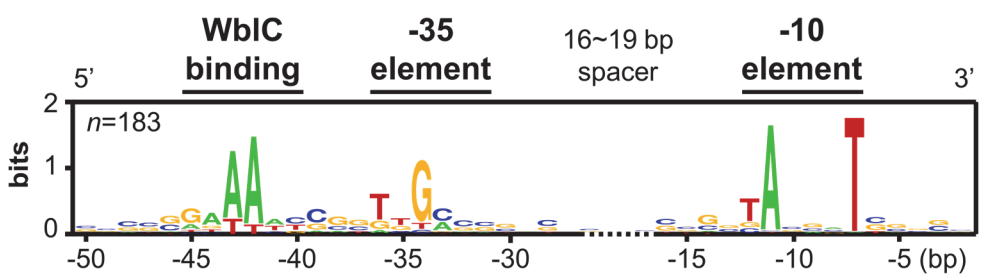

Figure 3-4. The conserved sequence motif of WblC regulon promoters activated by WblC.
n, total number of promoters with conserved sequence motif.

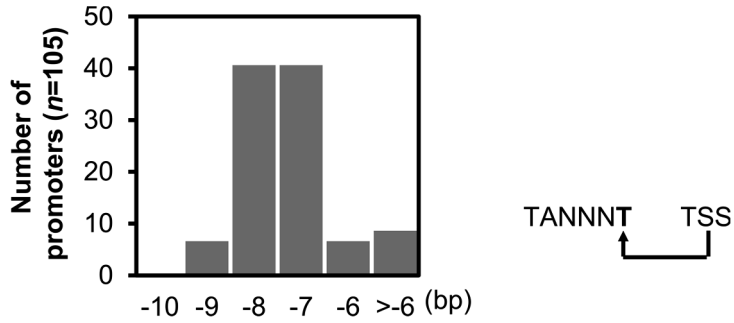

Figure 3-5. Locations of the last nucleotide of -10 elements relative to each TSS. Pairs of -10 element and TSS with ≤50 bp interval length were analyzed. *n*, total number of analyzed promoters; T, thymine; A, adenine, N, any base.

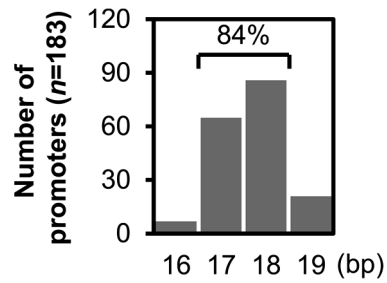

Figure 3-6. Distributions of spacer length between the promoter elements of WblC-activated promoter.
n, total number of analyzed promoters.

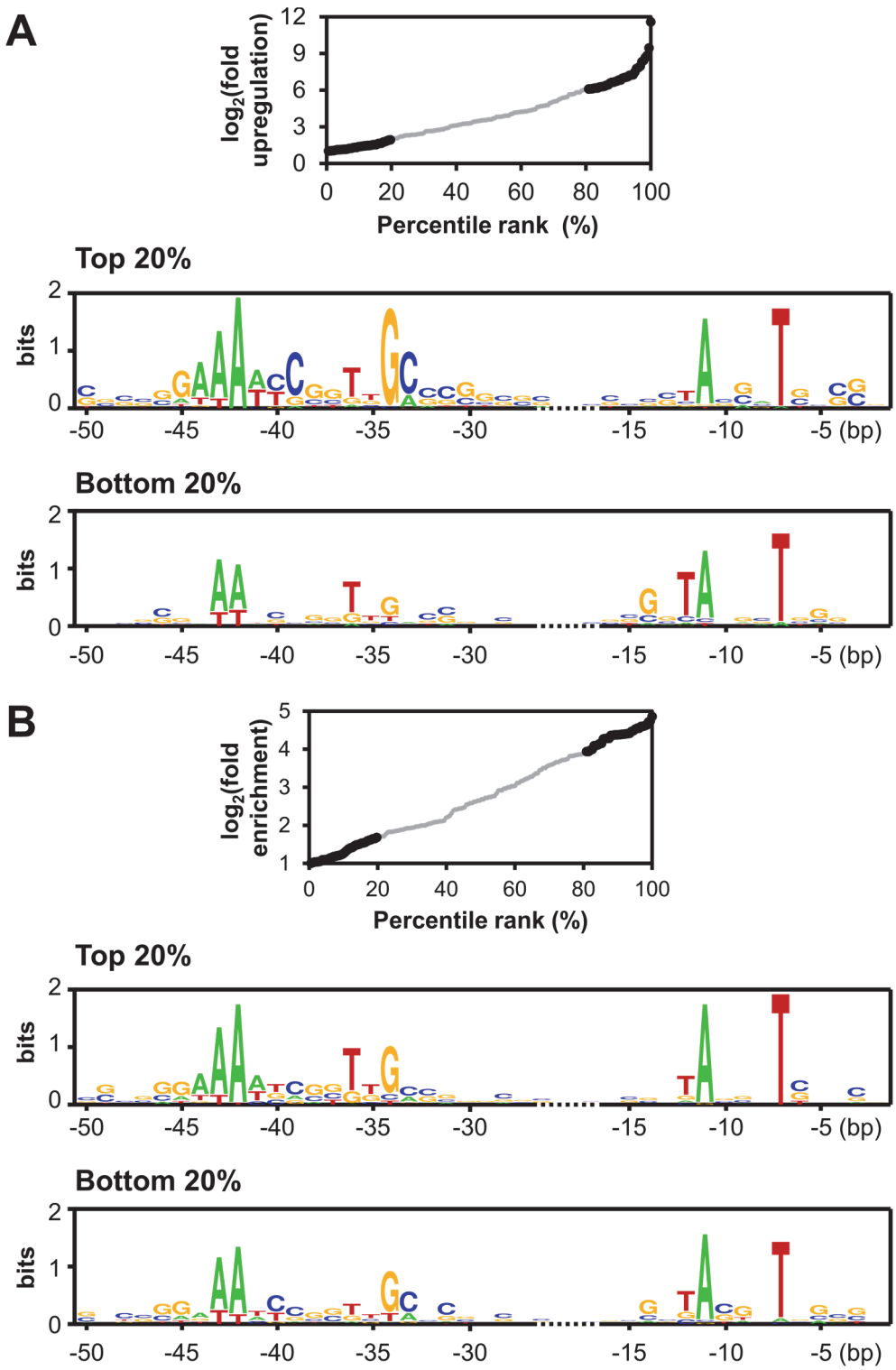

Figure 3-7. Relationship of the WblC-activated promoter sequence motif with fold upregulation by WblC (A) and the degree of WblC binding (B), respectively.

3-3. Different modes of WblC binding to activated and repressed regulon promoters

The co-occurrence of WhiB7-binding motif and the promoter elements in the target promoters have been thought to enable cooperative binding of the sigma factor SigA to the promoters along with WhiB7 and the subsequent transcription upregulation (Burian et al., 2012b; Burian et al., 2013). However, no direct observation of WhiB7-dependent recruitment of SigA (HrdB) to WhiB7 (WblC)-regulated promoters had been published. I assessed the fold enrichment of WblC-activated promoters by either WblC or HrdB ChIP from wild type and Δ*wblC* after treatment with 1μg/ml erythromycin for 1 hr. The WblC-activated *tuf3* and *tetM* promoters were 10~100-fold more enriched in WblC-ChIP samples of wild type than in the samples of Δ*wblC* (Figure 3-8). At the same time, these promoters exhibited ~100-fold greater enrichment in HrdB-ChIP samples of wild type than in samples of Δ*wblC* (Figure 3-8). This is a direct proof that HrdB is recruited to promoters activated by WblC in a *wblC*-dependent manner.

Meanwhile, the absence of conserved motif in WblC regulon promoter repressed by WblC led me to hypothesize that WblC would not bind to these promoters in the form of WblC-HrdB complex. In fact, while enrichment of WblC-repressed promoters by WblC ChIP was greater in erythromycin-treated wild type than in equally treated Δ*wblC*, enrichment of WblC-repressed promoters by HrdB ChIP was not greater in erythromycin-treated wild type than in equally treated Δ*wblC* (Figure 3-8). This demonstrates that WblC binds to the repressed WblC regulon promoters not as complexed with HrdB but by itself. Interestingly, promoters of SCO3064, *wblE*, and *citA* were enriched 5~27-fold less in HrdB-ChIP samples of wild type than in the samples of Δ*wblC* (Figure 3-8). This implies that WblC binding to these promoters may even hinder HrdB binding to these promoters, which in part explains the WblC-mediated transcription downregulation.

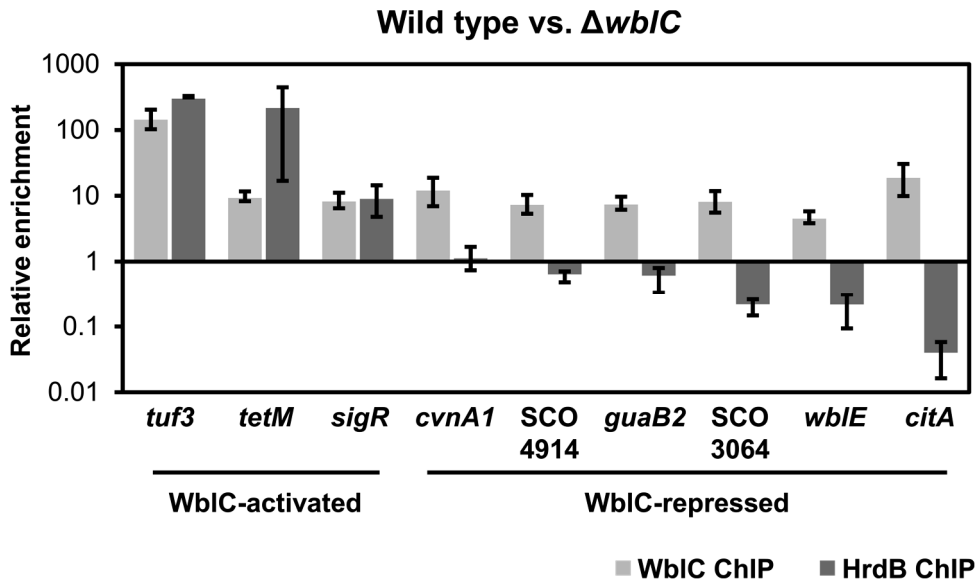

Figure 3-8. The dependency of HrdB recruitment on WblC binding in WblC-activated and WblC-repressed promoters.
Fold enrichment of WblC regulon promoters in erythromycin-treated WblC-ChIP and HrdB-ChIP samples were assessed by qPCR. Fold enrichment in wild type relative to that in Δ*wblC* is plotted for each promoter. Error bars indicate mean±standard error of 3 biologically independent experiments.

3-4. Noncoding RNA targets controlled by WblC

Besides mRNAs and 6 tRNAs of WblC regulon, I found some other noncoding RNAs directly regulated by WblC. 4 intergenic small RNAs and 12 antisense RNAs (asRNAs) showed *wblC*-dependent RNA level difference and >2-fold enrichment of the promoter region by WblC (Figure 3-9). Another interesting phenomenon was that 104 of the WblC regulon transcripts had long untranslated regions (UTRs) that overlapped adjacent gene(s) on the opposite direction, therefore may be considered both as an mRNA and an asRNA (Figure 3-9). This type of mRNA-asRNAs have been observed in other bacteria as well (Moody et al., 2013; Sesto et al., 2013). Nearly all the above noncoding RNAs – intergenic small RNAs, asRNAs, and mRNA-asRNAs – were upregulated in the presence of *wblC*, but levels of 2 asRNAs and 3 mRNA-asRNAs were downregulated by *wblC*. Intergenic small RNAs can post-transcriptionally regulate expression of other transcripts by complementary base pairing, although it is not so easy to predict their targets. asRNAs can regulate expression of the gene that they overlap with at the post-transcriptional stage. In conclusion, the noncoding RNA targets may expand the impact of WblC-mediated regulation on the transcriptome and proteome under antibiotic stress.

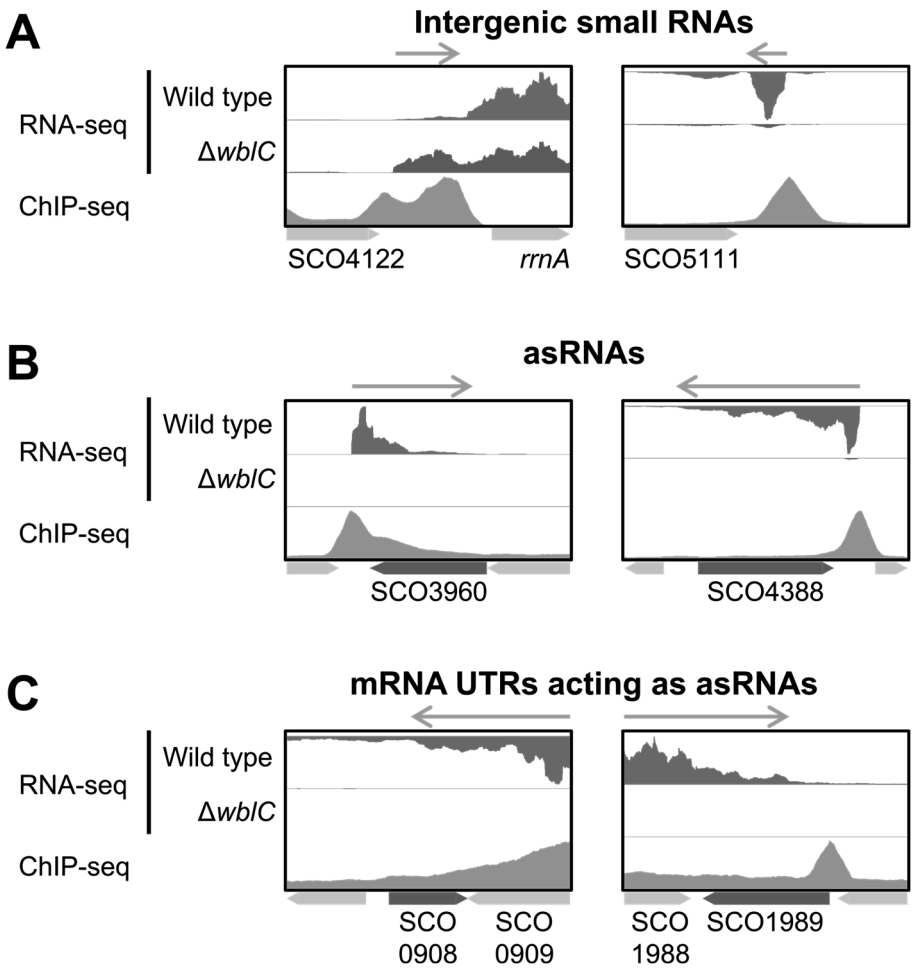

Figure 3-9. Selected examples of WblC-regulated noncoding RNAs.
Note that *y*-axis scales of RNA-seq and ChIP-seq data are variable among the panels. Genes corresponding to the antisense RNAs are represented under each plot as dark gray arrows. UTR, untranslated region.

Chapter 4. Antibiotic resistance conferred by ribosome-associated proteins of WblC regulon

4-1. Functions of WblC-upregulated regulon gene products and relationship with antibiotic resistance

I identified many genes involved in antibiotic resistance in a gene-by-gene investigation of WblC-upregulated regulon (Table 5). *lrm* encodes an *erm* family 23S rRNA methyltransferase that confers macrolide-lincosamide resistance (Jenkins and Cundliffe, 1991). *tetM* encodes a ribosomal GTPase that dislodges ribosome-bound tetracycline (Burdett, 1996; Donhofer et al., 2012). *hflX*, common to all previous-studied mycobacterial WhiB7 regulons and presumably rescues antibiotic-stalled ribosome (Duval et al., 2018; Hurst-Hess et al., 2017; Morris et al., 2005; Rudra et al., 2020), is also included in *S. coelicolor* WblC regulon. *smpB* that encodes another ribosome rescue factor, a tmRNA (transfer-messenger RNA, or SsrA)-binding protein involved in *trans*-translation, is also involved in antibiotic resistance (Li et al., 2013; Yang and Glover, 2009). Genes of aminoglycoside acetyltransferases Eis and Eis2 (Chen et al., 2011; Zaunbrecher et al., 2009), streptogramin B lease Vgb (Korczynska et al., 2007), as well as SCO4264, SCO0107, and SCO6090 are those encoding putative antibiotic-modifying enzymes that can inactivate translation-inhibitory antibiotics. *cmlR2* and *pep* encodes MFS proteins that confers chloramphenicol and streptogramin B resistance, respectively (Folcher et al., 2001; Vecchione et al., 2009), and SCO1840 is a close ortholog of *M. tuberculosis* Rv1473 encoding macrolide efflux ABC transporter (Duan et al., 2019). *sigR*, which contributes to multiple translation-inhibitory antibiotic resistance (Yoo et al., 2016), was also included in the WblC regulon of this study.

On the other hand, comprehensive functional analysis of the WblC-

upregulated regulon revealed prominent functions of WblC regulon gene products that may contribute to antibiotic resistance. I analyzed the functional annotations of WblC regulon by Gene Ontology terms, InterPro entries, and EggNOG classifications (Huerta-Cepas et al., 2016; Mitchell et al., 2019; The Gene Ontology Consortium, 2019). Analysis for overrepresented classes of functions revealed that several functions like tRNA aminoacylation, translation, N-acyltransferase activity, nucleotide-binding and NTPase activity, and ABC transporter activity are significantly enriched (BH-adjusted p-value<0.05) in the WblC-upregulated regulon compared to the genomic composition (Figure 4-1). Categorization of WblC-upregulated regulon genes according to the annotations supplemented the identification of represented functions (Table 6). The 20 ABC transporters and 39 integral membrane proteins encoded by WblC-upregulated regulon may include additional drug exporters. Some of the 16 Gcn5-related N-acetyltransferases may inactivate antibiotics, like the two *eis* genes.

Interestingly, many of the representative functions of WblC-upregulated genes relates to protein biosynthesis (Table 7). *tuf3*-encoded alternative elongation factor Tu (Olsthoorn-Tieleman et al., 2001; van Wezel et al., 1995), *fusB*-encoded alternative elongation factor G, SCO4278-encoded peptidyl-tRNA hydrolase, and 6 tRNAs are products of WblC regulon directly involved in protein biosynthesis. Additionally, WblC regulon includes genes encoding ribosome biogenesis-involved RsgA, Der, and RbfA, 13 aminoacyl-tRNA synthetases, 3 misacylated tRNA-editing enzymes, and tRNA processing enzymes TruB and MiaA. Under tetracycline stress, RNA levels of some of these genes surpassed the RNA level of their paralogs that are dominantly expressed in normal growth condition (Figure 4-2). This indicates that these WblC-upregulated genes may replace its paralogs upon encountering antibiotic stress, which may be important for maintaining the translation-related functions in the stress condition. In conclusion, I speculated that many of the WblC-upregulated regulon genes would function to enhance translation under antibiotic stress condition.

Table 5. WblC-upregulated regulon genes involved in antibiotic resistance.

Gene ID	Product	Function	Fold diff.*
Ribosome protection/rescue			
SCO6089	Lrm	Macrolide-lincosamide-streptogramin B resistance 23S rRNA adenine methyltransferase	406.7
SCO0783	TetM	Tetracycline-dissociating ribosomal GTPase	179.5
SCO5796	HflX	Ribosome-associated GTPase	18
SCO2966	SmpB	SsrA-binding protein	7.4
Antibiotic inactivation			
SCO4264	-	Putative aminoglycoside phosphotransferase	230
SCO2625	Eis2	Aminoglycoside acetyltransferase	72.8
SCO0107	-	Putative aminoglycoside nucleotidyltransferase	56.2
SCO6090	-	Putative macrolide glycosyltransferase	20.7
SCO4186	Eis	Aminoglycoside acetyltransferase	19.8
SCO4449	Vgb	Streptogramin B lyase	2.9
Antibiotic efflux			
SCO7662	CmlR2	Chloramphenicol efflux MFS protein	6.7
SCO4024	Pep	Streptogramin B efflux MFS protein	9.0
SCO1840	-	Putative macrolide efflux ABC transporter (Rv1473 ortholog)	3.0

* Fold difference of RNA level in wild type from that in Δ*wblC*.

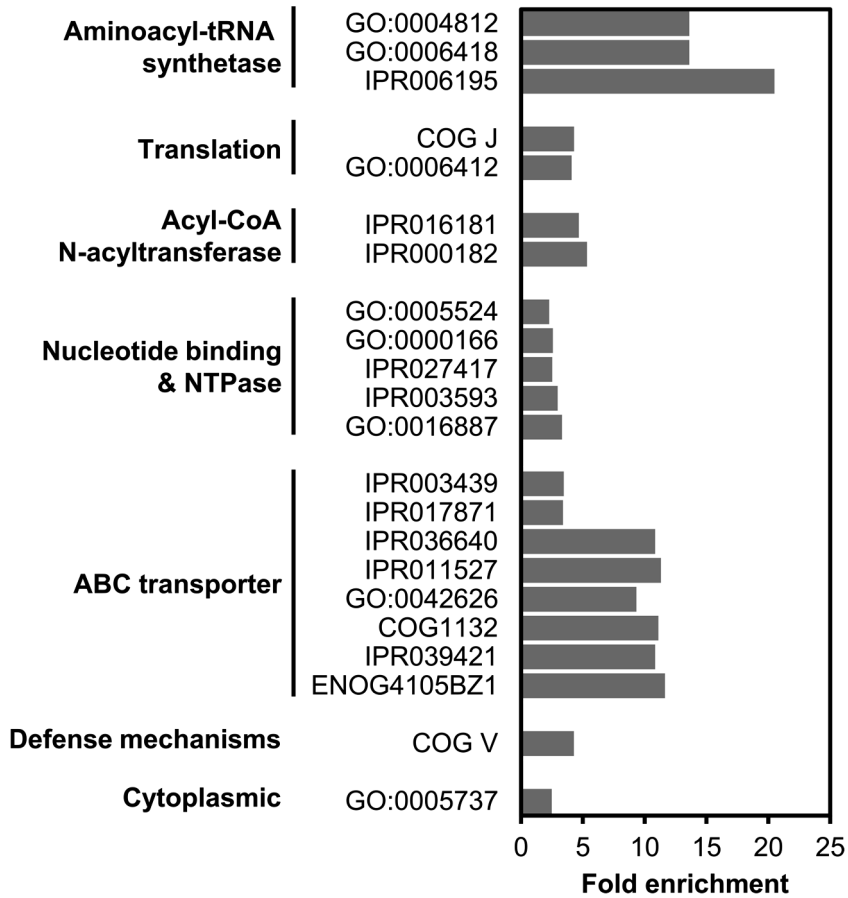

Figure 4-1. Functions overrepresented in WblC-upregulated regulon.
Gene Ontology terms, InterPro entries, and EggNOGs with BH-adjusted Fisher's exact test *p*-values of <0.05 are presented. CoA, coenzyme A.

Table 6. Functional classification of WblC-upregulated regulon genes.

Category	Number of genes	Representative genes
1. Aminoacyl-tRNA synthesis & editing enzymes	16	*thrS2*, *lysS*, *alaS2*, *trpS*
2. P-loop NTPases	35	
2A. ABC transporters with transmembrane domains	10	SCO1147, SCO5451
2B. ABC transporter ABC proteins	10	SCO6512, SCO3824
2C. Other ATPases	9	SCO2532, *hrpA*, *helY*
2D. GTPases	6	*hflX*, *der*, *tetM*, *tuf3*
3. Transferases	32	SCO4264, SCO7710
3A. Gcn5-related N-acetyltransferases	16	*eis*, *eis2*
3B. Methyltransferases	7	*lrm*
4. Integral membrane proteins	39	SCO2896, SCO1362
4A. MFS proteins	11	*cmlR2*, *pep*
5. Oxidoreductases	16	*asd1*, *pntA*
6. Hydrolases	16	*arfB*
7. Transcription regulators	19	*wblC*, *sigR*, *ndgR*
8. tRNAs	6	
Others	109	*hsp15*, SCO5707, *vgb*, *smpB*

Table 7. WblC-upregulated regulon genes involved in translation.

Gene	Product	Function	Fold diff.*
Elongation			
SCO1321	EF-Tu3	Elongation factor Tu	99.6
SCO6589	EF-G2	Elongation factor G	86.7
Ribosome recycling			
SCO4278	ArfB	Peptidyl-tRNA hydrolase	148.7
SCO1991	Hsp15	Ribosome-associated heat shock protein	14.5
Ribosome biogenesis			
SCO6149	RsgA	30S subunit assembly GTPase	68.4
SCO1758	Der	50S subunit assembly GTPase	6.3
SCO5708	RbfA	30S subunit assembly cold shock protein	5.4
Aminoacyl-tRNA synthesis			
SCO3778	ThrS2	Threonyl-tRNA synthetase	56
SCO7600	AlaS2	Alanyl-tRNA synthetase	41.6
SCO5699	proS	Prolyl-tRNA synthetase	6.7
SCO3303	lysS	Lysyl-tRNA synthetase	4.8
SCO1595	pheS	Phenylalanyl-tRNA synthetase subunit A	4.6
SCO3961	serS	Seryl-tRNA synthetase	4.1
SCO1508	hisS	Histidyl-tRNA synthetase	3.5
SCO2615	ValS	Valyl-tRNA synthetase	3.5
SCO2076	ileS	Isoleucyl-tRNA synthetase	3.2
SCO3304	ArgS	Arginyl-tRNA synthetase	3.1
SCO1594	pheT	Phenylalanyl-tRNA synthetase subunit B	2.6
SCO3334	TrpS1	Tryptophanyl-tRNA synthetase	2.3
SCO3795	AspS	Aspartyl-tRNA synthetase	2.1
Aminoacyl-tRNA editing			
SCO3165	YbaK	Cysteinyl-tRNA deacylase	24.4
SCO5498	GatC	Aspartyl/Glutamyl-tRNA amidotransferase subunit C	3.4
SCO5499	GatA	Aspartyl/Glutamyl-tRNA amidotransferase subunit A	2.7
tRNA modification			
SCO5709	TruB	tRNA pseudouridine synthase	6.6
SCO5791	MiaA	tRNA isopentenyltransferase	5.3
tRNA			
SCOt63	-	tRNA-Pro	4
SCOt45	-	tRNA-Lys	2.9
SCOt44	-	tRNA-Glu	2.8
SCOt62	-	tRNA-Leu	2.6
SCOt55	-	tRNA-Arg	2.4
SCOt18	-	tRNA-Arg	2.1

* Fold difference of RNA level in wild type from that in Δ*wblC*.

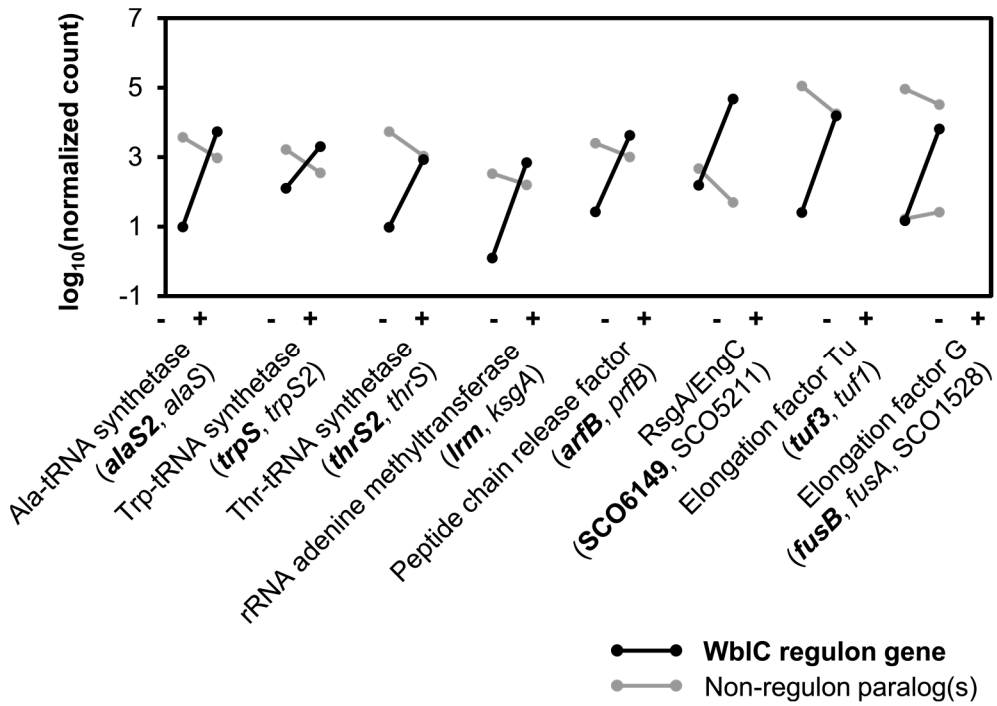

Figure 4-2. RNA levels of translation-involved gene paralogs before (-) and after (+) tetracycline treatment.
Normalized count, mapped read count normalized by DESeq2 (Love et al., 2014); Ala-tRNA, alanyl-tRNA; Trp-tRNA, tryptophanyl-tRNA; Thr-tRNA, threonyl-tRNA.

4-2. Maintenance of translation rate by WblC during antibiotic stress

In order to see the effect of WblC-mediated gene regulation on translation efficiency during antibiotic stress, I tried measuring the incorporation rates of radioisotopic amino acids into cells, which is a method of measuring *in vivo* protein synthesis rate (Cheverton et al., 2016; Esposito and Kinzy, 2014). The incorporation rates were not different for wild type and Δ*wblC* in the absence of antibiotic stress, indicating that WblC has no effect on translation rate at normal growth condition (Figure 4-3). However, when the strains were treated with either 0.25 μg/ml tetracycline or 5 μg/ml chloramphenicol for 1 hr, the rates were significantly different (p-value <0.01) between the strains; the rate was decreased by 20~50% in wild type, whereas the rate was decrease by about 80% in Δ*wblC*, compared to the rates at untreated condition (Figure 4-3). Meanwhile, the incorporation rates were lowered to about 20% of that of untreated condition for both strains when the concentration of tetracycline treatment was increased to 1 μg/ml (Figure 4-3). These results indicated WblC is required for maintaining translation rate when subjected to low concentrations of antibiotics.

I also measured growth of the strains after treating with the same antibiotic concentrations used in the *in vivo* amino acid incorporation rate measurements, and discovered that growth rates highly correlated with the incorporation rates in all conditions. Growth of wild type and Δ*wblC* were nearly identical without antibiotic treatment, and growth of both strains were suppressed greatly when they were treated with 1 μg/ml tetracycline (Figure 4-4). Moreover, treatment with 0.25 μg/ml tetracycline or 5 μg/ml chloramphenicol substantially suppressed the growth of Δ*wblC*, while wild type grew considerably well (Figure 4-4). Because global translation efficiency is thought to be a major factor of determining growth rate (Klumpp et al., 2013; Zhu and Dai, 2018), I suppose that the maintenance of translation rate by WblC-mediated regulation is what enables sustained growth in

wild type.

WblC-dependent maintenance of translation rate under translation-inhibitory antibiotic stress can arise from two different levels of WblC-regulated gene functions. WblC regulon products such as drug exporters and antibiotic-inactivating enzymes function on antibiotics; preventing decrease in translation rate by diminishing effective intracellular concentration of translation-inhibitory antibiotics. Alternatively, the WblC-upregulated gene products related to translation may function on translational machinery; sustaining translation rate against the action of antibiotics by blocking antibiotic action, restoring translational machineries impaired by antibiotics, or modulating the process of translation. However, it should be noted that *in vivo* amino acid incorporation assay does not distinguish protein synthesis rate from amino acid uptake rate.

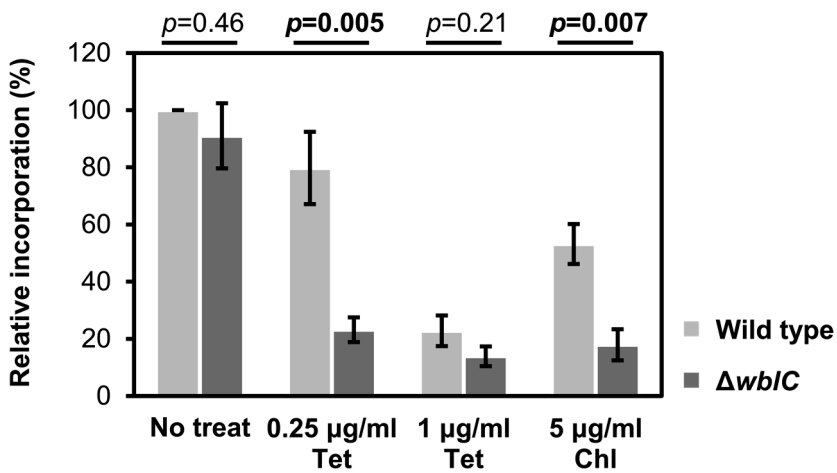

Figure 4-3. *In vivo* ^{35}S-methionine/cysteine incorporation rates of wild type and Δ*wblC* at different culture conditions.
Incorporation rates are plotted relative to the rate of untreated (no treat) wild type. Error bars indicate mean±standard error of 4 biologically independent experiments. Student's *t*-test *p*-values (*p*) are denoted for each comparison between strains. Tet, tetracycline; Chl, chloramphenicol.

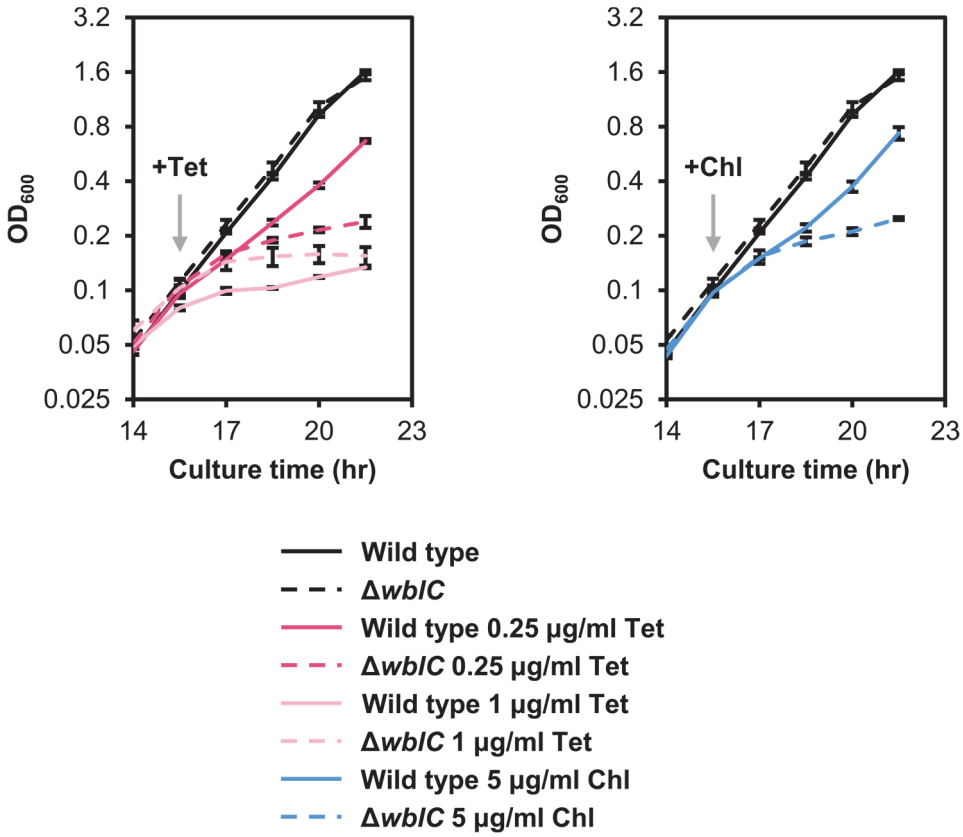

Figure 4-4. Growth of wild type and Δ*wblC* at different culture conditions. Antibiotics were treated after culture for 15.5 hr (indicated by gray arrows). Error bars indicate mean±standard error of 3 biologically independent experiments. Tet, tetracycline; Chl, chloramphenicol.

4-3. Association of WblC-upregulated gene products with ribosome

In order to see if translational machinery is WblC-dependently modulated during antibiotic stress to possibly facilitate translation, I quantitatively analyzed the protein composition of ribosomes, which proteomic analysis was performed by Dr. Jong-Seo Kim and Mr. Jeesoo Kim. Proteomic profiles of 70S ribosomes isolated from tetracycline-treated wild type was compared with that of either untreated wild type or tetracycline-treated Δ*wblC*. The condition of tetracycline treatment was 0.25 μg/ml for 2 hr. 12 proteins were significantly more abundant (BH-adjusted *p*-value<0.05) by >2-fold in wild-type ribosomes from tetracycline-treated samples than in those from untreated samples (Figure 4-5A). Likewise, 54 proteins were significantly more abundant (BH-adjusted *p*-value<0.05) by >2-fold in tetracycline-treated sample-derived ribosomes of wild type than in those of Δ*wblC* (Figure 4-5B). 9 proteins were discovered to be significantly more abundant in both comparisons, which are therefore tetracycline-dependently and WblC-dependently enriched ribosome-associated proteins (Table 8).

7 out of these 9 proteins were encoded by WblC-upregulated regulon, reinforcing the idea that many of the WblC-upregulated gene products function on translational machinery in response to antibiotic stress (Table 8). Hsp15 is known as a ribosome-associated heat shock protein that recycles aborted 50S subunits in *E. coli* (Jiang et al., 2009; Korber et al., 2000), which function may also be effective in recovering translation from antibiotic stress. The annotated functions of peptidyl hydrolase domain-containing protein of SCO4278 and PhoH-like ATPase protein of SCO2532 were ambiguous, so I analyzed the phylogenetic relativity of these proteins with their orthologs. SCO4278 protein was more homologous to *E. coli* ArfB (YaeJ) than to PrfA/B (release factors 1 and 2) of various species, so I re-annotated it as ArfB (Figure 4-6A). ArfB is a ribosome-rescuing alternative release factor that hydrolyses peptidyl-tRNA of stalled ribosome in a codon-independent

manner (Chadani et al., 2011; Handa et al., 2011), which intrigues a proposal that ArfB may also rescue antibiotic-stalled ribosome. SCO2532 protein was more homologous to *E. coli* YbeZ than to phosphate starvation-induced *E. coli* PhoH or *M. tuberculosis* RNA helicase-RNase PhoH2 (Figure 4-6B) (Andrews and Arcus, 2015; Kazakov et al., 2003). *E. coli* YbeZ is co-transcribed with its physically interacting partner YbeY (Vercruysse et al., 2016), which is an RNase that can degrade defective 70S ribosomes during heat stress and treatment of kasugamycin, a translation-inhibitory antibiotic (Jacob et al., 2013). *E. coli* YbeZ and `*E. coli* ortholog of ATP-dependent DEAH-box RNA helicase HrpA, another WblC-dependently enriched ribosome-associated WblC regulon protein, had been identified as ribosome-associated proteins in multiple large-scale protein-protein interaction studies (Arifuzzaman et al., 2006; Butland et al., 2005; Hu et al., 2009). HelY is another ATP/dATP-dependent RNA helicase (Uson et al., 2015). Der (EngA) is known as an essential ribosomal GTPase involved in 50S ribosomal subunit maturation (Hwang and Inouye, 2001, 2006), and depletion of Der results in sensitization of the organism to cold stress as well as aminoglycoside treatment (Bharat and Brown, 2014), implying the linkage of Der-mediated ribosome maturation with stress response. The uncharacterized SCO5707 protein shares a conserved synteny with genes encoding 30S ribosomal subunit maturation factors RimP and RbfA, initiation factor 2, tRNA modification/maturation factor TruB, and ribosomal protein S15, which supports its relationship with translation (Figure 4-7). In summary, these WblC regulon-encoded proteins showing increased ribosome association during antibiotic stress seems to be either resolving the negative effects of translation-inhibitory antibiotics or assisting translation.

2 non-WblC regulon proteins were WblC- and tetracycline-dependently enriched in ribosomes. HPF (ribosome hibernation-promoting factor) facilitates ribosome inactivation and ScoF4 is a cold shock protein, both of which are involved in modulating translation during stressful conditions.

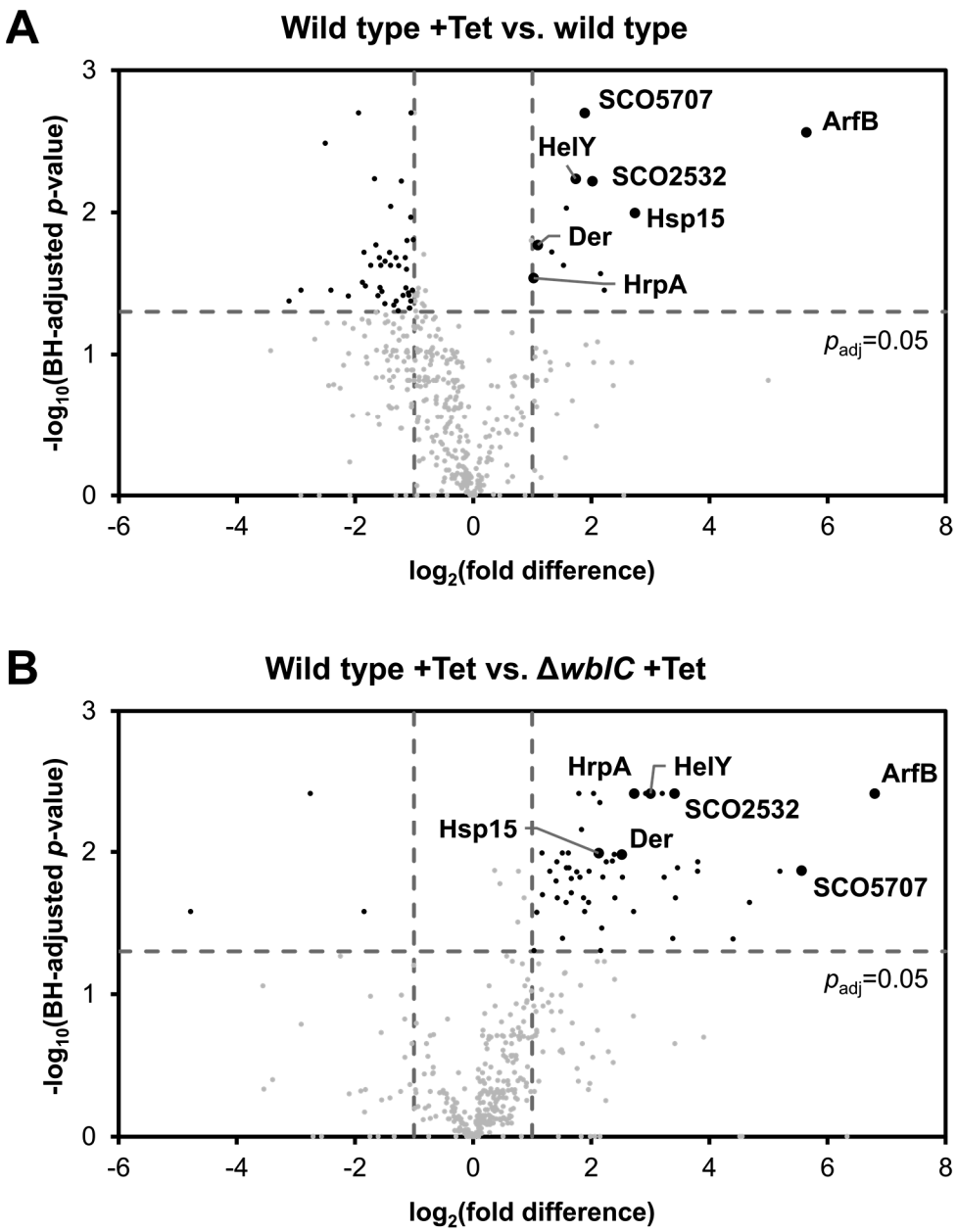

Figure 4-5. Tetracycline- and *wblC*-dependent changes in ribosomal proteome. Volcano plots comparing ribosomal proteomes of tetracycline-treated and untreated wild type (A) or tetracycline-treated wild type and Δ*wblC* (B). Proteins of significantly different abundance (black dots) are defined by BH-adjusted *p*-value (p_{adj}) and fold difference thresholds (gray dashed lines). WblC regulon proteins with abundances increased by both tetracycline and *wblC* (bigger black dots) are labeled. Tet, tetracycline.

Table 8. Proteins that were tetracycline- and *wblC*-dependently associated with ribosome.

Name	Gene ID	Description	Fold diff.*	
			Tet vs. None	Wt vs. Δ*wblC*
WblC regulon gene products				
HrpA	SCO4092	ATP-dependent RNA helicase	2.0	6.6
SCO2532	SCO2532	PhoH-like protein, ortholog of *E. coli* YbeZ	4.0	10.6
ArfB	SCO4278	Alternative ribosome rescue factor B	49.7	111.4
HelY	SCO1631	ATP-dependent RNA helicase	3.3	8.0
Hsp15 (HslR)	SCO1991	Ribosome-associated heat shock protein	6.6	4.4
Der (EngA)	SCO1758	Ribosome-associated GTPase	2.1	5.7
SCO5707	SCO5707	Uncharacterized protein, with DUF503	3.7	47.2
Other proteins				
HPF	SCO3009	Ribosome hibernation promoting factor	3.0	7.6
ScoF4	SCO4295	Cold shock protein	2.5	10.8

* Fold difference between conditions. Tet, tetracycline; None, no treatment; Wt, wild type.

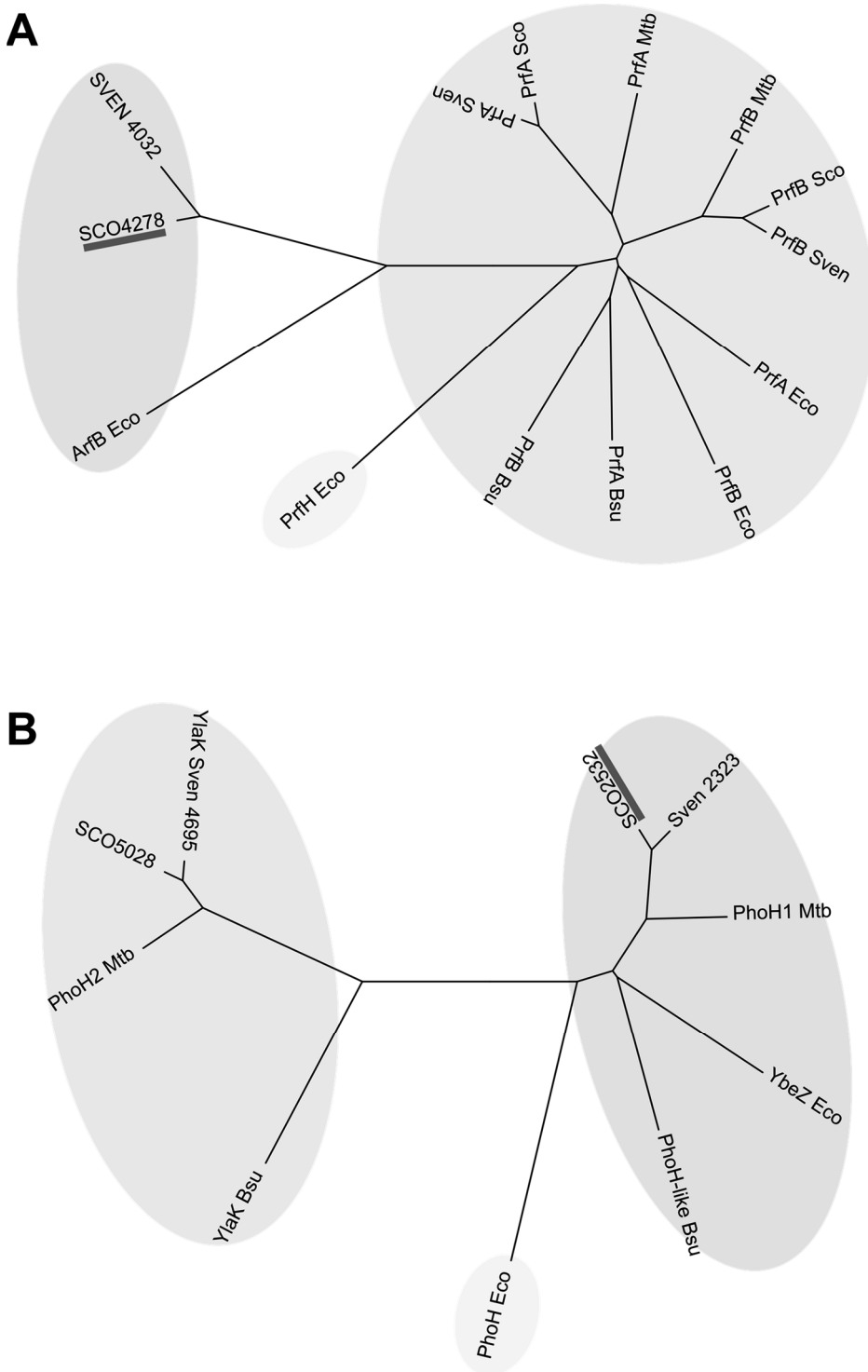

Figure 4-6. Phylogeny analysis of SCO4278 protein and SCO2532 protein.
Neighbor-joining trees of SCO4278 protein (A) and SCO2523 protein (B) homologs in 5 species. Bsu, *Bacillus subtilis*; Eco, *E. coli*; Mtb, *M. tuberculosis*; SCO, *S. coelicolor*; SVEN, *Streptomyces venezuelae*.

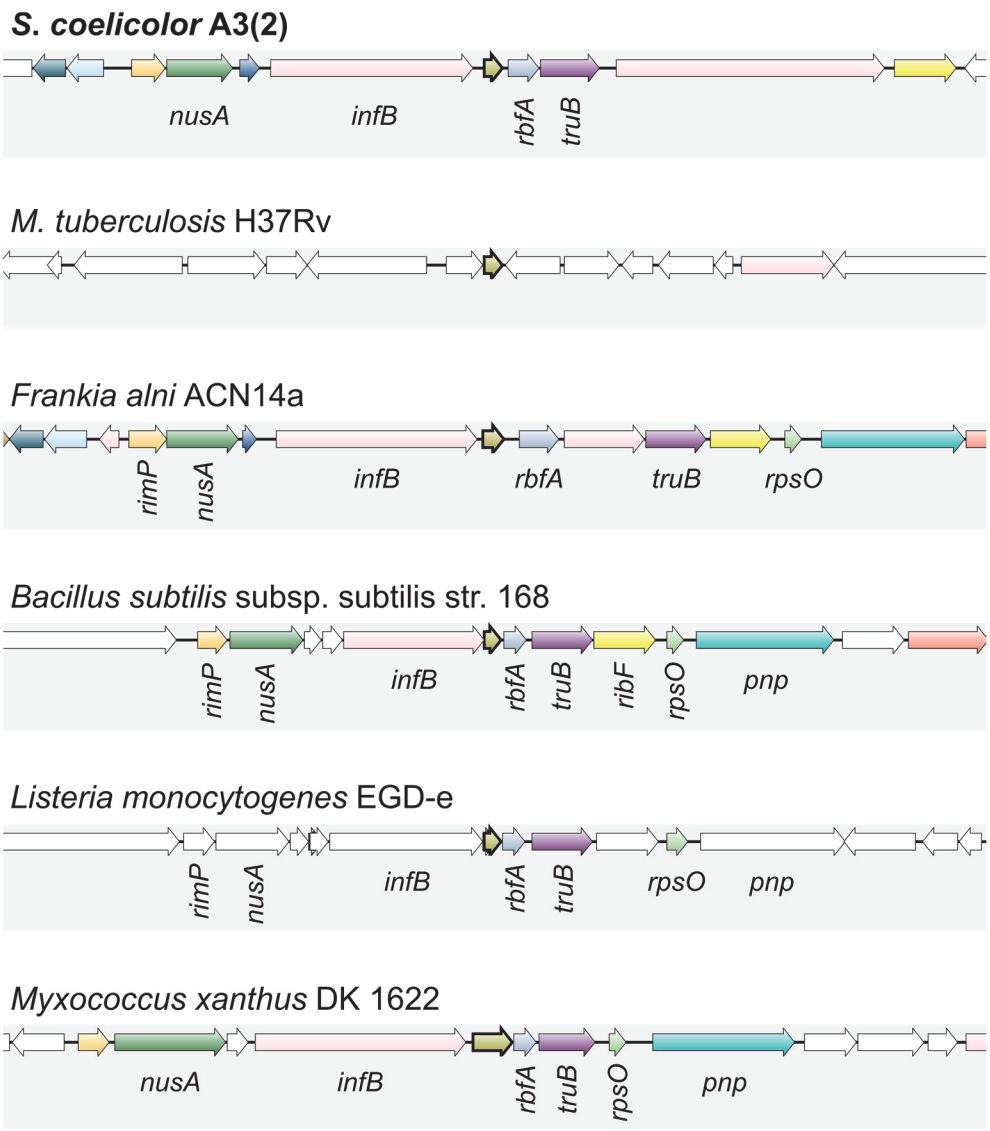

Figure 4-7. Conserved synteny of SCO5707.
Orthologs of SCO5707 are shown as arrows with thicker outlines. Proteins encoded by the genes of the conserved synteny are as follows: *rimP*, ribosome maturation factor; *nusA*, transcription termination/antitermination protein; *infB*, initiation factor 2; *rbfA*, ribosome-binding factor A; *truB*, tRNA pseudouridine synthase B; *rpsO*, 30S ribosomal protein S15; *ribF*, riboflavin biosynthesis protein; *pnp*, polyribonucleotide nucleotidyltransferase.

4-4. Contribution of ribosome-associated WblC regulon gene products to intrinsic resistance

I tested if WblC-upregulated genes encoding ribosome-associated proteins can actually contribute to antibiotic resistance. The antibiotic susceptibility profiles of mutant strains lacking *hflX*, *arfB*, SCO2532, *hrpA*, or *helY* were tested compared to that of wild type. Susceptibility to erythromycin, tetracycline, and lincomycin was tested, to which antibiotics Δ*wblC* was ≥4-fold more susceptible than wild type (Table 9). Δ*hflX* was 4-fold more sensitive to erythromycin (Figure 4-8), validating HflX as an erythromycin resistance factor as observed in other studies (Duval et al., 2018; Rudra et al., 2020). *hrpA* knockout mutant was 8-fold more sensitive to tetracycline and 4-fold more sensitive to erythromycin (Figure 4-8). Also, deletion of SCO2532 led to 4-fold and 2-fold greater sensitivity to tetracycline and erythromycin, respectively (Figure 4-8). Meanwhile, *helY* knockout only resulted in 2-fold greater sensitivity to tetracycline, and *arfB* knockout caused no increased sensitivity to any of the tested antibiotics. These results are likely because of the fact that *S. coelicolor* retains SCO1152 that is paralogous to *helY* and SsrA-SmpB trans-translation system that is functionally redundant with ArfB (Chadani et al., 2011).

Respective genetic complementation of *hflX*, *hrpA*, and SCO2532 mutants resulted in almost full recovery of the intrinsic antibiotic resistance almost to the resistance profile of wild type with empty vector used for complementation (Figure 4-8), verifying that *hflX*, *hrpA*, and SCO2532 are indeed responsible for intrinsic resistance to the antibiotics. These results suggest that other WblC-upregulated genes encoding ribosome-associated proteins that were not tested in this study may also be responsible for intrinsic resistance to translation-inhibitory antibiotics.

Table 9. Antibiotic susceptibility profiles of wild type and Δ*wblC*.

Antibiotic	MIC (μg/ml)*	
	Wild type	Δ*wblC*
Erythromycin	20	0.3125
Tetracycline	10	0.15625
Lincomyin	80	10
Chloramphenicol	40	20
Fusidic acid	0.625	0.3125
Hygromycin B	20	10
Linezolid	1.25	0.625
Streptomycin	2.5	1.25
Thiostrepton	0.4	0.2
Puromycin	640	640
Spectinomycin	160	160

* Median of three independent experiments.

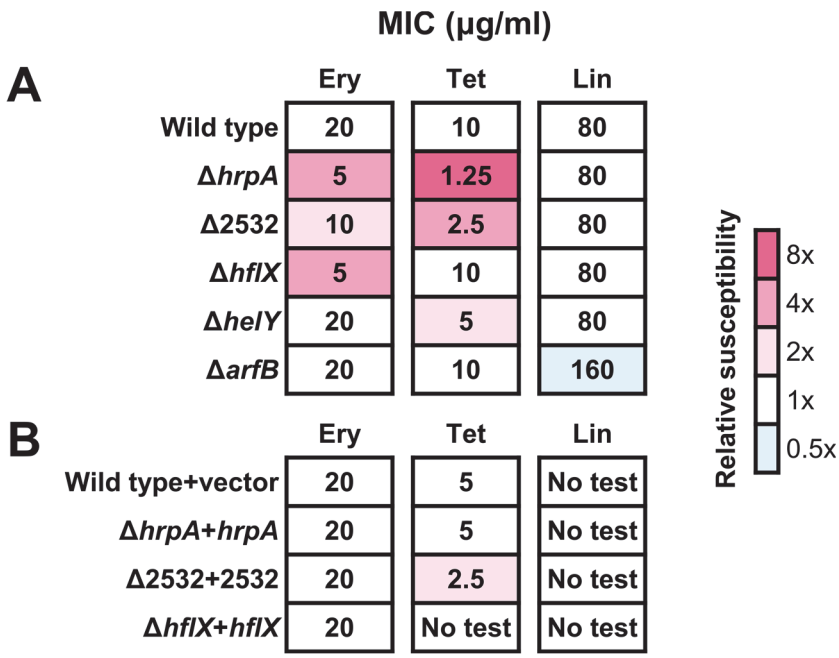

Figure 4-8. Contributions of ribosome-associated proteins of WblC regulon to erythromycin and tetracycline resistance.
Presented values are median MICs of three independent experiments. Background color indicates susceptibility of either a mutant strain (in panel A) or complemented strain (in panel B) to the antibiotic compared to the susceptibility of the reference strain, which is either wild type (in panel A) or wild type+vector (in panel B). Ery, erythromycin; Tet, tetracycline; Lin, lincomycin.

Chapter 5. The mechanism of *wblC* induction by translation stress

5-1. Conservation of ribosome-mediated transcriptional attenuation of *wblC*/*whiB7* orthologs

wblC/*whiB7* expression is thought to be regulated by ribosome-mediated attenuation, for which uORF and putative RIT must be present in the leader sequence. Because former studies insisted the conservation of these sequence elements but provided insufficient data, I checked how extensively these sequence features are conserved among *wblC*/*whiB7* leader sequences. Motif search within upstream sequences of 36 *wblC*/*whiB7* orthologs revealed 3 conserved motifs (Figure 5-1). *wblC*/*whiB7* promoter motif that includes WblC-binding site plus -35 element was discovered in the sequences of all but 1 species (Figure 5-1). Another conserved motif that corresponds to the ribosome-binding site and start codon of uORF was discovered in all of the 35 *wblC*/*whiB7* leader sequences determined based on the location of promoter motifs (Figure 5-1). Downstream to the uORF was the stem-loop and uridine-rich tail of putative RIT, conserved in most of the species (Figure 5-1). In conclusion, wide conservation of uORF and putative RIT among *wblC*/*whiB7* leader sequences supported that ribosome-mediated transcriptional attenuation is a common regulatory mechanism of *wblC*/*whiB7* expression.

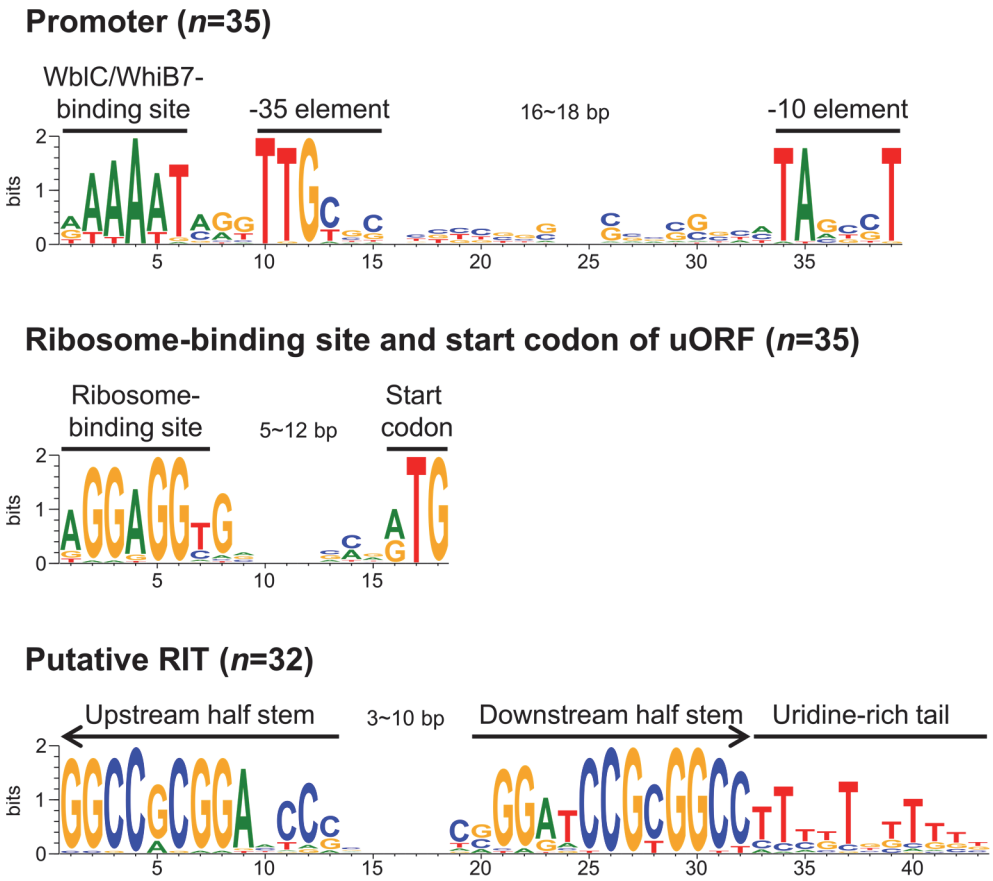

Figure 5-1. Conserved motifs in *wblC*/*whiB7* upstream intergenic sequences. *n*, number of sequences with the identified motif. Analyzed were *wblC*/*whiB7* upstream intergenic sequences of 36 species: *Acidothermus cellulolyticus*, *Actinoplanes missouriensis*, *Actinospica robinae*, *Actinosynnema mirum*, *Amycolatopsis mediterranei*, *Beutenbergia cavernae*, *Catenulispora acidiphila*, *Cellulomonas fimi*, *Frankia alni*, *Gordonia bronchialis*, *Hoyosella subflava*, *Jonesia denitrificans*, *Kitasatospora setae*, *Micromonospora aurantiaca*, *M. smegmatis*, *M. tuberculosis*, *N. farcinica*, *Nocardiopsis dassonvillei*, *Pseudonocardia dioxanivorans*, *Rhodococcus jostii*, *Saccharomonospora viridis*, *Saccharopolyspora erythraea*, *Saccharothrix esapnaensis*, *Salinispora tropica*, *Sanguibacter keddieii*, *Segniliparus rotundus*, *Stackebrandtia nassauensis*, *Streptacidiphilus albus*, *S. coelicolor*, *S. venezuelae*, *Streptosporangium roseum*, *Thermobifida fusca*, *Thermobispora bispora*, *Thermomonospora curvata*, *Tsukamurella paurometabola*, and *Xylanomonas cellulosilytica*.

5-2. Attenuation caused by leader RIT

In order to validate that premature transcription termination occurs at the conserved putative RIT in *wblC* leader, I analyzed the 3' end of *wblC* leader transcript in untreated or tetracycline-treated wild type *S. coelicolor*. In both conditions, a probe fragment with a length of ~145 nt was observed, which size is nearly identical to ~150 nt fragment that is predicted to be produced by premature termination at the putative RIT (Figure 5-2). At the same time, another fragment of a size corresponding to full length of the probed region was observed in tetracycline-treated samples (Figure 5-2). This fragment indicates presence of a transcript that traverses the putative RIT ('read-through' transcript), which means that transcription continued into *wblC* instead of terminating at the putative RIT. The 'read-through' product is barely detectable in untreated sample (Figure 5-2), indicating that tetracycline treatment suppresses attenuation. In conclusion, the result implied that transcription termination occurs at a location nearly identical to that of the putative RIT, and antibiotic stress facilitates transcription readthrough at this location.

To show that the putative RIT is indeed the element that functions as a transcriptional attenuator in *wblC* leader sequence, I constructed a series of uORF-*wblC* mutant (ΔuORF*wblC*) strains carrying *wblC* leader-*gusA* reporter transcriptional fusions with sequence variations in the putative RIT as in Figure 5-3A. For each strain, I assessed *wblC* leader RNA levels near the TSS and past the putative RIT in either before or after 2 μg/ml erythromycin treatment for 30 min. Readthrough ratio, calculated as the RNA level past the putative RIT divided by the RNA level near the TSS, was ≈0.2 and ≈0.9 before and after erythromycin treatment, respectively, for wild-type *wblC* leader (Figure 5-3B). The readthrough ratio before treatment was significantly increased to ≈0.6 when either the upstream ('Up-switched') or the downstream ('Down-switched') half of putative RIT stem was partially switched into complementary sequences (Figure 5-3B), suggesting

that disruption of RIT sequence causes impairment of attenuation. When sequences of both strands of the RIT stem were switched, which would recover base pairing between the strands ('Swap-paired'), readthrough ratio without erythromycin treatment was significantly lowered back to ≈0.2 (Figure 5-3B), confirming that the RIT sequence causes attenuation in the absence of antibiotic stress.

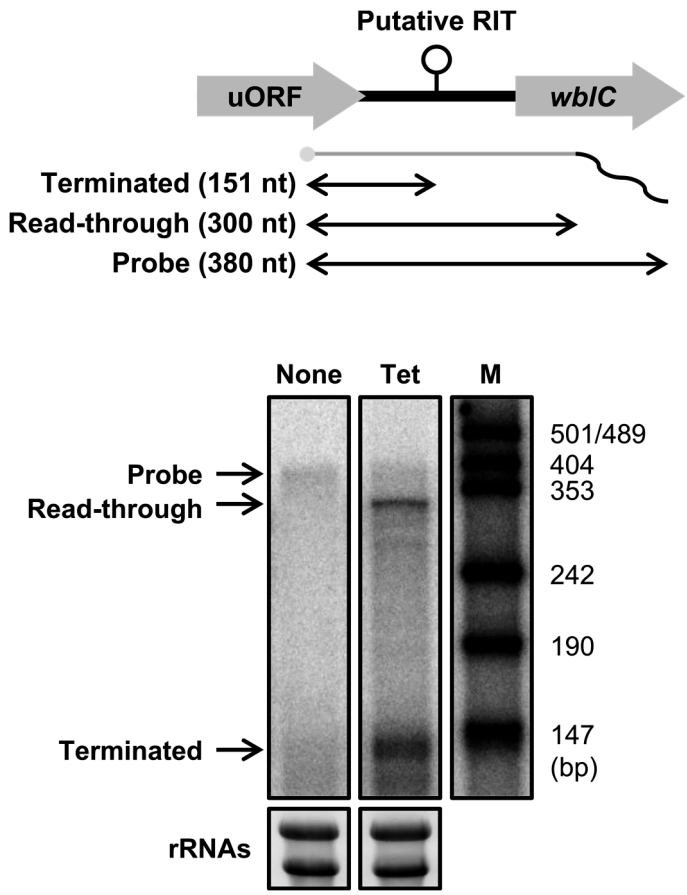

Figure 5-2. Locations of *wblC* leader RNA 3' ends in different conditions.
3' end S1 nuclease mapping of *wblC* leader RNA. 23S and 16S rRNAs are shown as control. Radiolabeled DNA size marker (M) is shown in parallel. None, no treatment; Tet, 2 μg/ml tetracycline treatment for 30 min.

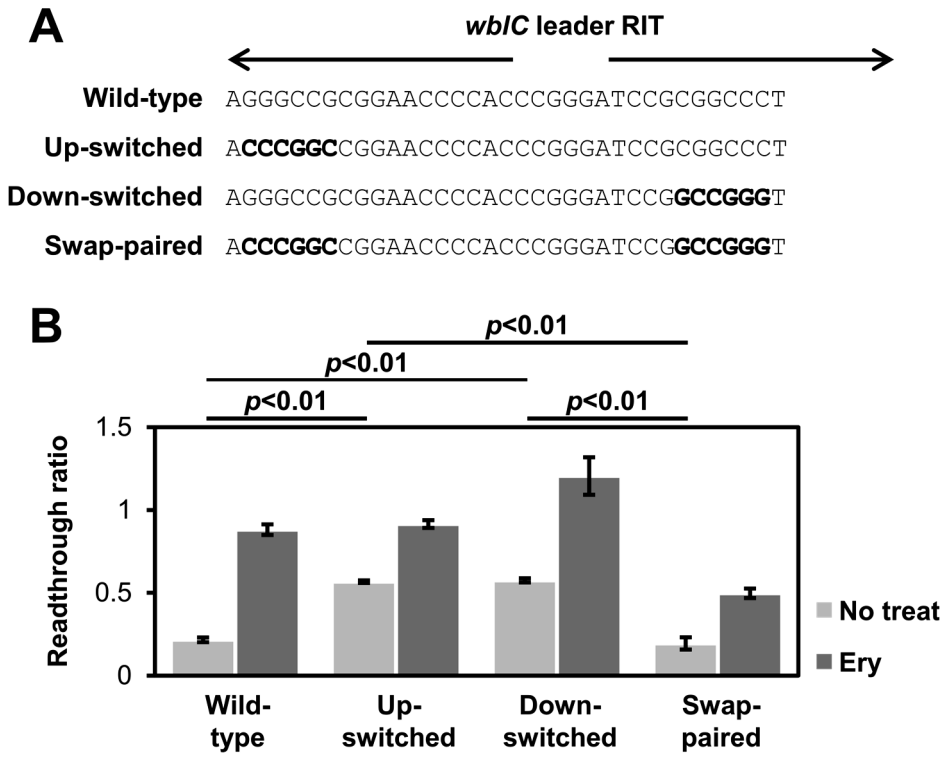

Figure 5-3. Effects of sequence variations of putative RIT on *wblC* leader readthrough ratio.

(A) Sequence variations of the putative RIT of *wblC* leader. The switched complementary sequences are marked in bold. (B) Readthrough ratio of each *wblC* leader sequence variant was assessed by qRT-PCR in untreated (No treat) and erythromycin (Ery)-treated conditions. Error bars indicate mean±standard error of 3 biologically independent experiments. Student's *t*-test *p*-values (*p*) are denoted for each comparison.

5-3. Conservation of putative antiterminator structure in *wblC* leader sequences

Interestingly, readthrough ratio after erythromycin treatment was ≈0.5 for *wblC* leader with 'Swap-paired' RIT, which is significantly smaller than the readthrough ratio of ≈0.9 for wild-type leader after treatment (Figure 5-3B). This implied that the sequence of RIT is involved not only in premature termination but also in suppressing attenuation during antibiotic stress. Considering the canonical model of antibiotic-responsive transcriptional attenuation (Figure 1-3), I suspected that an antiterminator RNA structure may be conserved in leader sequences of *S. coelicolor wblC* orthologs. Sequence alignment revealed that sequences of the upstream vicinity of *wblC* leader RITs are relatively well-conserved among the order of streptomycetales, and multiple palindromic sequences that spans the upstream half of RIT was discovered in the consensus (Figure 5-4A). RNA structures predicted from the conserved multiple palindromic sequences were similar among streptomycetales (Figure 5-5A). Alignment of orthologous *wblC*/*whiB7* leader sequences of other clades of actinomycetes revealed the same characteristics of relatively high conservation in the upstream vicinity of RIT and a consensus of multiple palindromic sequences spanning half of RITs (Figure 5-4B~D). Predicted RNA structures were similar within each clade but different from those of other clades (Figure 5-5B).

Remarkably, all of the predicted structures encompassed stop codons of uORFs in their apical region (Figure 5-5). This implies that ribosomes translating uORFs would prevent folding of these predicted structures (Figure 5-6A). Therefore, absence of translation stress will favor the formation of *wblC* leader RIT instead of antiterminator (Figure 5-6A). However, if antibiotics interrupt uORF translation, the RNA structure will fold at the end of the ribosome-free uORF sequence and function as an antiterminator that would exclude folding of leader RIT, thereby facilitating transcription readthrough of RIT (Figure 5-6B).

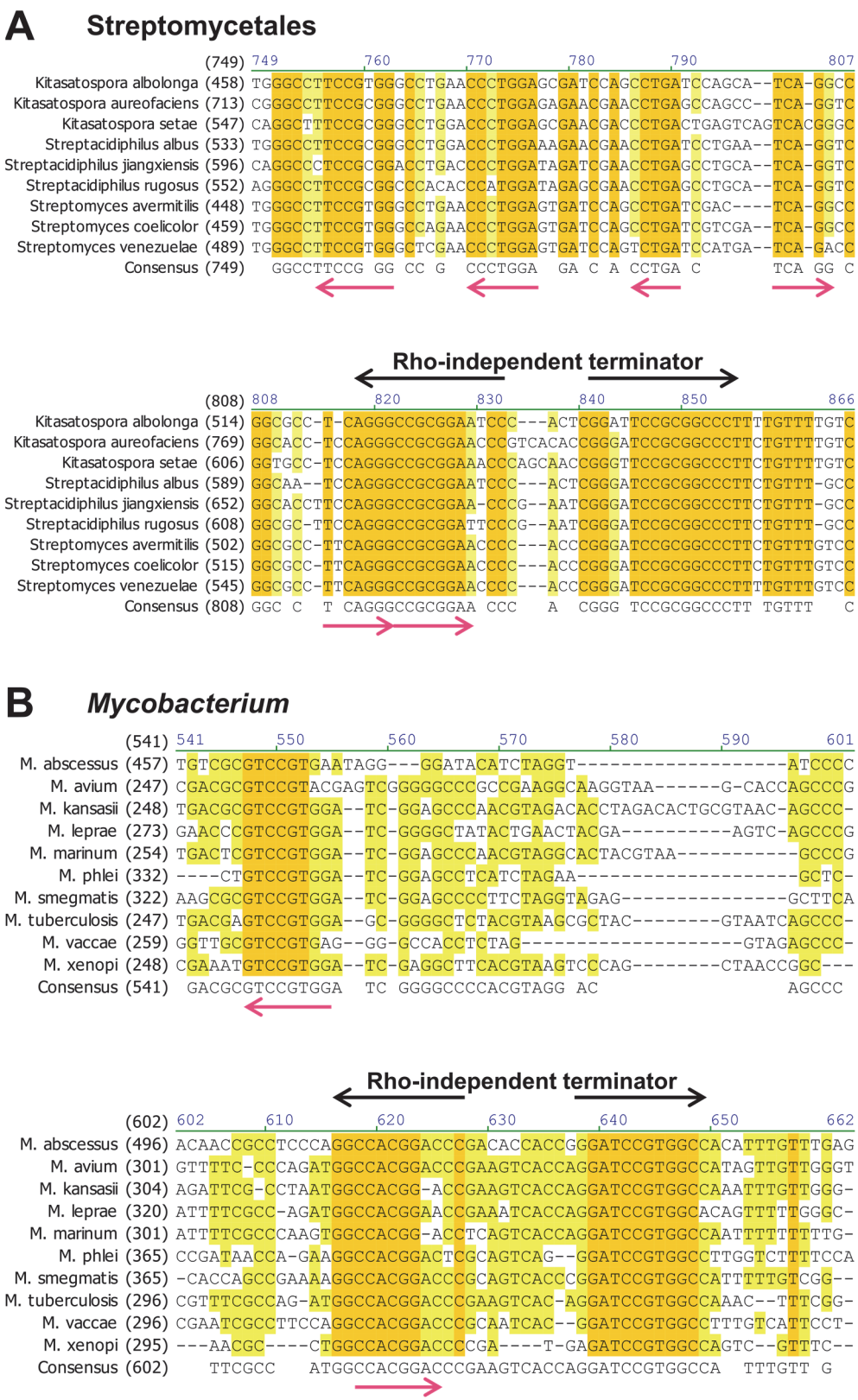
A
Streptomycetales
(749) 749 760 770 780 790 807
Kitasatospora albolonga (458) TGGGCCTTCCGTGGGCCTGAACCCTGGAGCGATCCAGCCTGATCCAGCA--TCA-GGCC
Kitasatospora aureofaciens (713) CGGGCCTTCCGCGGGCCTGAACCCTGGAGAGAACGAACCTGAGCCAGCC--TCA-GGTC
Kitasatospora setae (547) CAGGCTTTCCGCGGGCCTGGACCCTGGAGCGAACGACCCTGACTGAGTCAGTCACGGGC
Streptacidiphilus albus (533) TGGGCCTTCCGCGGGCCTGGACCCTGGAAAGAACGAACCTGATCCTGAA--TCA-GGTC
Streptacidiphilus jiangxiensis (596) CAGGCCCTCCGCGGACCTGACCCCTGGATAGATCGAACCTGAGCCTGCA--TCA-GGTC
Streptacidiphilus rugosus (552) AGGGCCTTCCGCGGCCCACACCCATGGATAGAGCGAACCTGAGCCTGCA--TCA-GGTC
Streptomyces avermitilis (448) TGGGCCTTCCGTGGGCCTGAACCCTGGAGTGATCCAGCCTGATCGAC----TCA-GGCC
Streptomyces coelicolor (459) TGGGCCTTCCGTGGGCCAGAACCCTGGAGTGATCCAGCCTGATCGTCGA--TCA-GGCC
Streptomyces venezuelae (489) TGGGCCTTCCGTGGGCTCGAACCCTGGAGTGATCCAGTCTGATCCATGA--TCA-GACC
Consensus (749) GGCCTTCCG GG CC G CCCTGGA GA C A CCTGA C TCA GG C
Rho-independent terminator
(808) 808 820 830 840 850 866
Kitasatospora albolonga (514) GGCGCC-T-CAGGGCCGCGGAATCCC---ACTCGGATTCCGCGGCCCTTTTGTTTTGTC
Kitasatospora aureofaciens (769) GGCACC-TCCAGGGCCGCGGAACCCGTCACACCGGGATCCGCGGCCCTTCTGTTTTGTC
Kitasatospora setae (606) GGTGCC-TCCAGGGCCGCGGAAACCCAGCAACCGGGTTCCGCGGCCCTTCTGTTTTGTC
Streptacidiphilus albus (589) GGCAA--TCCAGGGCCGCGGAATCCC---ACTCGGGATCCGCGGCCCTTCTGTTT-GCC
Streptacidiphilus jiangxiensis (652) GGCACCTTCCAGGGCCGCGGAA-CCCG--AATCGGGATCCGCGGCCCTTCTGTTT-GCC
Streptacidiphilus rugosus (608) GGCGC-TTCCAGGGCCGCGGATTCCCG--AATCGGGATCCGCGGCCCTTCTGTTT-GCC
Streptomyces avermitilis (502) GGCGCC-TTCAGGGCCGCGGAACCCC---ACCCGGGATCCGCGGCCCTTCTGTTTGTCC
Streptomyces coelicolor (515) GGCGCC-TTCAGGGCCGCGGAACCCC---ACCCGGGATCCGCGGCCCTTCTGTTTGTCC
Streptomyces venezuelae (545) GGCGCC-TTCAGGGCCGCGGAACCCC---ACCCGGGATCCGCGGCCCTTTTGTTTGTCC
Consensus (808) GGC C T CAGGGCCGCGGAA CCC A CGGG TCCGCGGCCCTT TGTTT C
B
Mycobacterium
(541) 541 550 560 570 580 590 601
M. abscessus (457) TGTCGCGTCCGTGAATAGG---GGATACATCTAGGT------------------ATCCCC
M. avium (247) CGACGCGTCCGTACGAGTCGGGGGCCCGCCGAAGGCAAGGTAA------G-CACCAGCCCG
M. kansasii (248) TGACGCGTCCGTGGA--TC-GGAGCCCAACGTAGACACCTAGACACTGCGTAAC-AGCCC-
M. leprae (273) GAACCCGTCCGTGGA--TC-GGGGCTATACTGAACTACGA----------AGTC-AGCCCG
M. marinum (254) TGACTCGTCCGTGGA--TC-GGAGCCCAACGTAGGCACTACGTAA----------GCCCG
M. phlei (332) ----CTGTCCGTGGA--TC-GGAGCCTCATCTAGAA-----------------GCTC-
M. smegmatis (322) AAGCGCGTCCGTGGA--TC-GGAGCCCCTTCTAGGTAGAG---------------GCTTCA
M. tuberculosis (247) TGACGAGTCCGTGGA--GC-GGGGCTCTACGTAAGCGCTAC--------GTAATCAGCCC-
M. vaccae (259) GGTTGCGTCCGTGAG--GG-GCCACCTCTAG--------------------GTAGAGCCC-
M. xenopi (248) CGAAATGTCCGTGGA--TC-GAGGCTTCACGTAAGTCCCAG--------CTAACCGGC---
Consensus (541) GACGCGTCCGTGGA TC GGGGCCCCACGTAGG AC AGCCC
Rho-independent terminator
(602) 602 610 620 630 640 650 662
M. abscessus (496) ACAACCGCCTCCCAGGCCACGGACCCGACACCACCGGGATCCGTGGCCACATTTGTTTGAG
M. avium (301) GTTTTC-CCCAGATGGCCACGGACCCGAAGTCACCAGGATCCGTGGCCATAGTTGTTGGGT
M. kansasii (304) AGATTCG-CCTAATGGCCACGG-ACCGAAGTCACCAGGATCCGTGGCCAAATTTGTTGGG-
M. leprae (320) ATTTTCGCC-AGATGGCCACGGAACCGAAATCACCAGGATCCGTGGCACAGTTTTTGGGC-
M. marinum (301) ATTTTCGCCCAAGTGGCCACGG-ACCTCAGTCACCAGGATCCGTGGCCAATTTTTTTTTG-
M. phlei (365) CCGATAACCA-GAAGGCCACGGACTCGCAGTCAG--GGATCCGTGGCCTTGGTCTTTTCCA
M. smegmatis (365) -CACCAGCCGAAAAGGCCACGGACCCGCAGTCACCCGGATCCGTGGCCATTTTTGTCGG--
M. tuberculosis (296) CGTTTCGCCAG-ATGGCCACGGACCCGAAGTCAC-AGGATCCGTGGCCAAAC--TTTCGG-
M. vaccae (296) CGAATCGCCTTCCAGGCCACGGACCCGCAATCAC--GGATCCGTGGCCTTTGTCATTCCT-
M. xenopi (295) ---AACGC----CTGGCCACGGACCCCGA----T-GAGATCCGTGGCCAGTC--GTTTC--
Consensus (602) TTCGCC ATGGCCACGGACCCGAAGTCACCAGGATCCGTGGCCA TTTGTT G

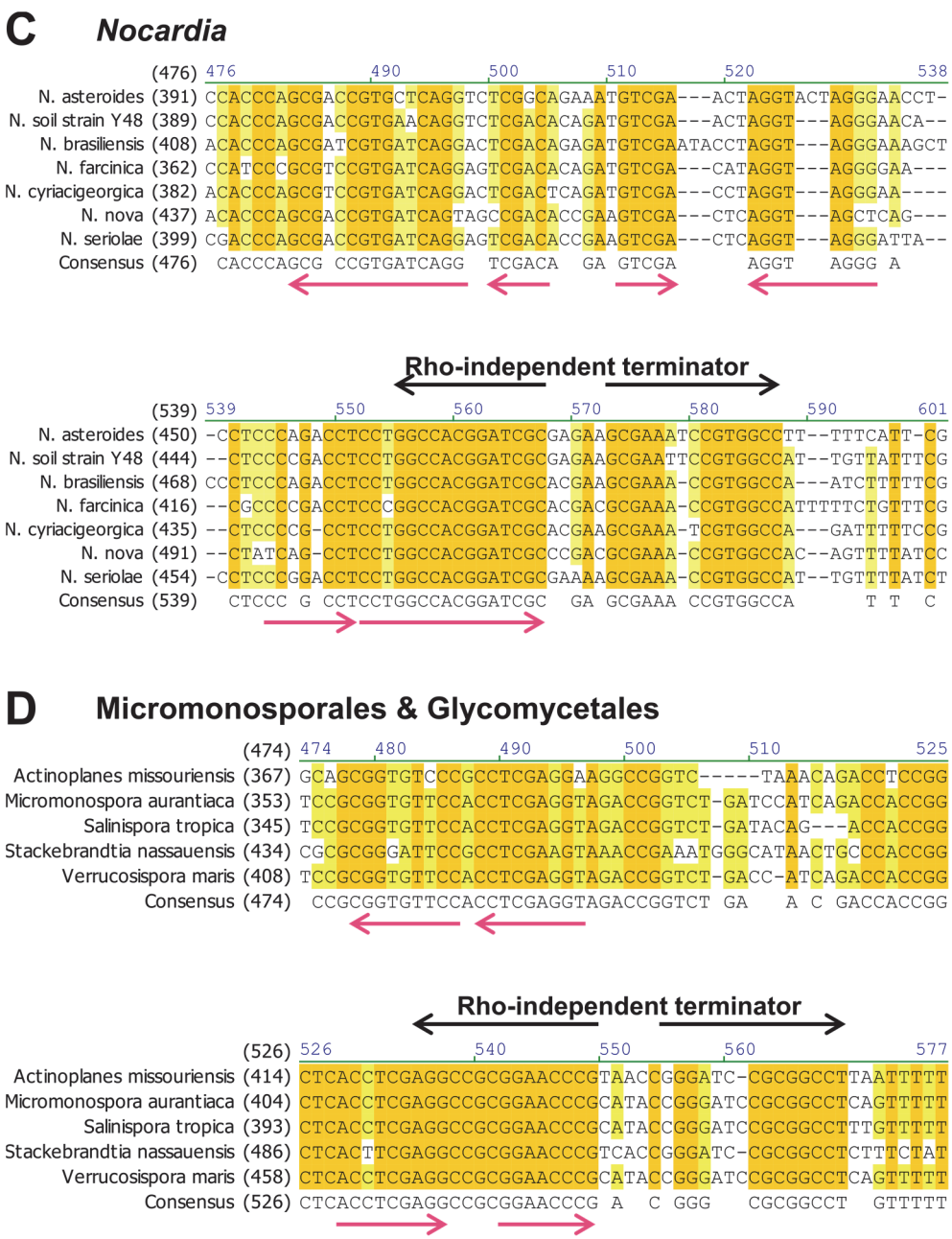

Figure 5-4. Conservation of RIT-overlapping multiple palindromes in *wblC*/*whiB7* leader sequences of each sub-clade of actinomycetes.
Sequence alignment of *wblC*/*whiB7* leader sequences of order Streptomycetales (A), genus *Mycobacteria* (B), genus *Nocardia* (C), and orders Micromonosporales and Glycomycetales (D). The conserved palindromes are denoted below aligned sequences as pairs of divergent arrows in magenta. Bases conserved in 100% (orange shade) and ≥80% (yellow shade) of the aligned sequences are indicated.

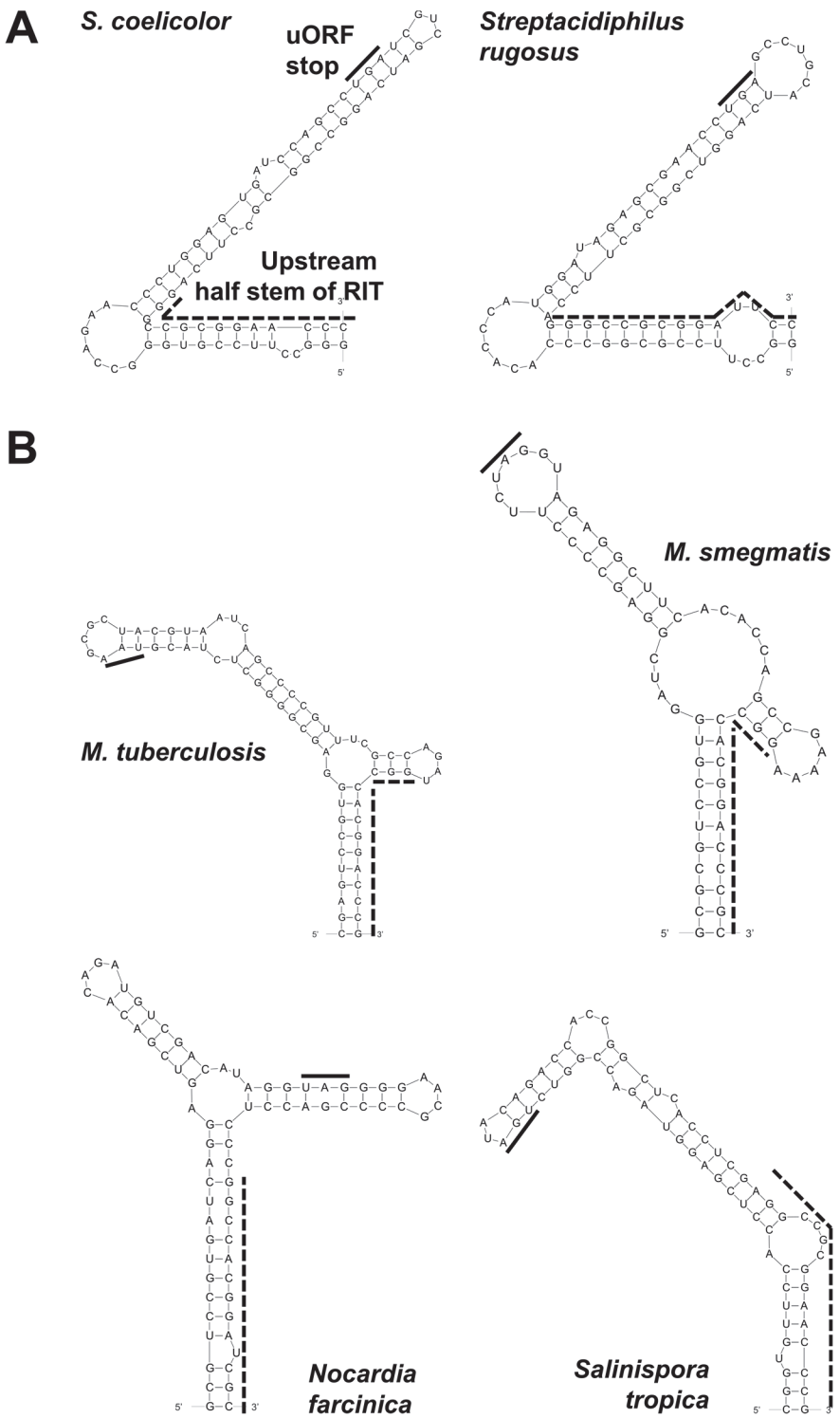

Figure 5-5. Putative antiterminator structures in *wblC*/*whiB7* leader sequences of streptomycetales (A) and other actinomycetes (B).
Upstream half stem (dashed lines) and uORF stop codon (solid lines) are indicated.

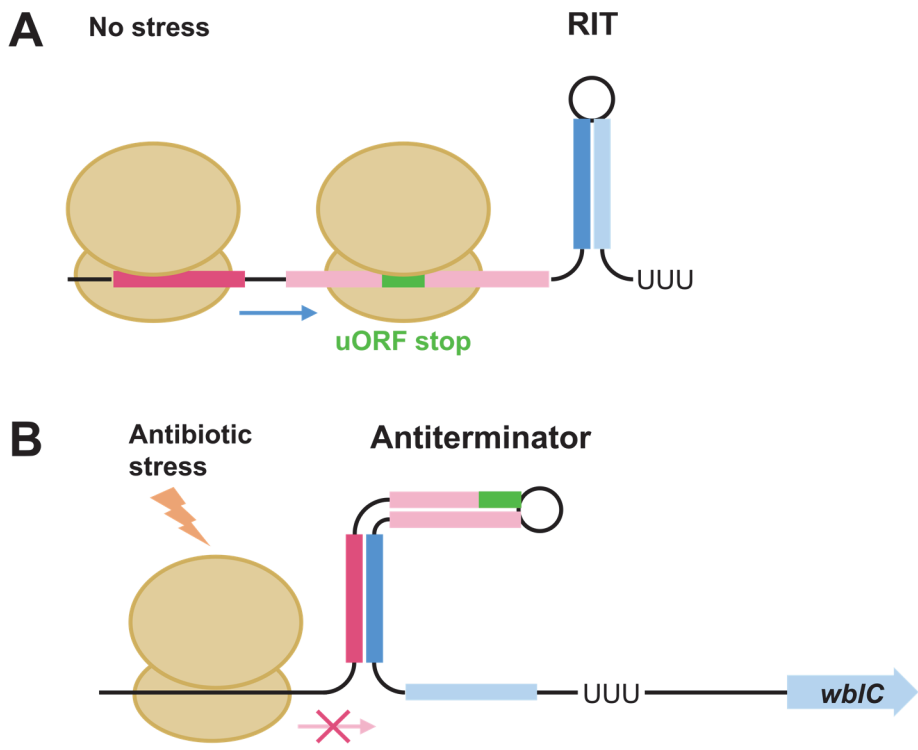

Figure 5-6. Models of transcriptional attenuation (A) and conditional anti-termination (B) at *wblC* leader RIT.
Ribosome-mediated sensing of antibiotic stress leads to suppression of premature termination at leader RIT by formation of the antiterminator RNA structure. U, uridine.

5-4. Transcription readthrough caused by antiterminator formation during antibiotic stress

Functionality of the predicted antiterminator was tested in *wblC* leader sequence of *S. coelicolor* by disrupting the putative antiterminator sequence that would pair with the region of 'Up-switched' variation of RIT (Figure 5-7A). This 'Anti-switched' *wblC* leader exhibited constitutive attenuation regardless of antibiotic stress, which is even greater than the partial decrease in readthrough ratio by 'Swap-paired' sequence variation (Figure 5-7B).

I also checked if these sequence variations would affect WblC-dependent induction of antibiotic resistance. Growth of ΔuORF*wblC* with an empty vector was inhibited by low concentrations of antibiotics, whereas complementation with the vector carrying wild-type *wblC* operon increased resistance to erythromycin, tetracycline, and lincomycin by 64-fold, 8-fold, and 2-fold (Figure 5-8). Introduction of 'Anti-switched' *wblC* operon was practically incapable of antibiotic resistance recovery, demonstrating that impairing the antiterminator nullifies WblC-mediated antibiotic resistance. On the other hand, 'Swap-paired' *wblC* operon had partial effect in recovering antibiotic resistance, being 4-fold defective than the wild-type operon in recovering erythromycin resistance but equally efficient in recovering tetracycline and lincomycin resistance (Figure 5-8). This is likely due to the partial antitermination activity of 'Swap-paired' *wblC* leader (Figure 5-7B). Collectively, these results show that the antiterminator causes transcription readthrough of *wblC* leader RIT during antibiotic stress and subsequent induction of WblC-dependent multidrug resistance.

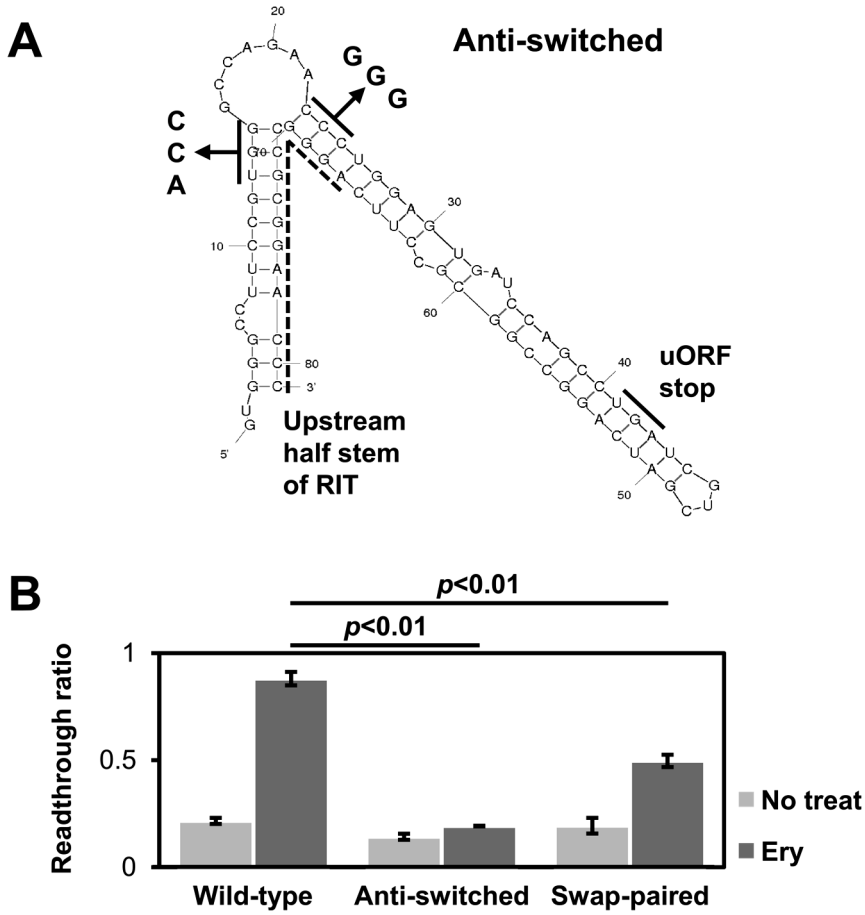

Figure 5-7. Effects of sequence variations in the putative antiterminator on *wblC* leader readthrough ratio.
(A) The 'Anti-switched' sequence variation. Regions switched into complementary sequences are indicated. (B) Readthrough ratio was assessed by qRT-PCR in untreated (No treat) and erythromycin (Ery)-treated conditions. Error bars indicate mean±standard error of 3 biologically independent experiments. Student's *t*-test *p*-values (*p*) are denoted for each comparison.

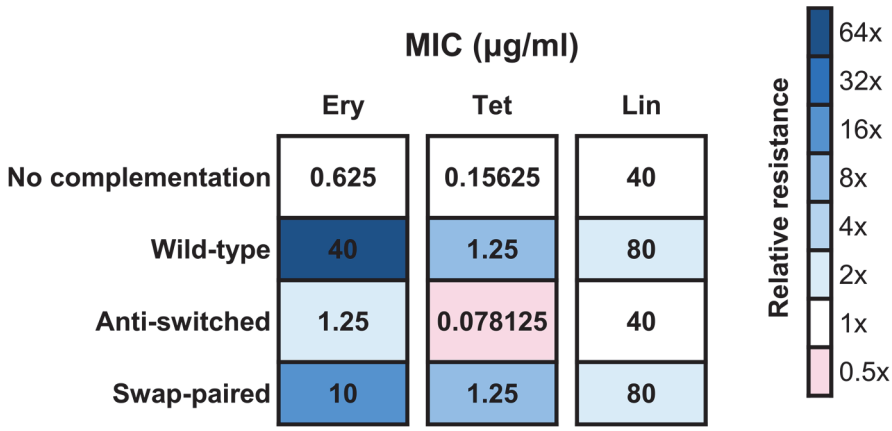

Figure 5-8. Antibiotic resistance profiles of ΔuORF*wblC* complemented with *wblC* operons possessing antiterminator sequence variations.
Presented values are median MIC of three independent experiments. Background color indicates resistance of a strain to the antibiotic compared to the resistance of the reference strain ΔuORF*wblC*+pSET162 (No complementation). Ery, erythromycin; Tet, tetracycline; Lin, lincomycin.

5-5. Induction of *wblC* by amino acid starvation

Because *wblC* is induced by numerous translation-inhibitory antibiotics of different mode of action, I suspected that other translation stress conditions may induce *wblC* expression as well. By monitoring *wblC* RNA level at different conditions, I discovered that treatment of serine hydroxamate, a seryl-tRNA synthetase inhibitor induces *wblC* (Figure 5-9A), implying that insufficient supply of serine during translation can cause induction of *wblC*. Changing the culture medium into NMMP without casamino acids in the middle of early-mid exponential growth also induced *wblC* (Figure 5-9B). On the contrary, *wblC* was not induced when the medium was changed into either normal, ammonium-deficient, or sodium-potassium-phosphate buffer-deficient NMMP, and weakly induced when the medium was changed into glucose-deficient NMMP (Figure 5-9B). mRNA levels of WblC regulon genes were also increased by changing the medium to NMMP without casamino acids, in a *wblC*-dependent manner (Figure 5-10). Amino acid starvation seems to be the common cause of *wblC* induction by serine hydroxamate treatment and the medium change.

Translation decrease upon amino acid starvation could be either a direct result of short substrate supply to protein synthesis or due to stringent response that is signaled by guanosine tetraphosphate (ppGpp, also known as alarmone). In wild type (strain M600) and *relA* knockout strain (M570) that is incapable of ppGpp synthesis (Chakraburtty and Bibb, 1997), medium change into NMMP without casamino acid induced *wblC* to an identical degree (Figure 5-11), disproving the involvement of ppGpp signaling in *wblC* induction by amino acid starvation. Meanwhile, *wblC* was induced by medium change into NMMP without casamino acid in a similar kinetics with induction by tetracycline treatment. Swift achievement of a nearly full induction of *wblC* was observed in both conditions (Figure 5-12), implying that the mode of induction is similar. I therefore observed if amino acid starvation causes anti-termination at *wblC* leader sequence and

observed an increased readthrough of leader RIT upon medium change to NMMP without casamino acids (Figure 5-13). In summary, ribosome-mediated attenuation of *wblC* can directly sense decreased supply of amino acid during translation of uORF.

I also found that expression of *wblC* is slightly increased from mid-late exponential phase to transition phase, which is the period of entering stationary phase (Figure 5-14A). Interestingly, growth of Δ*wblC* was significantly retarded in comparison with wild type at during transition to stationary phase (Figure 5-14B), indicating the role of WblC and WblC regulon gene products at this timing when of culture medium becomes depleted of nutrients.

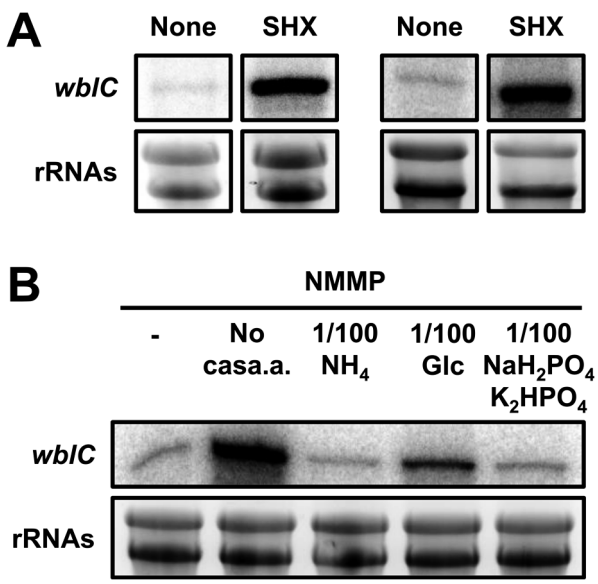

Figure 5-9. Induction of *wblC* by amino acid starvation.
S1 nuclease protection assay of *wblC* mRNA. 23S and 16S rRNAs are shown as control. (A) RNA levels before (None) and after 25 mM serine hydroxamate (SHX) treatment for 30 min. (B) RNA levels 30 min after changing medium into either normal NMMP (-) or NMMPs of modified compositions; without casamino acids (No casa.a.), with 1/100 NH_4, with 1/100 glucose (Glc), or with 1/100 NaH_2PO_4/K_2HPO_4 buffer.

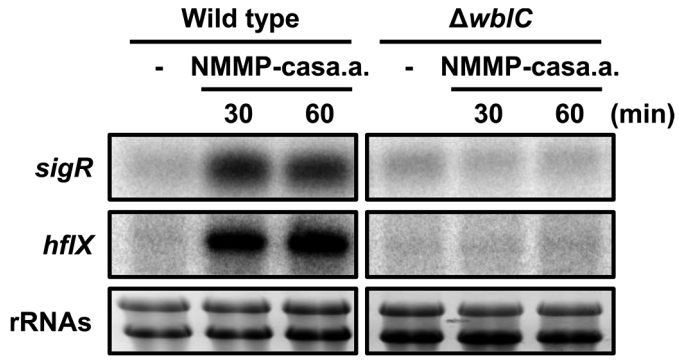

Figure 5-10. WblC-dependent upregulation of WblC regulon genes during amino acid starvation.
S1 nuclease protection assay of mRNAs. 23S and 16S rRNAs are shown as control. NMMP-casa.a., change of medium into NMMP without casamino acids.

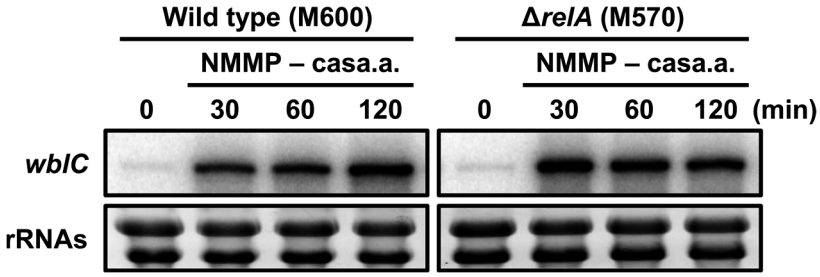

Figure 5-11. Irrelevance of *wblC* induction by amino acid starvation with ppGpp signaling.
S1 nuclease protection assay of *wblC* mRNA. 23S and 16S rRNAs are shown as control. NMMP-casa.a., change of medium into NMMP without casamino acids.

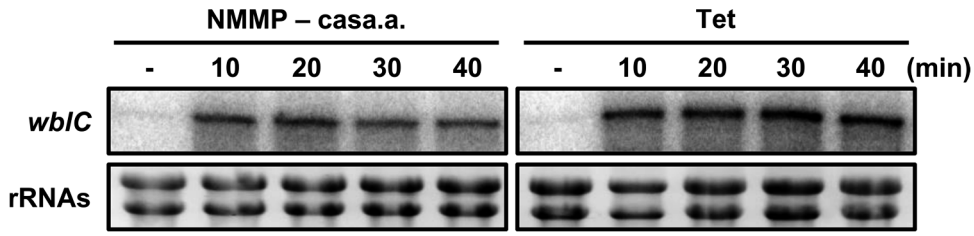

Figure 5-12. Time-course observation of *wblC* induction by amino acid starvation and tetracycline treatment.
S1 nuclease protection assay of *wblC* mRNA. 23S and 16S rRNAs are shown as control. NMMP-casa.a., change of medium into NMMP without casamino acids; Tet, 2 μg/ml tetracycline treatment.

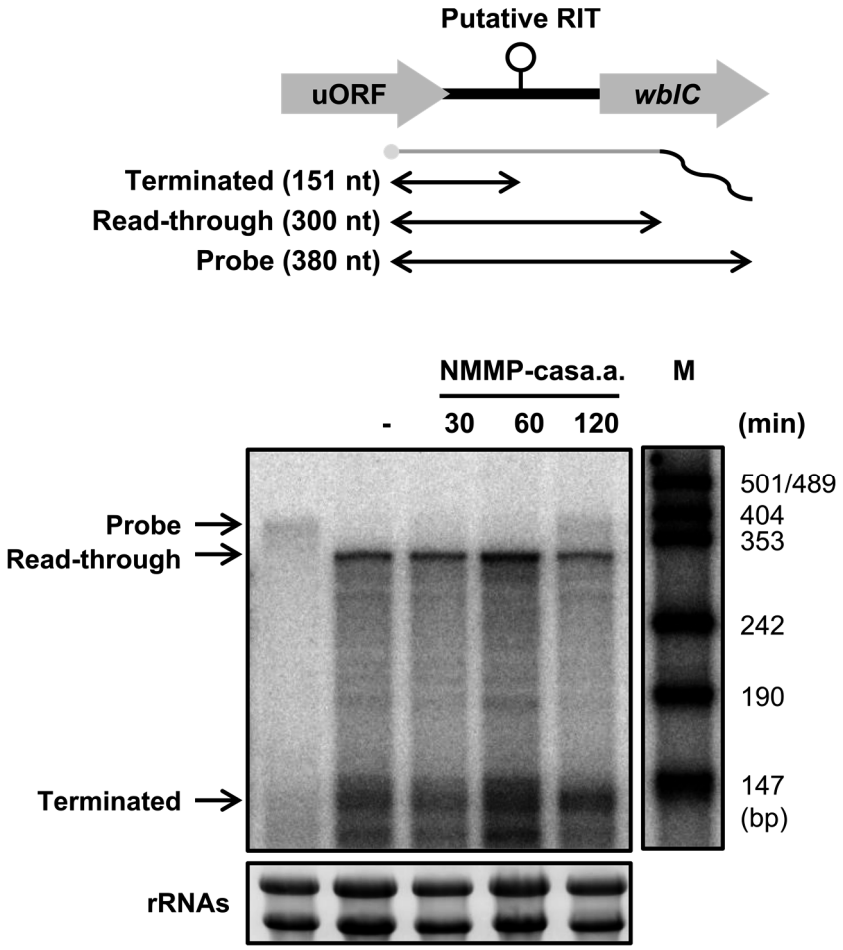

Figure 5-13. Effect of amino acid starvation on premature termination at *wblC* leader RIT.
3' end S1 nuclease mapping of *wblC* leader RNA. 23S and 16S rRNAs are shown as control. Radiolabeled DNA size marker (M) is shown in parallel. NMMP-casa.a., change of medium into NMMP without casamino acids.

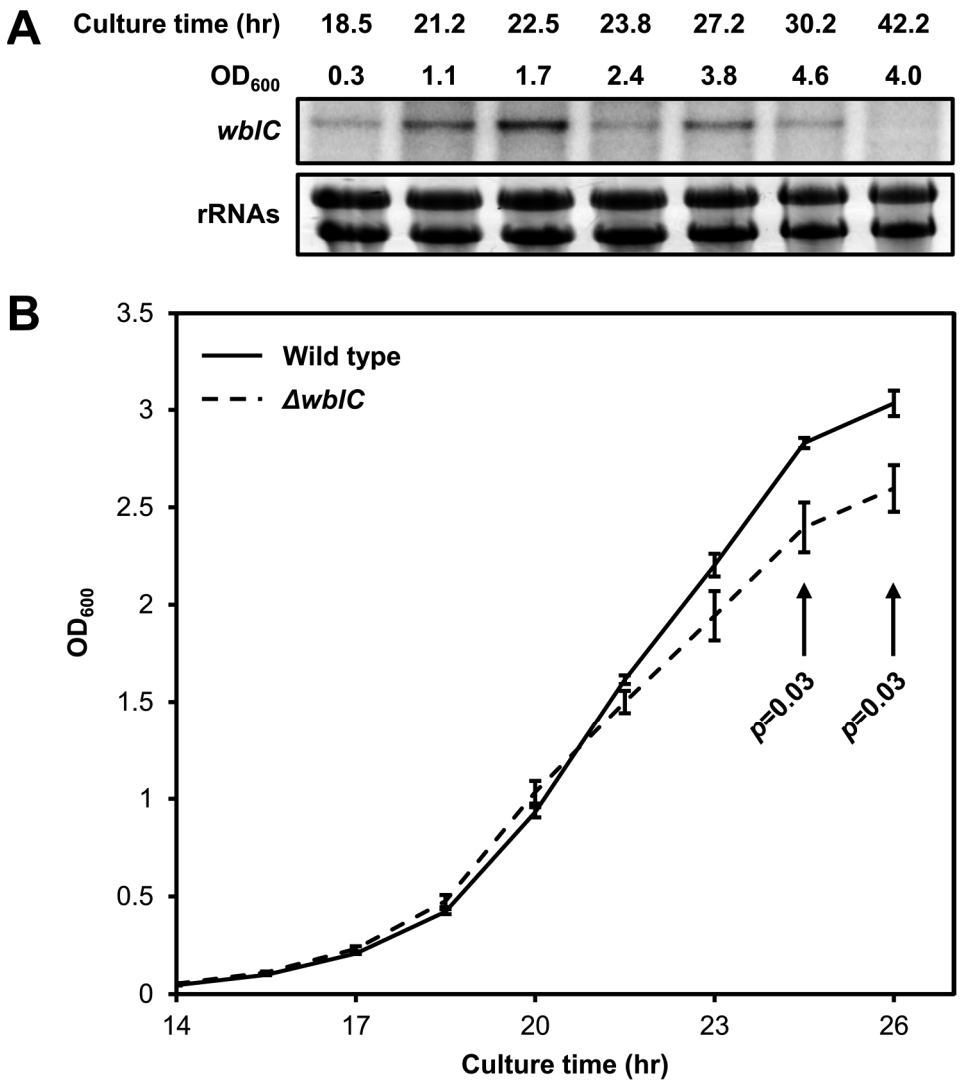

Figure 5-14. The role of *wblC* in growth during transition phase.
(A) S1 nuclease protection assay of *wblC* mRNA. 23S and 16S rRNAs are shown as control. (B) Growth of wild type and Δ*wblC*. Error bars indicate mean±standard error of 3 independent experiments. Student's *t*-test *p*-values (*p*) are denoted for each comparison between strains.

Chapter 6. Discussion

6-1. Transcriptional regulation by WblC

WblC exerts its regulatory function over a great number of genes. 312 genes, or 4% of the chromosomal genes of *S. coelicolor*, were found in this study to be directly regulated by WblC, as well as a number of noncoding RNA targets. MarA, another antibiotic-responsive transcriptional regulator, is also known to bind to >30 locations in *E. coli* genome and either directly or indirectly regulate expression of >60 genes (Barbosa and Levy, 2000; Sharma et al., 2017). However, no many bacterial transcription factors are known to globally control hundreds of target genes (Martinez-Antonio and Collado-Vides, 2003) (see also; regulondb.ccg.unam.mx (Santos-Zavaleta et al., 2019)). Meanwhile, the composition of WblC/WhiB7 regulon is highly variable among species (Hurst-Hess et al., 2017; Morris et al., 2005). This vast and variable regulation by WblC/WhiB7 orthologs may be due, in part, to the fact that WblC is a principal sigma factor-interacting monomeric transcriptional regulator, as most WhiB-like proteins (Feng et al., 2016). The sequence requirement of WblC target promoters is quite little; a few adenine or thymine at certain positions upstream of -35 element, as discovered in this study. Low sequence specificity of WblC is also probably the reason why WblC binding was observed in 830 locations in *S. coelicolor* genome but only about 200 of them corresponds to WblC-regulated promoters. Also, this could be the reason why the WhiB7 regulon of human pathogen *M. tuberculosis* is so compact in comparison with that of *M. smegmatis*, *M. abscessus*, and *S. coelicolor*. The pathogen would encounter antibiotic stress by much less chance than the environmental microbes *Streptomyces* or *M. smegmatis* and *M. abscessus*, which could have prompted erosion of antibiotic-responsive regulation by WhiB7. Low sequence specificity of WblC would probably facilitate diversification of the

composition of WblC/WhiB7 regulon across species and strains, which can lead to different intrinsic resistance profiles controlled by WblC/WhiB7 (Ramon-Garcia et al., 2013). Moreover, this may be a general situation for other WhiB-family transcriptional regulators that commonly exhibits low sequence specificity (Bush, 2018).

Another interesting discovery regarding gene regulation by WblC is that expression of several genes seem to be repressed by direct regulation of WblC. 24 genes exhibited both WblC binding at promoters and *wblC*-dependent decrease of mRNA level. WblC bound to these 'WblC-repressed' promoters in a different mode from WblC-HrdB complex binding seen in WblC-activated promoters. This can be indicating that WblC functions as a regulator and a repressor on different target genes, which was suggested as well for another WhiB-like regulator WhiB1 of *M. tuberculosis* (Kudhair et al., 2017), Alternatively, WblC binding to these promoters and *wblC*-dependent decrease in expression may just be a coincidence. The large number of WblC-binding locations across *S. coelicolor* genome may have caused such coincidence at multiple genes of which expression level are indirectly decreased by WblC. Further studies are required to verify a causal relationship between WblC binding and *wblC*-dependent downregulation of these genes.

6-2. Antibiotic resistance and functions of WblC regulon

The *S. coelicolor* WblC regulon comprehend many intrinsic resistance mechanisms to translation-inhibitory antibiotics. Antibiotic resistance genes of both established mechanisms and newly discovered genes were included in WblC regulon. Considering both the extent of transcriptional regulation exerted by WblC over hundreds of genes and the spectrum of antibiotic resistance conferred by the genes, WblC seems to be a regulatory hub of transcriptional responses that helps to resist translation inhibition by multiple classes of antibiotics. Resistance-conferring

mechanisms of novel antibiotic resistance genes discovered in this study, *hrpA* and SCO2532 protein, is yet unknown and deserves further investigations. SCO2532 protein is likely to be functioning in concert with SCO2533 protein, the ortholog of *E. coli* YbeY. HrpA have been reported to regulate gene expression at a post-transcriptional level in *E. coli* and Lyme disease-causing spirochete (Koo et al., 2004; Salman-Dilgimen et al., 2011; Salman-Dilgimen et al., 2013), so I guess HrpA would be functioning on its target mRNAs as associated to ribosome during *S. coelicolor* under antibiotic stress as well.

Many other ribosome-associated proteins encoded by WblC-upregulated regulon may contribute to intrinsic resistance. Highly promising candidates are Hsp15, ArfB, HelY, Der, and SCO5707. Although Δ*helY* and Δ*arfB* were not susceptible to erythromycin, tetracycline, and lincomycin, there still is a chance that *helY* and *arfB* may contribute to antibiotic resistance. It should be noted that antibiotic susceptibility of the mutants could not be tested for several aminoglycosides to which *aac(3)IV* that replaces gene of interest during knockout is known to confer cross-resistance (Gust et al., 2003; Kieser et al., 2000). Regarding ArfB, no specific stress condition and regulator that induces expression of this ribosome rescue factor have been reported to my knowledge, and induction of ArfB by WblC during antibiotic stress is the first one to be reported.

I also proposed that functions of WblC and its regulon products seems to be required during nutrient-starving conditions during prolonged culture. Presumably, that many translation-enhancing functions of WblC regulon would be involved in this phenomenon. Similarly, WblC regulon genes may be either induced or promote growth at other translation stresses such as heat shock.

6-3. The mechanism of *wblC* induction by translation stress

In this study, the model of ribosome-mediated transcriptional attenuation of

wblC/*whiB7* expression was revised to include the mechanism of conditional *wblC* induction by formation of antiterminator RNA structure in response to defect in translation. One interesting point was that the antiterminator is differently conserved in the sub-clades of actinomycetes, in contrast to the conservation of RIT across actinomycetes. This may indicate the greater importance of attenuating *wblC* expression than the importance of inducing it to the overall fitness of bacteria to the environment. Minor defects caused by sequence alterations in the antiterminator would not harm normal growth as WblC seems to have little role in the absence of translation stress, as demonstrated by the comparative transcriptome analysis of wild type and Δ*wblC*, which could have allowed variations in the antiterminator sequence and structure. On the contrary, uncontrolled expression of *wblC* may be detrimental to bacteria, which is in accordance with the common understanding that antibiotic resistance mechanisms impose a fitness cost to bacteria and thus need to be regulated for conditional expression.

One important remaining question about antibiotic-responsive induction of *wblC*/*whiB7* is the broad spectrum of inducers (Burian et al., 2012a). Some of the well-studied examples of antibiotic-responsive attenuation, such as *ermC* leader and *catA86* leader, exhibit high antibiotic selectivity, which is determined by ribosome stalling at certain region in uORF due to specific nascent peptide sequence that promotes stalling (Gupta et al., 2016; Lovett, 1996). This may be due to the striking length of *wblC*/*whiB7* leader uORF. The *wblC*/*whiB7* uORF is composed of 111 codons in *S. coelicolor*, 80 codons in *M. smegmatis*, and 41 codons in *M. tuberculosis*. These lengthy uORF may either encode multiple peptide sequence motifs that collectively endow responsiveness to multiple classes of antibiotics, or the length of uORF itself may form a sensor of translation rate. It should be considered that uORF-encoded peptide sequence is not conserved among *wblC*/*whiB7* leader sequences, which seems to be discordant with the former possibility. Further investigations are needed to discriminate these two possibilities, and sensitivity of *wblC* attenuation to amino acid starvation may aid the endeavor.

Bibliography

Agarwal, N., and Tyagi, A.K. (2006). Mycobacterial transcriptional signals: requirements for recognition by RNA polymerase and optimal transcriptional activity. Nucleic Acids Res *34*, 4245-4257.

Ainsa, J.A., Blokpoel, M.C., Otal, I., Young, D.B., De Smet, K.A., and Martin, C. (1998). Molecular cloning and characterization of Tap, a putative multidrug efflux pump present in Mycobacterium fortuitum and Mycobacterium tuberculosis. Journal of bacteriology *180*, 5836-5843.

Aminov, R.I., and Mackie, R.I. (2007). Evolution and ecology of antibiotic resistance genes. FEMS Microbiol Lett *271*, 147-161.

Andrews, E.S., and Arcus, V.L. (2015). The mycobacterial PhoH2 proteins are type II toxin antitoxins coupled to RNA helicase domains. Tuberculosis (Edinb) *95*, 385-394.

Arifuzzaman, M., Maeda, M., Itoh, A., Nishikata, K., Takita, C., Saito, R., Ara, T., Nakahigashi, K., Huang, H.C., Hirai, A.*, et al.* (2006). Large-scale identification of protein-protein interaction of Escherichia coli K-12. Genome Res *16*, 686-691.

Bailey, T.L., Boden, M., Buske, F.A., Frith, M., Grant, C.E., Clementi, L., Ren, J., Li, W.W., and Noble, W.S. (2009). MEME SUITE: tools for motif discovery and searching. Nucleic Acids Res *37*, W202-208.

Barbosa, T.M., and Levy, S.B. (2000). Differential expression of over 60 chromosomal genes in Escherichia coli by constitutive expression of MarA. Journal of bacteriology *182*, 3467-3474.

Basu, A., and Yap, M.N. (2017). Disassembly of the Staphylococcus aureus hibernating 100S ribosome by an evolutionarily conserved GTPase. Proceedings of the National Academy of Sciences of the United States of America *114*, E8165-E8173.

Bedard, A.V., Hien, E.D.M., and Lafontaine, D.A. (2020). Riboswitch regulation mechanisms: RNA, metabolites and regulatory proteins. Biochim Biophys Acta Gene Regul Mech *1863*, 194501.

Bharat, A., and Brown, E.D. (2014). Phenotypic investigations of the depletion of EngA in Escherichia coli are consistent with a role in ribosome biogenesis. FEMS Microbiol Lett *353*, 26-32.

Bierman, M., Logan, R., O'Brien, K., Seno, E.T., Rao, R.N., and Schoner, B.E. (1992). Plasmid cloning vectors for the conjugal transfer of DNA from Escherichia coli to Streptomyces spp. Gene *116*, 43-49.

Blair, J.M., Webber, M.A., Baylay, A.J., Ogbolu, D.O., and Piddock, L.J. (2015). Molecular mechanisms of antibiotic resistance. Nature reviews Microbiology *13*, 42-51.

Bolger, A.M., Lohse, M., and Usadel, B. (2014). Trimmomatic: a flexible trimmer for Illumina sequence data. Bioinformatics *30*, 2114-2120.

Brodersen, D.E., Clemons, W.M., Jr., Carter, A.P., Morgan-Warren, R.J., Wimberly, B.T., and Ramakrishnan, V. (2000). The structural basis for the action of the antibiotics tetracycline, pactamycin, and hygromycin B on the 30S ribosomal subunit. Cell *103*, 1143-1154.

Burdett, V. (1996). Tet(M)-promoted release of tetracycline from ribosomes is GTP dependent. Journal of bacteriology *178*, 3246-3251.

Burian, J., Ramon-Garcia, S., Howes, C.G., and Thompson, C.J. (2012a). WhiB7, a transcriptional activator that coordinates physiology with intrinsic drug resistance in Mycobacterium tuberculosis. Expert Rev Anti Infect Ther *10*, 1037-1047.

Burian, J., Ramon-Garcia, S., Sweet, G., Gomez-Velasco, A., Av-Gay, Y., and Thompson, C.J. (2012b). The mycobacterial transcriptional regulator whiB7 gene links redox homeostasis and intrinsic antibiotic resistance. The Journal of biological chemistry *287*, 299-310.

Burian, J., and Thompson, C.J. (2018). Regulatory genes coordinating antibiotic-

induced changes in promoter activity and early transcriptional termination of the mycobacterial intrinsic resistance gene whiB7. Molecular microbiology *107*, 402-415.

Burian, J., Yim, G., Hsing, M., Axerio-Cilies, P., Cherkasov, A., Spiegelman, G.B., and Thompson, C.J. (2013). The mycobacterial antibiotic resistance determinant WhiB7 acts as a transcriptional activator by binding the primary sigma factor SigA (RpoV). Nucleic Acids Res *41*, 10062-10076.

Buroni, S., Manina, G., Guglierame, P., Pasca, M.R., Riccardi, G., and De Rossi, E. (2006). LfrR is a repressor that regulates expression of the efflux pump LfrA in Mycobacterium smegmatis. Antimicrob Agents Chemother *50*, 4044-4052.

Bush, M.J. (2018). The actinobacterial WhiB-like (Wbl) family of transcription factors. Molecular microbiology *110*, 663-676.

Butland, G., Peregrin-Alvarez, J.M., Li, J., Yang, W., Yang, X., Canadien, V., Starostine, A., Richards, D., Beattie, B., Krogan, N.*, et al.* (2005). Interaction network containing conserved and essential protein complexes in Escherichia coli. Nature *433*, 531-537.

Carter, A.P., Clemons, W.M., Brodersen, D.E., Morgan-Warren, R.J., Wimberly, B.T., and Ramakrishnan, V. (2000). Functional insights from the structure of the 30S ribosomal subunit and its interactions with antibiotics. Nature *407*, 340-348.

Chadani, Y., Ono, K., Kutsukake, K., and Abo, T. (2011). Escherichia coli YaeJ protein mediates a novel ribosome-rescue pathway distinct from SsrA- and ArfA-mediated pathways. Molecular microbiology *80*, 772-785.

Chakraburtty, R., and Bibb, M. (1997). The ppGpp synthetase gene (relA) of Streptomyces coelicolor A3(2) plays a conditional role in antibiotic production and morphological differentiation. Journal of bacteriology *179*, 5854-5861.

Chakravorty, S., Lee, J.S., Cho, E.J., Roh, S.S., Smith, L.E., Lee, J., Kim, C.T., Via,

L.E., Cho, S.N., Barry, C.E., 3rd, *et al.* (2015). Genotypic susceptibility testing of Mycobacterium tuberculosis isolates for amikacin and kanamycin resistance by use of a rapid sloppy molecular beacon-based assay identifies more cases of low-level drug resistance than phenotypic Lowenstein-Jensen testing. J Clin Microbiol *53*, 43-51.

Chandra, G., and Chater, K.F. (2014). Developmental biology of Streptomyces from the perspective of 100 actinobacterial genome sequences. FEMS microbiology reviews *38*, 345-379.

Chater, K.F. (2016). Recent advances in understanding Streptomyces. F1000Res *5*, 2795.

Chen, W., Biswas, T., Porter, V.R., Tsodikov, O.V., and Garneau-Tsodikova, S. (2011). Unusual regioversatility of acetyltransferase Eis, a cause of drug resistance in XDR-TB. Proceedings of the National Academy of Sciences of the United States of America *108*, 9804-9808.

Cheverton, A.M., Gollan, B., Przydacz, M., Wong, C.T., Mylona, A., Hare, S.A., and Helaine, S. (2016). A Salmonella Toxin Promotes Persister Formation through Acetylation of tRNA. Molecular cell *63*, 86-96.

Coatham, M.L., Brandon, H.E., Fischer, J.J., Schummer, T., and Wieden, H.J. (2016). The conserved GTPase HflX is a ribosome splitting factor that binds to the E-site of the bacterial ribosome. Nucleic Acids Res *44*, 1952-1961.

Cox, G., and Wright, G.D. (2013). Intrinsic antibiotic resistance: mechanisms, origins, challenges and solutions. Int J Med Microbiol *303*, 287-292.

Crooks, G.E., Hon, G., Chandonia, J.M., and Brenner, S.E. (2004). WebLogo: a sequence logo generator. Genome Res *14*, 1188-1190.

Cundliffe, E., and Demain, A.L. (2010). Avoidance of suicide in antibiotic-producing microbes. J Ind Microbiol Biotechnol *37*, 643-672.

D'Costa, V.M., King, C.E., Kalan, L., Morar, M., Sung, W.W., Schwarz, C., Froese, D., Zazula, G., Calmels, F., Debruyne, R., *et al.* (2011). Antibiotic

resistance is ancient. Nature *477*, 457-461.

D'Costa, V.M., McGrann, K.M., Hughes, D.W., and Wright, G.D. (2006). Sampling the antibiotic resistome. Science *311*, 374-377.

Dar, D., Shamir, M., Mellin, J.R., Koutero, M., Stern-Ginossar, N., Cossart, P., and Sorek, R. (2016). Term-seq reveals abundant ribo-regulation of antibiotics resistance in bacteria. Science *352*, aad9822.

Dar, D., and Sorek, R. (2017). Regulation of antibiotic-resistance by non-coding RNAs in bacteria. Current opinion in microbiology *36*, 111-117.

De Rossi, E., Blokpoel, M.C., Cantoni, R., Branzoni, M., Riccardi, G., Young, D.B., De Smet, K.A., and Ciferri, O. (1998). Molecular cloning and functional analysis of a novel tetracycline resistance determinant, tet(V), from Mycobacterium smegmatis. Antimicrob Agents Chemother *42*, 1931-1937.

Dersch, P., Khan, M.A., Muhlen, S., and Gorke, B. (2017). Roles of Regulatory RNAs for Antibiotic Resistance in Bacteria and Their Potential Value as Novel Drug Targets. Front Microbiol *8*, 803.

Dey, S., Biswas, C., and Sengupta, J. (2018). The universally conserved GTPase HflX is an RNA helicase that restores heat-damaged Escherichia coli ribosomes. J Cell Biol *217*, 2519-2529.

Dinan, A.M., Tong, P., Lohan, A.J., Conlon, K.M., Miranda-CasoLuengo, A.A., Malone, K.M., Gordon, S.V., and Loftus, B.J. (2014). Relaxed selection drives a noisy noncoding transcriptome in members of the Mycobacterium tuberculosis complex. MBio *5*, e01169-01114.

Donhofer, A., Franckenberg, S., Wickles, S., Berninghausen, O., Beckmann, R., and Wilson, D.N. (2012). Structural basis for TetM-mediated tetracycline resistance. Proceedings of the National Academy of Sciences of the United States of America *109*, 16900-16905.

Duan, W., Li, X., Ge, Y., Yu, Z., Li, P., Li, J., Qin, L., and Xie, J. (2019). Mycobacterium tuberculosis Rv1473 is a novel macrolides ABC Efflux Pump regulated by WhiB7. Future Microbiol *14*, 47-59.

Dunkle, J.A., Xiong, L., Mankin, A.S., and Cate, J.H. (2010). Structures of the Escherichia coli ribosome with antibiotics bound near the peptidyl transferase center explain spectra of drug action. Proceedings of the National Academy of Sciences of the United States of America *107*, 17152-17157.

Duval, M., Dar, D., Carvalho, F., Rocha, E.P.C., Sorek, R., and Cossart, P. (2018). HflXr, a homolog of a ribosome-splitting factor, mediates antibiotic resistance. Proceedings of the National Academy of Sciences of the United States of America *115*, 13359-13364.

Esposito, A.M., and Kinzy, T.G. (2014). In vivo [35S]-methionine incorporation. Methods in enzymology *536*, 55-64.

Fajardo, A., Martinez-Martin, N., Mercadillo, M., Galan, J.C., Ghysels, B., Matthijs, S., Cornelis, P., Wiehlmann, L., Tummler, B., Baquero, F.*, et al.* (2008). The neglected intrinsic resistome of bacterial pathogens. PloS one *3*, e1619.

Feng, L., Chen, Z., Wang, Z., Hu, Y., and Chen, S. (2016). Genome-wide characterization of monomeric transcriptional regulators in Mycobacterium tuberculosis. Microbiology *162*, 889-897.

Folcher, M., Morris, R.P., Dale, G., Salah-Bey-Hocini, K., Viollier, P.H., and Thompson, C.J. (2001). A transcriptional regulator of a pristinamycin resistance gene in Streptomyces coelicolor. The Journal of biological chemistry *276*, 1479-1485.

Forsberg, K.J., Reyes, A., Wang, B., Selleck, E.M., Sommer, M.O., and Dantas, G. (2012). The shared antibiotic resistome of soil bacteria and human pathogens. Science *337*, 1107-1111.

Fowler-Goldsworthy, K., Gust, B., Mouz, S., Chandra, G., Findlay, K.C., and Chater, K.F. (2011). The actinobacteria-specific gene wblA controls major developmental transitions in Streptomyces coelicolor A3(2). Microbiology *157*, 1312-1328.

Genilloud, O. (2017). Actinomycetes: still a source of novel antibiotics. Natural product reports *34*, 1203-1232.

Gibson, M.K., Forsberg, K.J., and Dantas, G. (2015). Improved annotation of antibiotic resistance determinants reveals microbial resistomes cluster by ecology. ISME J *9*, 207-216.

Green, M.R., and Sambrook, J. (2012). Molecular Cloning: A Laboratory Manual (Cold Spring Harbor Laboratory Press).

Gupta, P., Liu, B., Klepacki, D., Gupta, V., Schulten, K., Mankin, A.S., and Vazquez-Laslop, N. (2016). Nascent peptide assists the ribosome in recognizing chemically distinct small molecules. Nature chemical biology *12*, 153-158.

Gust, B., Challis, G.L., Fowler, K., Kieser, T., and Chater, K.F. (2003). PCR-targeted Streptomyces gene replacement identifies a protein domain needed for biosynthesis of the sesquiterpene soil odor geosmin. Proceedings of the National Academy of Sciences of the United States of America *100*, 1541-1546.

Hanahan, D. (1983). Studies on transformation of Escherichia coli with plasmids. J Mol Biol *166*, 557-580.

Handa, Y., Inaho, N., and Nameki, N. (2011). YaeJ is a novel ribosome-associated protein in Escherichia coli that can hydrolyze peptidyl-tRNA on stalled ribosomes. Nucleic Acids Res *39*, 1739-1748.

Hu, P., Janga, S.C., Babu, M., Diaz-Mejia, J.J., Butland, G., Yang, W., Pogoutse, O., Guo, X., Phanse, S., Wong, P*., et al.* (2009). Global functional atlas of Escherichia coli encompassing previously uncharacterized proteins. PLoS Biol *7*, e96.

Huerta-Cepas, J., Forslund, K., Coelho, L.P., Szklarczyk, D., Jensen, L.J., von Mering, C., and Bork, P. (2017). Fast Genome-Wide Functional Annotation through Orthology Assignment by eggNOG-Mapper. Mol Biol Evol *34*, 2115-2122.

Huerta-Cepas, J., Szklarczyk, D., Forslund, K., Cook, H., Heller, D., Walter, M.C., Rattei, T., Mende, D.R., Sunagawa, S., Kuhn, M.*, et al.* (2016). eggNOG 4.5: a hierarchical orthology framework with improved functional annotations for eukaryotic, prokaryotic and viral sequences. Nucleic Acids Res *44*, D286-293.

Hurst-Hess, K., Rudra, P., and Ghosh, P. (2017). Mycobacterium abscessus WhiB7 Regulates a Species-Specific Repertoire of Genes To Confer Extreme Antibiotic Resistance. Antimicrob Agents Chemother *61*.

Hwang, J., and Inouye, M. (2001). An essential GTPase, der, containing double GTP-binding domains from Escherichia coli and Thermotoga maritima. The Journal of biological chemistry *276*, 31415-31421.

Hwang, J., and Inouye, M. (2006). The tandem GTPase, Der, is essential for the biogenesis of 50S ribosomal subunits in Escherichia coli. Molecular microbiology *61*, 1660-1672.

Jacob, A.I., Kohrer, C., Davies, B.W., RajBhandary, U.L., and Walker, G.C. (2013). Conserved bacterial RNase YbeY plays key roles in 70S ribosome quality control and 16S rRNA maturation. Molecular cell *49*, 427-438.

Jenkins, G., and Cundliffe, E. (1991). Cloning and characterization of two genes from Streptomyces lividans that confer inducible resistance to lincomycin and macrolide antibiotics. Gene *108*, 55-62.

Jeong, Y., Kim, J.N., Kim, M.W., Bucca, G., Cho, S., Yoon, Y.J., Kim, B.G., Roe, J.H., Kim, S.C., Smith, C.P.*, et al.* (2016). The dynamic transcriptional and translational landscape of the model antibiotic producer Streptomyces coelicolor A3(2). Nature communications *7*, 11605.

Jiang, L., Schaffitzel, C., Bingel-Erlenmeyer, R., Ban, N., Korber, P., Koning, R.I., de Geus, D.C., Plaisier, J.R., and Abrahams, J.P. (2009). Recycling of aborted ribosomal 50S subunit-nascent chain-tRNA complexes by the heat shock protein Hsp15. J Mol Biol *386*, 1357-1367.

Jiang, X., Ellabaan, M.M.H., Charusanti, P., Munck, C., Blin, K., Tong, Y., Weber,

T., Sommer, M.O.A., and Lee, S.Y. (2017). Dissemination of antibiotic resistance genes from antibiotic producers to pathogens. Nature communications *8*, 15784.

Kannan, K., and Mankin, A.S. (2011). Macrolide antibiotics in the ribosome exit tunnel: species-specific binding and action. Annals of the New York Academy of Sciences *1241*, 33-47.

Kaur, S., Rana, V., Singh, P., Trivedi, G., Anand, S., Kaur, A., Gupta, P., Jain, A., and Sharma, C. (2016). Novel mutations conferring resistance to kanamycin in Mycobacterium tuberculosis clinical isolates from Northern India. Tuberculosis (Edinb) *96*, 96-101.

Kazakov, A.E., Vassieva, O., Gelfand, M.S., Osterman, A., and Overbeek, R. (2003). Bioinformatics classification and functional analysis of PhoH homologs. In Silico Biol *3*, 3-15.

Kieser, T., Bibb, M.J., Buttner, M.J., Chater, K.F., and Hopwood, D.A. (2000). Practical *Streptomyces* Genetics (Norwich: John Innes Foundation).

Kim, I.K., Lee, C.J., Kim, M.K., Kim, J.M., Kim, J.H., Yim, H.S., Cha, S.S., and Kang, S.O. (2006). Crystal structure of the DNA-binding domain of BldD, a central regulator of aerial mycelium formation in Streptomyces coelicolor A3(2). Molecular microbiology *60*, 1179-1193.

Kim, J.E., Choi, J.S., Kim, J.S., Cho, Y.H., and Roe, J.H. (2020). Lysine acetylation of the housekeeping sigma factor enhances the activity of the RNA polymerase holoenzyme. Nucleic Acids Res *48*, 2401-2411.

Klumpp, S., Scott, M., Pedersen, S., and Hwa, T. (2013). Molecular crowding limits translation and cell growth. Proceedings of the National Academy of Sciences of the United States of America *110*, 16754-16759.

Koo, J.T., Choe, J., and Moseley, S.L. (2004). HrpA, a DEAH-box RNA helicase, is involved in mRNA processing of a fimbrial operon in Escherichia coli. Molecular microbiology *52*, 1813-1826.

Korber, P., Stahl, J.M., Nierhaus, K.H., and Bardwell, J.C. (2000). Hsp15: a

ribosome-associated heat shock protein. The EMBO journal *19*, 741-748.

Korczynska, M., Mukhtar, T.A., Wright, G.D., and Berghuis, A.M. (2007). Structural basis for streptogramin B resistance in Staphylococcus aureus by virginiamycin B lyase. Proceedings of the National Academy of Sciences of the United States of America *104*, 10388-10393.

Koser, C.U., Bryant, J.M., Parkhill, J., and Peacock, S.J. (2013). Consequences of whiB7 (Rv3197A) mutations in Beijing genotype isolates of the Mycobacterium tuberculosis complex. Antimicrob Agents Chemother *57*, 3461.

Kudhair, B.K., Hounslow, A.M., Rolfe, M.D., Crack, J.C., Hunt, D.M., Buxton, R.S., Smith, L.J., Le Brun, N.E., Williamson, M.P., and Green, J. (2017). Structure of a Wbl protein and implications for NO sensing by M. tuberculosis. Nature communications *8*, 2280.

Kumar, S., Stecher, G., and Tamura, K. (2016). MEGA7: Molecular Evolutionary Genetics Analysis Version 7.0 for Bigger Datasets. Mol Biol Evol *33*, 1870-1874.

Langmead, B., and Salzberg, S.L. (2012). Fast gapped-read alignment with Bowtie 2. Nat Methods *9*, 357-359.

Li, J., Ji, L., Shi, W., Xie, J., and Zhang, Y. (2013). Trans-translation mediates tolerance to multiple antibiotics and stresses in Escherichia coli. J Antimicrob Chemother *68*, 2477-2481.

Liao, Y., Smyth, G.K., and Shi, W. (2014). featureCounts: an efficient general purpose program for assigning sequence reads to genomic features. Bioinformatics *30*, 923-930.

Love, M.I., Huber, W., and Anders, S. (2014). Moderated estimation of fold change and dispersion for RNA-seq data with DESeq2. Genome Biol *15*, 550.

Lovett, P.S. (1996). Translation attenuation regulation of chloramphenicol resistance in bacteria--a review. Gene *179*, 157-162.

Martinez-Antonio, A., and Collado-Vides, J. (2003). Identifying global regulators

in transcriptional regulatory networks in bacteria. Current opinion in microbiology *6*, 482-489.

Merino, E., and Yanofsky, C. (2005). Transcription attenuation: a highly conserved regulatory strategy used by bacteria. Trends Genet *21*, 260-264.

Metsalu, T., and Vilo, J. (2015). ClustVis: a web tool for visualizing clustering of multivariate data using Principal Component Analysis and heatmap. Nucleic Acids Res *43*, W566-570.

Mi, H., Muruganujan, A., Ebert, D., Huang, X., and Thomas, P.D. (2019). PANTHER version 14: more genomes, a new PANTHER GO-slim and improvements in enrichment analysis tools. Nucleic Acids Res *47*, D419-D426.

Mitchell, A.L., Attwood, T.K., Babbitt, P.C., Blum, M., Bork, P., Bridge, A., Brown, S.D., Chang, H.Y., El-Gebali, S., Fraser, M.I.*, et al.* (2019). InterPro in 2019: improving coverage, classification and access to protein sequence annotations. Nucleic Acids Res *47*, D351-D360.

Moody, M.J., Young, R.A., Jones, S.E., and Elliot, M.A. (2013). Comparative analysis of non-coding RNAs in the antibiotic-producing Streptomyces bacteria. BMC genomics *14*, 558.

Morris, R.P., Nguyen, L., Gatfield, J., Visconti, K., Nguyen, K., Schnappinger, D., Ehrt, S., Liu, Y., Heifets, L., Pieters, J.*, et al.* (2005). Ancestral antibiotic resistance in Mycobacterium tuberculosis. Proceedings of the National Academy of Sciences of the United States of America *102*, 12200-12205.

Myronovskyi, M., Welle, E., Fedorenko, V., and Luzhetskyy, A. (2011). Beta-glucuronidase as a sensitive and versatile reporter in actinomycetes. Applied and environmental microbiology *77*, 5370-5383.

Nessar, R., Cambau, E., Reyrat, J.M., Murray, A., and Gicquel, B. (2012). Mycobacterium abscessus: a new antibiotic nightmare. J Antimicrob Chemother *67*, 810-818.

Nguyen, L., and Thompson, C.J. (2006). Foundations of antibiotic resistance in

bacterial physiology: the mycobacterial paradigm. Trends in microbiology *14*, 304-312.

Oberto, J. (2013). SyntTax: a web server linking synteny to prokaryotic taxonomy. BMC Bioinformatics *14*, 4.

Olsthoorn-Tieleman, L.N., Plooster, L.J., and Kraal, B. (2001). The variant tuf3 gene of Streptomyces coelicolor A3(2) encodes a real elongation factor Tu, as shown in a novel Streptomyces in vitro translation system. European journal of biochemistry / FEBS *268*, 3807-3815.

Paget, M.S., Chamberlin, L., Atrih, A., Foster, S.J., and Buttner, M.J. (1999). Evidence that the extracytoplasmic function sigma factor sigmaE is required for normal cell wall structure in Streptomyces coelicolor A3(2). Journal of bacteriology *181*, 204-211.

Park, A.K., Kim, H., and Jin, H.J. (2010). Phylogenetic analysis of rRNA methyltransferases, Erm and KsgA, as related to antibiotic resistance. FEMS Microbiol Lett *309*, 151-162.

Peterson, E., and Kaur, P. (2018). Antibiotic Resistance Mechanisms in Bacteria: Relationships Between Resistance Determinants of Antibiotic Producers, Environmental Bacteria, and Clinical Pathogens. Front Microbiol *9*, 2928.

Pryjma, M., Burian, J., Kuchinski, K., and Thompson, C.J. (2017). Antagonism between Front-Line Antibiotics Clarithromycin and Amikacin in the Treatment of Mycobacterium abscessus Infections Is Mediated by the whiB7 Gene. Antimicrob Agents Chemother *61*.

Ramon-Garcia, S., Ng, C., Jensen, P.R., Dosanjh, M., Burian, J., Morris, R.P., Folcher, M., Eltis, L.D., Grzesiek, S., Nguyen, L.*, et al.* (2013). WhiB7, an Fe-S-dependent transcription factor that activates species-specific repertoires of drug resistance determinants in actinobacteria. The Journal of biological chemistry *288*, 34514-34528.

Reeves, A.Z., Campbell, P.J., Sultana, R., Malik, S., Murray, M., Plikaytis, B.B., Shinnick, T.M., and Posey, J.E. (2013). Aminoglycoside cross-resistance in

Mycobacterium tuberculosis due to mutations in the 5' untranslated region of whiB7. Antimicrob Agents Chemother *57*, 1857-1865.

Rodnina, M.V. (2018). Translation in Prokaryotes. Cold Spring Harbor perspectives in biology *10*.

Rudra, P., Hurst-Hess, K.R., Cotten, K.L., Partida-Miranda, A., and Ghosh, P. (2020). Mycobacterial HflX is a ribosome splitting factor that mediates antibiotic resistance. Proceedings of the National Academy of Sciences of the United States of America *117*, 629-634.

Salman-Dilgimen, A., Hardy, P.O., Dresser, A.R., and Chaconas, G. (2011). HrpA, a DEAH-box RNA helicase, is involved in global gene regulation in the Lyme disease spirochete. PloS one *6*, e22168.

Salman-Dilgimen, A., Hardy, P.O., Radolf, J.D., Caimano, M.J., and Chaconas, G. (2013). HrpA, an RNA helicase involved in RNA processing, is required for mouse infectivity and tick transmission of the Lyme disease spirochete. PLoS Pathog *9*, e1003841.

Santos-Zavaleta, A., Salgado, H., Gama-Castro, S., Sanchez-Perez, M., Gomez-Romero, L., Ledezma-Tejeida, D., Garcia-Sotelo, J.S., Alquicira-Hernandez, K., Muniz-Rascado, L.J., Pena-Loredo, P*., et al.* (2019). RegulonDB v 10.5: tackling challenges to unify classic and high throughput knowledge of gene regulation in E. coli K-12. Nucleic Acids Res *47*, D212-D220.

Sesto, N., Wurtzel, O., Archambaud, C., Sorek, R., and Cossart, P. (2013). The excludon: a new concept in bacterial antisense RNA-mediated gene regulation. Nature reviews Microbiology *11*, 75-82.

Sharma, P., Haycocks, J.R.J., Middlemiss, A.D., Kettles, R.A., Sellars, L.E., Ricci, V., Piddock, L.J.V., and Grainger, D.C. (2017). The multiple antibiotic resistance operon of enteric bacteria controls DNA repair and outer membrane integrity. Nature communications *8*, 1444.

Shin, J.H., Singh, A.K., Cheon, D.J., and Roe, J.H. (2011). Activation of the SoxR regulon in Streptomyces coelicolor by the extracellular form of the

pigmented antibiotic actinorhodin. Journal of bacteriology *193*, 75-81.

Sievers, F., and Higgins, D.G. (2018). Clustal Omega for making accurate alignments of many protein sequences. Protein Sci *27*, 135-145.

Smidova, K., Zikova, A., Pospisil, J., Schwarz, M., Bobek, J., and Vohradsky, J. (2019). DNA mapping and kinetic modeling of the HrdB regulon in Streptomyces coelicolor. Nucleic Acids Res *47*, 621-633.

Smith, T., Wolff, K.A., and Nguyen, L. (2013). Molecular biology of drug resistance in Mycobacterium tuberculosis. Curr Top Microbiol Immunol *374*, 53-80.

Sun, J., Hesketh, A., and Bibb, M. (2001). Functional analysis of relA and rshA, two relA/spoT homologues of Streptomyces coelicolor A3(2). Journal of bacteriology *183*, 3488-3498.

The Gene Ontology Consortium (2019). The Gene Ontology Resource: 20 years and still GOing strong. Nucleic Acids Res *47*, D330-D338.

Tu, D., Blaha, G., Moore, P.B., and Steitz, T.A. (2005). Structures of MLSBK antibiotics bound to mutated large ribosomal subunits provide a structural explanation for resistance. Cell *121*, 257-270.

Turnbough, C.L., Jr. (2019). Regulation of Bacterial Gene Expression by Transcription Attenuation. Microbiology and molecular biology reviews : MMBR *83*.

Tyanova, S., Temu, T., and Cox, J. (2016). The MaxQuant computational platform for mass spectrometry-based shotgun proteomics. Nature protocols *11*, 2301-2319.

Uson, M.L., Ordonez, H., and Shuman, S. (2015). Mycobacterium smegmatis HelY Is an RNA-Activated ATPase/dATPase and 3'-to-5' Helicase That Unwinds 3'-Tailed RNA Duplexes and RNA:DNA Hybrids. Journal of bacteriology *197*, 3057-3065.

van Wezel, G.P., Takano, E., Vijgenboom, E., Bosch, L., and Bibb, M.J. (1995). The tuf3 gene of Streptomyces coelicolor A3(2) encodes an inessential

elongation factor Tu that is apparently subject to positive stringent control. Microbiology *141 (Pt 10)*, 2519-2528.

Vecchione, J.J., Alexander, B., Jr., and Sello, J.K. (2009). Two distinct major facilitator superfamily drug efflux pumps mediate chloramphenicol resistance in Streptomyces coelicolor. Antimicrob Agents Chemother *53*, 4673-4677.

Vercruysse, M., Kohrer, C., Shen, Y., Proulx, S., Ghosal, A., Davies, B.W., RajBhandary, U.L., and Walker, G.C. (2016). Identification of YbeY-Protein Interactions Involved in 16S rRNA Maturation and Stress Regulation in Escherichia coli. MBio *7*.

Wilson, D.N. (2014). Ribosome-targeting antibiotics and mechanisms of bacterial resistance. Nature reviews Microbiology *12*, 35-48.

Wilson, D.N., Schluenzen, F., Harms, J.M., Starosta, A.L., Connell, S.R., and Fucini, P. (2008). The oxazolidinone antibiotics perturb the ribosomal peptidyl-transferase center and effect tRNA positioning. Proceedings of the National Academy of Sciences of the United States of America *105*, 13339-13344.

World Health Organization (2019). WHO consolidated guidelines on drug-resistant tuberculosis treatment (Geneva: World Health Organization).

Xu, W., DeJesus, M.A., Rucker, N., Engelhart, C.A., Wright, M.G., Healy, C., Lin, K., Wang, R., Park, S.W., Ioerger, T.R.*, et al.* (2017). Chemical Genetic Interaction Profiling Reveals Determinants of Intrinsic Antibiotic Resistance in Mycobacterium tuberculosis. Antimicrob Agents Chemother *61*.

Yang, C., and Glover, J.R. (2009). The SmpB-tmRNA tagging system plays important roles in Streptomyces coelicolor growth and development. PloS one *4*, e4459.

Yanofsky, C. (1981). Attenuation in the control of expression of bacterial operons. Nature *289*, 751-758.

Yoo, J.S., Oh, G.S., Ryoo, S., and Roe, J.H. (2016). Induction of a stable sigma factor SigR by translation-inhibiting antibiotics confers resistance to antibiotics. Sci Rep *6*, 28628.

Zaunbrecher, M.A., Sikes, R.D., Jr., Metchock, B., Shinnick, T.M., and Posey, J.E. (2009). Overexpression of the chromosomally encoded aminoglycoside acetyltransferase eis confers kanamycin resistance in Mycobacterium tuberculosis. Proceedings of the National Academy of Sciences of the United States of America *106*, 20004-20009.

Zhang, Y., Liu, T., Meyer, C.A., Eeckhoute, J., Johnson, D.S., Bernstein, B.E., Nusbaum, C., Myers, R.M., Brown, M., Li, W.*, et al.* (2008). Model-based analysis of ChIP-Seq (MACS). Genome Biol *9*, R137.

Zhang, Y., Mandava, C.S., Cao, W., Li, X., Zhang, D., Li, N., Zhang, Y., Zhang, X., Qin, Y., Mi, K.*, et al.* (2015). HflX is a ribosome-splitting factor rescuing stalled ribosomes under stress conditions. Nat Struct Mol Biol *22*, 906-913.

Zhu, M., and Dai, X. (2018). On the intrinsic constraint of bacterial growth rate: M. tuberculosis's view of the protein translation capacity. Crit Rev Microbiol *44*, 455-464.

Zuker, M. (2003). Mfold web server for nucleic acid folding and hybridization prediction. Nucleic Acids Res *31*, 3406-3415.

Appendix

List of abbreviations

A/T-rich	adenine-thymine-rich
ABC	ATP-binding cassette
asRNA	antisense RNA
ATP	adenosine 5’-triphosphate
ATPase	adenosine triphosphatase
BH-adjusted	Benjamini-Hochberg-adjusted
bp	base pair(s)
cDNA	complementary DNA
ChIP	chromatin immunoprecipitation
ChIP-seq	ChIP-sequencing
dATP	2’-deoxyadenosine 5’-triphosphate
DMSO	dimethyl sulfoxide
DNA	deoxyribonucleic acid
DNase	deoxyribonuclease
EDTA	ethylenediaminetetraacetic acid
GTP	guanosine 5’-triphosphate
GTPase	guanosine triphosphatase
IP	immunoprecipitation
MFS	major facilitator superfamily
MIC	minimum inhibitory concentration
mRNA	messenger RNA
nt	nucleotide(s)
NTPase	nucleoside triphosphatase
OD_{600}	optical density at 600 nm

ORF	open reading frame
PCR	polymerase chain reaction
ppGpp	guanosine tetraphosphate
p-value	probability value
qPCR	quantitative PCR
qRT-PCR	quantitative reverse transcription-PCR
RIT	Rho-independent terminator
RNA	ribonucleic acid
RNase	ribonuclease
RNA-seq	RNA sequencing
rRNA	ribosomal RNA
tRNA	transfer RNA
TSS	transcription start site
uORF	upstream ORF

Abstract in Korean

세균의 기초 대사인 단백질 합성 과정, 즉 번역은 수많은 항생제의 작용 표적이다. 번역 저해 항생제들은 다양한 작용 방식으로 리보솜을 중심으로 한 번역 기구들의 기능을 저해한다. 세균은 유전적 변화를 통한 저항성 획득 외에도 고유의 유전인자를 활용해 항생제에 대한 내재적 저항성을 보이곤 한다. 여러 유형의 내재적 저항성 기작이 알려져 있으나 아직 밝혀지지 않은 기작도 많이 존재함이 세균들에서 관찰되고 있다.

그람 양성 방선균문 (Actinobacteria)의 방선균목 (actinomycetes) 은 환경 미생물, 동식물 공생체, 병원균들을 포함한다. 상용 항생제 대다수를 생합성하는 한편 항생제 저항성 기작을 다수 보유하는 *Streptomyces* 속과 결핵균 등 항생제 저항성 문제를 일으키는 주요 병원균이 속한 *Mycobacterium* 속이 방선균목에 포함된다. WblC 혹은 WhiB7은 번역 저해 항생제에 대한 방선균의 내재적 저항성 인자이다. WblC (WhiB7)는 시그마 인자 HrdB (SigA)와 함께 표적 유전자 프로모터에 결합해 전사를 활성화한다고 알려져 있다. WblC (WhiB7) 표적 유전자 산물들은 다수의 항생제 저항성 기작을 수행한다. 하지만 WblC (WhiB7) 조절 표적 유전자군 (조절군)의 구성은 종 간에 매우 상이할 뿐 아니라 다수의 기능 불명 유전자를 포함한다. 또한 기존의 WhiB7 조절군의 정의 방식에는 몇 가지 문제점들이 있었다. 한편 *wblC* (*whiB7*)는 리보솜 매개 전사 감쇠 기작에 의한 발현 조절을 받는다고 여겨지는데 이에 대한 실험적 증명이 아직 부족하며 무엇보다 항생제 스트레스 시 어떻게 전사 감쇠가 억제되는지는 제시된 바가 없다.

본 연구는 *Streptomyces coelicolor*에서 WblC의 조절 표적들을 규명하였다. *S. coelicolor* 유전자의 7.8%가 항생제 스트레스 상황에서

WblC에 의한 전사량 변화를 보였으며, 이들 중 312개 유전자가 항생제 스트레스 상황에서 WblC의 직접적 프로모터 결합이 관찰되는 WblC 조절군 (regulon) 으로 파악되었다. WblC에 의해 발현이 증가하는 288개 조절군 유전자들의 프로모터들은 mycobacteria에서와 같이 2개의 프로모터 서열 인자와 WblC 결합 부위를 공통적으로 지니고 있었고, 이들 공통 서열의 보존성에 상응하는 WblC 결합 및 전사 활성화 정도를 보였으며, WblC 의존적 HrdB 결합 증가가 관찰되었다. 반면 WblC에 의한 발현 감소를 보이는 24개 조절군 유전자들의 프로모터들에서는 공통 서열이 발견되지 않았으며 WblC에 의한 HrdB 결합 유도도 일어나지 않았다. 한편 WblC는 조절군 유전자들 외에도 다수의 noncoding RNA 발현을 조절하였다.

WblC 조절군 산물 다수가 리보솜에 결합하며 새로운 항생제 저항성 인자들로 작용함도 확인하였다. *S. coelicolor*의 WblC 조절군은 기존에 알려진 항생제 저항성 유전자들을 다수 포함하는 한편 몇몇 기능 유형의 유전자들을 높은 비율로 포함하고 있었으며, 특히 다수의 단백질 합성 관여 유전자들을 포함하였다. WblC는 저농도 항생제 스트레스 상황에서 세포 내 전반적 번역 속도 증가와 이에 상응하는 생장 속도 증진을 유발했는데, 이는 WblC 조절군 산물들에 의한 유효 항생제 농도 저감 혹은 번역 촉진에 기인할 수 있다. 항생제 스트레스와 WblC에 의존적인 리보솜 결합량 증가가 일어나는 단백질들을 파악해 본 결과 대부분이 WblC 조절군의 산물이었으며 이들 중 상당수가 번역 스트레스의 해소에 관여한다는 보고들을 찾을 수 있었다. 리보솜 결합 단백질들을 암호화하는 3개 유전자의 변이가 erythromycin, tetracycline에 대한 저항성의 감소를 일으켰으며 변이된 유전자의 보완 시 항생제 저항성이 회복되었다.

본 연구는 또한 항생제에 의한 *wblC* 발현 유도 중 전사 감쇠가 억제되는 기작을 다루었다. 먼저 대다수의 방선균 *wblC* 선도 서열 (leader

sequence)에 전사 감쇠의 서열 인자들이 보존되어 있음을 확인하였다. 그리고 선도 서열 내 Rho 비의존적 종결자가 일으키는 전사 종결이 *wblC* 발현 감쇠를 일으킴을 검증하였다. 방선균목 하위 분류군들의 선도 서열 내에 보존된 항종결인자 (antiterminator) 추정 RNA 구조가 발견되었고, *S. coelicolor*의 해당 항종결인자 추정 서열은 실제로 항생제 스트레스 상황에서 전사 감쇠를 억제하는 기작으로 작용하였다. 마지막으로, 아미노산 고갈 역시 전사 조기 종결을 억제해 *wblC* 발현을 유도함을 발견함으로써 *wblC*의 리보솜 매개 전사 감쇠는 다양한 번역 결함에 반응함을 제시하였다.

주요어 : WblC (WhiB7), 항생제 저항성, 조절군, 리보솜 매개 전사 감쇠, 항종결인자, *Streptomyces*

학 번 : 2014-21296